

Norwegian University of Life Sciences
Faculty of Environmental Science and
Technology
Department of Mathematical Sciences and
Technology

Master Thesis 2014
30 credits

CFD Flow Simulation and Testing of Coolant Pressure Drop in a Marine Heat Exchanger

Lasse Flåt Isaksen

Preface

This thesis concludes my Master of Science degree in Machinery and Product Development at The Norwegian University of Life Sciences. The work done has been performed during my 10th semester, spring 2014, at the Department of Mathematical Sciences and Technology in the Faculty of Environmental Science and Technology.

My thesis is a result of collaboration with Sperre Coolers AS, where Sperre's contribution includes, but is not limited to, a facility for experimental testing and CAD-models.

I would like to thank Rune Myklebust, President of Sperre Coolers AS, for this opportunity to work with them and engage in their products. Kenneth Myklebust, V.P. Technical, and his teammates Roger Døving and Lars Einar Endresen also deserve thanks, for providing me with all information requested, CAD-models for simulation and experimental testing expertise.

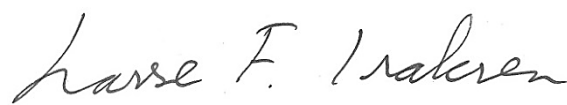
Secondly, I would like to thank my supervisors, Professor John Mosbye for keeping the thesis on track in the right direction, and associate professor Dr. Carlos Salas Bringas for guiding me into the world of Flow Simulation, and supporting me through it.

At last, I would like to thank my wonderful fiancée Lene, for bringing my spirits back up during the rough periods of simulation.

Thank you!

Norwegian University of Life Sciences, Ås, Norway

May 15th, 2014



Lasse Flåt Isaksen

Abstract

As the focus on energy consumption increase, so does the use of heat exchangers. Utilizing natural temperature differences, is a safe and efficient way to cool fluid medium. Through collaboration in a previous course, Sperre Coolers introduced me to the Rack Cooler, as a new, efficient and stable alternative for engine cooling in the maritime industry. In their process of calculating its total efficiency they were very interested in the pressure drop of the internal coolant through their heat exchanger, and methods of determining it. The method questioned is Computational Fluid Dynamic (CFD) analysis. Since the Rack Cooler is available in a large number of different configurations, three main sizes were selected by Sperre, on request. Each of these three main sizes is in turn available in three different heights, and two different flow patterns, which makes a total of 18 specific configurations.

First we performed experimental testing of pressure drop, in Sperre's own test facility. Because of reading error in instruments used and a system whose specifications did not match the needs for the testing, these results ended up with a broad spectrum. Still, the results are compared to the CFD results, with various degrees of success.

The CFD analyses were done in SolidWorks Flow Simulation, with 3D-models mostly converted from Inventor. Through simplifications of the 3D-model and a long phase of mesh optimization, a final mesh was set for the rack with the highest number of pipes. Through comparisons of simulating one single pipe in different heights, and simulations of two similar racks, with only difference in height, eight (8) was found as correlation factor. This factor was used to find the pressure drop of the racks higher than those simulated in their fully extend. In an attempt to further refine the mesh, a smaller rack then the optimization was done on, was used. This resulted in a much lower pressure drop simulated in the same rack. This initiated an investigation why, and the result show clearly a mesh which is too coarse for these simulations. The most unambiguously result, which is supported both of the testing and all the simulations, is that the pressure drop in a 2-pass configuration is more or less half of the pressure drop in a 4-pass configuration. The conclusion states that the need of computer power (due to the need of further mesh refinement) far exceeds what was available at the time of the work on this thesis.

Further development of the test facility and improved computer capacity is required for more applicable and accurate results.

Sammendrag

Rørvarmevekslere er en effektiv og sikker måte å overføre varme på, fra en væske til en annen. Denne metoden blir brukt i mange forskjellige bransjer og variasjoner, men felles for dem alle er at en varmeveksler utnytter temperaturforskjellen i væsker eller gasser, for å flytte på varmen. Sperre Coolers AS er et firma som har utviklet en ny og sikrere varmeveksler for å kjøle motorer i skip tilknyttet offshore industrien. Gjennom et tidligere samarbeid har de uttrykt et ønske om å få bedre data på trykktapet gjennom varmeveksleren, samt metoder for å finne dette. Dette er viktig for å kunne finne den totale effektiviteten. Metoden som er brukt er et datasimuleringsverktøy laget for å simulere blant annet væskestrøm (Flow Simulation), i en 3D-modell bygget opp i modelleringsverktøyet SolidWorks. Sperre valgte ut tre hovedmodeller de mente var viktigst, hvor alle kommer i tre forskjellige høyder. Det er to mulige måter å sette opp varmeveksleren på, slik at totalt 18 forskjellige konfigurasjoner er vurdert.

Det ble først utført fysiske tester på en fullskalamodell i Sperres eget lokale. På grunn av ukalibrerte instrumenter og et testsystem som ikke var spesifikt bygget for testene, ble det et stort spenn i resultatene. Resultatene ble senere sammenliknet med simuleringsresultatene med varierende grad av overlapping.

For å finne en best mulig elementoppdeling (mesh) av én modell, ble 3D-modellen forenklet og en fase med testsimuleringer utført. Deretter ble resten av de tre hovedmodellene simulert med samme mesh, i begge oppsettene. Ved å simulere kun ett enkelt gjennomsnittsrør i hver av vekslerene, med ulik lengde, ble det funnet en faktor på åtte, som ble brukt for å utnytte de tidligere simuleringsresultatene på høyere vekslere. I et forsøk på å optimalisere meshen enda mer, i en mindre veksler enn først brukt, viste resultatene et mye lave trykktap. Derfor ble det viktig å finne ut hvorfor forskjellen var så stor. Det viste seg at meshen som ble anvendt, var på langt nær så god som den burde vært, for å få pålitelige resultater. Derfor må man ha kraftigere datamaskiner, bygget til formålet, for å kunne fullføre simuleringer med den nødvendig meshen.

Forskjellen i trykktapet i de to ulike måtene å sette opp veksleren på, ble verifisert av alle simuleringene og testene, til å ha en faktor på to(2). Det vil si at når vannet går gjennom rørene to ganger, vil det bli dobbelt trykktap enn hva det vil bli med kun en gjennomstrømning. Dette er med lik dimensjonerende vannhastighet i rørene.

Table of Contents	Page
Preface.....	i
Abstract.....	ii
Sammendrag	iii
1. Introduction	8
1.1 Background	9
1.2 Product description.....	10
1.2.1 Basic principles	10
1.2.2 System placement	11
1.2.3 Physical dimensions.....	12
1.2.4 System Components.....	15
1.3 Goals.....	16
1.3.1 Main goal	16
1.3.2 Project goals.....	16
1.3.3 Sperres goal.....	16
1.4 Limitations	17
2. Methods	18
2.1 Experimental testing – system setup	18
2.2 Test setup and configurations.....	23
2.2.1 No rack.....	24
2.2.2 2-pass half rack	25
2.2.3 2-pass full rack.....	26
2.2.4 4-pass rack	28
2.3 Computational Fluid Dynamics (CFD).....	29
2.3.1 Overview of capabilities	29
2.3.2 Computational domain:.....	31
2.3.3 Mesh.....	31



2.3.4	The calculations	31
2.4	Simulation model	32
2.4.1	File conversion.....	32
2.4.2	Model simplification.....	34
2.5	Mesh optimization.....	40
2.5.1	Global mesh	41
2.5.2	Bend mesh.....	42
2.5.3	Inlet/outlet mesh.....	44
2.6	Rack simulation setup	46
2.6.1	General settings.....	47
2.6.2	Input data	48
2.7	Rack simulation configurations.....	50
2.7.1	Experimental test configurations	50
2.7.2	Real configurations	51
2.8	Single pipe simulation.....	52
2.8.1	Principle	52
2.8.2	Result treatment	54
2.8.3	Result treatment of improved mesh simulations.....	55
3.	Results	56
3.1	Experimental test results	56
3.1.1	Raw results.....	56
3.1.2	Sorted and ordered results.....	57
3.1.3	Adjusted results.....	61
3.2	Single pipe simulations	63
3.2.1	Pipe flow profile	63
3.2.2	Pressure results.....	63
3.3	Rack Simulation Results	65

3.4	Combined results.....	70
3.4.1	Experimental combined results.....	71
3.4.2	Rack simulation results.....	73
4	Discussion and investigation of 600-1000S rack results.....	77
4.1	Result summary comparison.....	77
4.1.1	Results.....	78
4.1.2	Goals and convergence.....	79
4.1.3	Minimum and maximum.....	80
4.2	Cut plot comparison.....	81
4.3	Cell size and amount of cells.....	86
4.3.1	Total amount of cells.....	86
4.3.2	Types of cells.....	88
4.3.3	Simple pipe comparison.....	88
5	Discussion.....	94
5.1	The experimental testing.....	94
5.1.1	Factors of influence.....	94
5.1.2	Result adjustment.....	98
5.2	The simulations.....	98
5.2.1	Inlet conditions.....	98
5.2.2	Mesh.....	99
5.2.3	Computer capabilities.....	99
5.3	Results.....	100
6	Conclusion.....	101
6.1	Experimental testing.....	101
6.2	CFD simulations.....	101
6.3	Results.....	102
6.4	Future work.....	102



6.4.1	Experimental testing	102
6.4.2	CFD simulations	103
7	Reference List.....	104
Appendix I	List of current available rack-sizes ⁶	106
Appendix II	Pump sheet	107
Appendix III	Picture of original output file from loggings.....	108
Appendix IV	Raw test data with standard deviation.....	109
Appendix V	Result file from SolidWorks Flow Simulation.....	110
Appendix VI	Full report 600-1000S 4-pass Simulation (Mesh 5).....	111
Appendix VII	Full report 600-1000S 4-pass Simulation (Mesh 4)	116

1. Introduction

International Energy Agency's World Energy Outlook 2013, predicts the energy demand for the future to increase. Today, 1,3 billion people lack electricity, and 2,6 billion people relying on solid mass for cooking. As access to electricity spreads to less developed regions, the demand will increase drastically.

As the demand increases, the renewable contribution to the global energy source mix is not expected to cover the demand. Fossil fuels are today responsible for 82% of the energy, and even though it will decrease, it is predicted to still account for 75% of the global primary energy source in 2035. ¹ As oil and gas are two of the main sources of fossil fuels, these will still have a large growth of demand during the next decades. Projections vary greatly, but most expect oil and gas to still account for at least 50% of the total demand. To meet these needs, the oil and gas industry is constantly working to go deeper and further from land, as well as in arctic conditions and increasing the extraction of existing fields, by utilizing new technology placed on the sea bed.

The market for subsea production and processing systems is expected to have a compound annual growth rate (CAGR) of 6% till 2018. ² The maritime industry of offshore support vessels is closely tied to the activity of offshore exploration, and especially the subsea activity. This market includes anchor handling vessels, towing & supply vessels, platform supply vessels, multi-purpose service vessels, crew boats and standby & rescue vessels. This market is expected a CAGR of 5,7% towards 2018.³

Parallel to the increasing energy demand globally, there is a rising awareness and understanding of human impact of our planet. This influences the way people think about the future. The use of fossil energy sources and its effects on the environment is not consistent with the future energy demands. In order to meet the future energy demands with as little negative impact as possible, energy consumption needs to decrease. New regulations in many industries have been, and will be implemented, in order to reduce its energy consumption and carbon footprint. All fields, from residential housing and automobiles, to aircrafts and the shipping industry are working for this indefinite goal.

Heat exchangers are used to transfer heat from one medium to another. In buildings they are used for heating and are called heat pumps. In warmer climates they are called air conditioners and are used for cooling. They represent an efficient tool for heating or



cooling, as it utilizes the temperature difference between two substances. In ships they are used in the same matter, but most specifically for cooling the engines. The energy needed to cool the engine, has to come from the engine itself, which means it is directly linked to the total efficiency. The lower the power consumption of the cooling equipment is, the higher the output for propulsion is. And further, when the power consumption decreases, the required gross power output from the power plant is cut.

The Sperre Rack Cooler is a heat exchanger designed especially for the growing market of offshore support vessels to decrease its total power consumption, among other main features.

1.1 Background

The total efficiency of a heat exchanger system is of importance when choosing what system a client needs. Because the system is pump driven, the energy needed to run these pumps are of interest to the builder to both find the efficiency of the system, but also to select the correct pumps for the system. The importance of selecting correct pumps to run the system are crucial to be sure the needed cooling will be achieved. The main parameters for selecting correct pump is the flow the system needs to achieve the desired water velocity in the pipes. For the pump to be able to achieve this flow, the pressure drop of the system needs to be known.

The spring semester of 2012 I attended a course called “Heat and Slow Simulation”, which made me interested in computational fluid dynamics. This interest resulted in me working as the teacher’s assistant by helping answering questions in the course, for the two next years.

During the autumn semester of 2013 I participated in the course “TIP300-concept and product realization”, where I wrote a project report named “Phase 1: Flow optimizing of heat exchanger”. In this project I went through several different ideas for how to reduce the pressure loss in the heat exchanger. The idea I went forward with, and examined in detail, was the inlets and outlets of the cooling pipes for the coolant. I concluded that by changing the shape of this region, the pressure drop in that specific region could be reduced by 18-42 per cent. These changes are not included in this thesis.

1.2 Product description

The Sperre Rack Cooler will in this chapter be introduced and explained to the extent needed for this thesis.

1.2.1 Basic principles

The Sperre Rack Cooler is a water to water heat exchanger, designed to efficient cooling of ships main engines, during all operating conditions. The coolant fluid from the engine is run through a series of cooling racks, to transfer its heat to sea water. This is done by convection to the pipes the fluid runs through, conduction through the pipe, and finally convection to the colder sea water. Compared to conventional box coolers used in many ships of today, the rack cooler uses forced convection, to secure a better transfer the heat, in every condition.

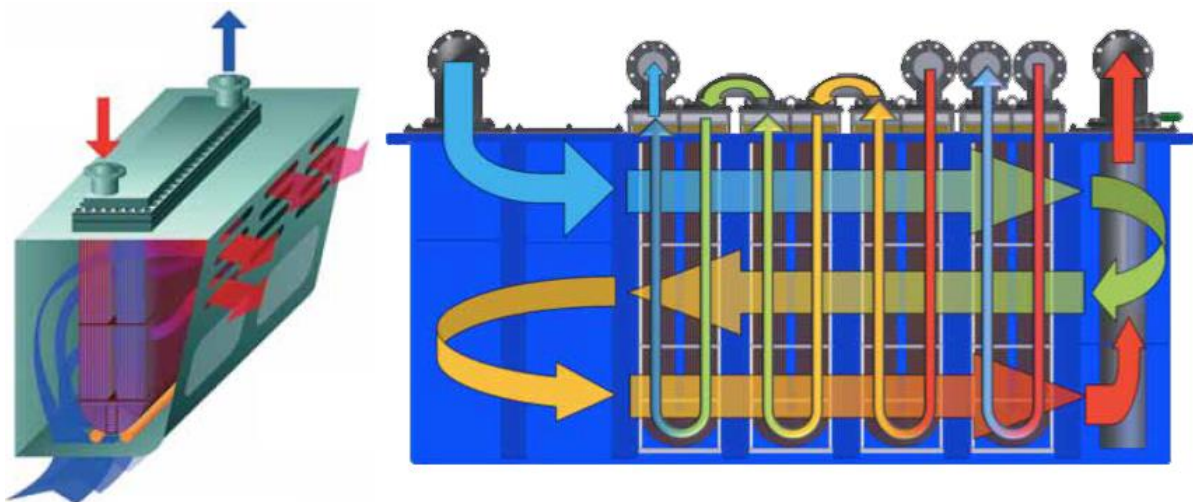


Figure 1: To the left is the flow situation of a box cooler⁴, and to the right is the flow situation of a rack cooler system.

Conventional box coolers are dependant of natural convection of the cooling fluid. The cooling fluid in the system is the sea water, and because it heats up during the contact with the warmer pipes “holding” the engine coolant fluid, the sea water will create a natural upwards drafts, because warmer water is less dense than colder water. When the ship moves, this cooling will increase because the sea water will have a horizontal flow over the pipes, as well as the natural convection. In many offshore supply vessels, among others, the heavy load on the ships engines creates the need for high and stable cooling, even during standstill or slow moving operations (dynamic positioning).

Because the rack utilizes forced convection in both fluids of the heat exchanger, the need for pumps making these fluid flow, is larger. Pumps are to be used both to pump the engine coolant through the cooling pipes, as well as pump the sea water around the pipes to extract its heat. This increased need for pumping power is a negative effect of the increased stability in cooling, and is to be investigated.

The coolant water used in the system is fresh water, with a small amount of glycol added. In all the calculations Sperre does on this water, the glycol effect is neglected. The temperature the coolant has when entering the cooler can differ from system to system, but most often in the range of 40°-60° C, with an exit temperature after the entire cycle of 35°-40° C. For all simulations done here, the temperature of the water is set to 50°C.

1.2.2 System placement

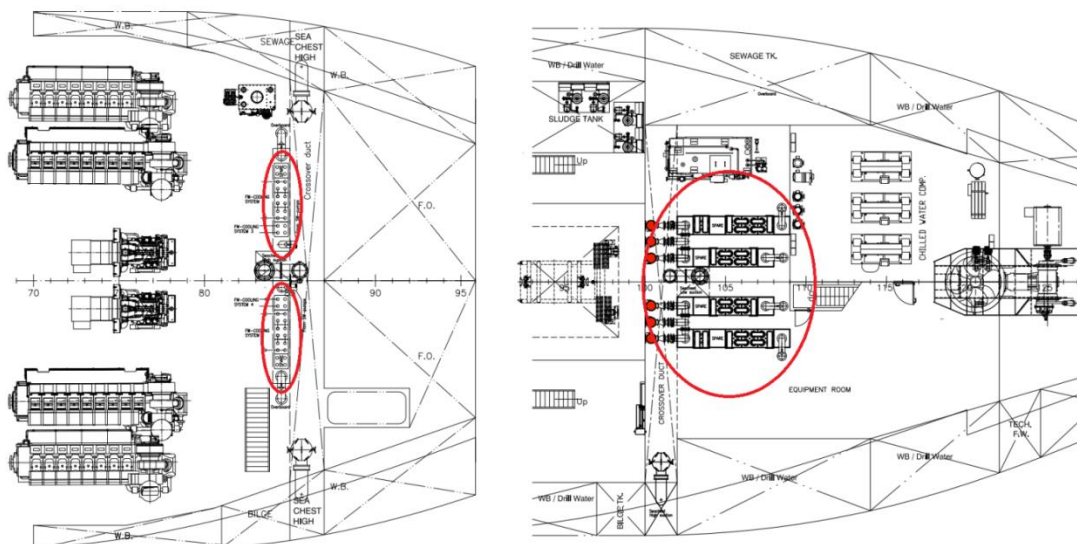


Figure 2: Two possible positions of the cooling system in a ships lowest deck. The coolers are circled in red, and the front of the ships is to the right.

The rack cooler is placed under the lowest deck of the ship. Compared to the box coolers that has to be on the sides of the ship, these coolers are flexible to be positioned closer to the engines, more in the middle of the ship, and still out of sight. This makes the access of them to do maintenance and modifications better, because the ship does not have to be dry docked to reach the coolers. This saves time and money, because the coolers and be fully checked and maintained still at sea.

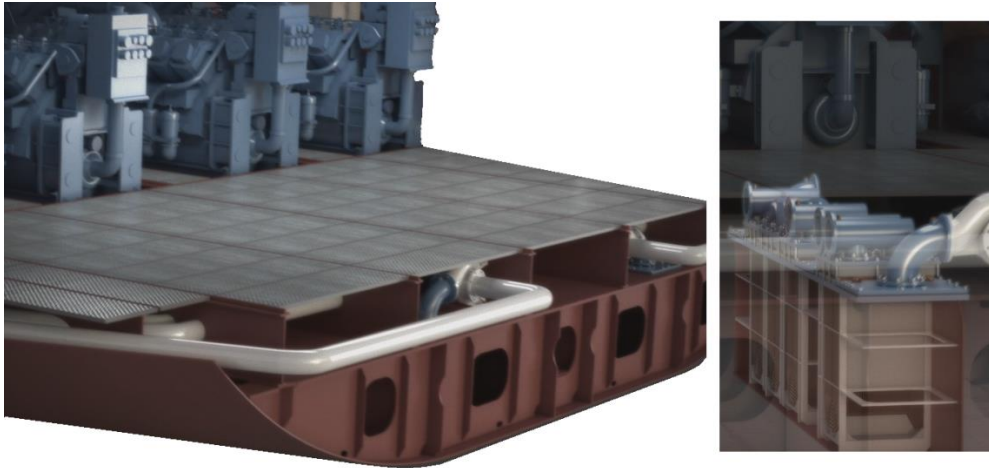


Figure 3: The ship is cut through to see the positioning of the cooling system under the lowest deck, on which the engine is placed on top of. To the left the deck is shown, and the white piping which leads to the system, and to the right the system is shown beneath the deck.

1.2.3 Physical dimensions

Because the rack is installed in the hull of the ship, its available dimensions can match the distances the frame of the ship is built around. The height is defined by the height available under the lowest deck, which is loosely defined by the size of the ballast tanks in the ship. When designing a system for a ship, the area available is defining for which size will be chosen, and the cooling requirement defines the number of racks needed. The total cooling equipment will consist of typically 2-6 more or less separate systems.

Table 1: A list of most relevant rack-models and their main dimensions. Surface area are from Sperre internal documents⁵ and ⁶.

Model (Width-Height (Standard/Compact))	Width [mm]	Height [mm]	Length [mm]	Cooling surface area [m ²]	Number of pipes
600-1000C	600	1000	400	29,3	367
600-1200C	600	1200	400	35,1	367
600-1500C	600	1500	400	43,9	367
600-1000S	600	1000	500	37,2	467
600-1200S	600	1200	500	44,7	467
600-1500S	600	1500	500	55,9	467
700-1000S	700	1000	600	56,5	709
700-1200S	700	1200	600	67,9	709
700-1500S	700	1500	600	84,8	709

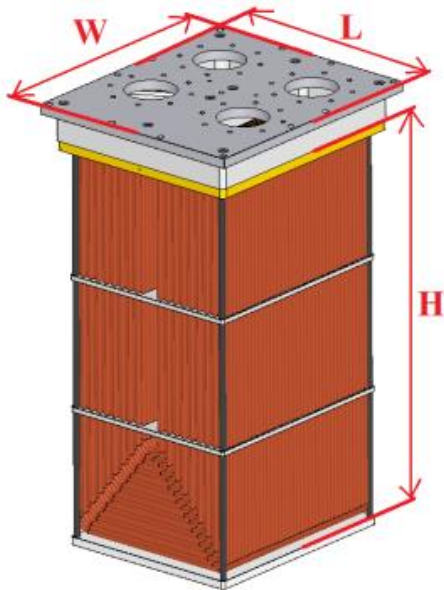


Figure 4: Picture of a single rack, and what each dimensions refers to.

The rack is made in many different models, to fit different physical needs. The available sizes have developed from it was launched, to meet the needs of the clients. A complete list of current available configurations is given in Appendix I, and in Table 1 the models of most interest/relevance are listed. The frame width is the first parameter in the model. Sperre has so far developed four different sizes, ranging from 500mm to 800mm, but as it turns out, the 600-series and the 700-series are the two with the most marked potential. According to ⁷ all of the ordered and/or delivered projects as of April 2014 are either of the 600-series or 700-series rack.

The rack height is a parameter that dictates the length of each individual pipe, and is chosen on the basis of what is available. The higher the rack is the larger its cooling surface area is, in relation to the footprint. The height needs to be high enough for the 3-pass of the sea water to pass over the rack, and there for the minimum desired height Sperre will supply is 800mm, but most used is between 1000mm and 1500mm, and that is why these are the ones listed.

The length of each rack in a system is always a compromise between long and few racks, and having shorter and more racks. This dimension is linked to the width, in the way that it is 100mm less than it in the standard configuration (S). The compact configuration (C) is a further 100mm shorter, in order to fit more racks in the same length. The number of pipes in the standard and compact are different, and there for the cooling surface are also different.

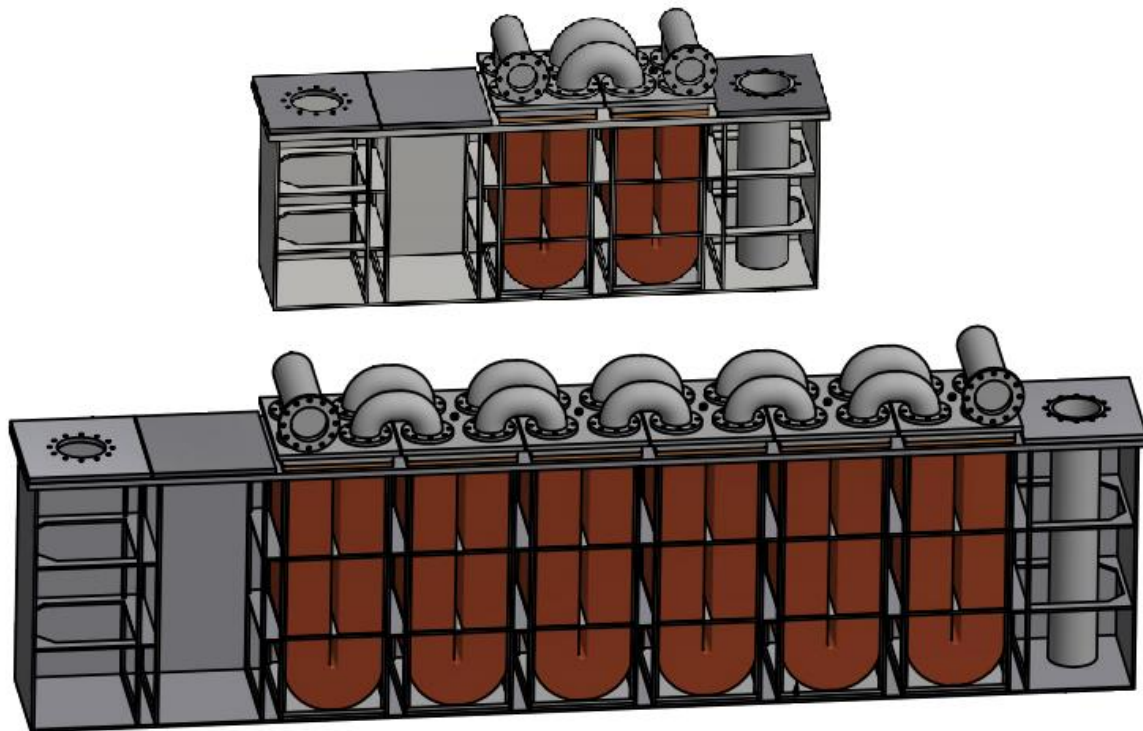


Figure 5: Two different rack systems. The top one is a 600-1000S system with two racks and a spare slot, and the bottom one is a 700-15000S system with six racks and one spare slot.

Each system is placed in a separate box, where the racks will be installed. Each box contains a certain number of slots, which defines the maximum number of how many racks can be installed. The first and last slots are used for inlet and outlet of the sea water, but the rest will house one rack each. Every box is usually designed with a spare slot, in which a spare rack can be installed if the need of cooling is underestimated or increases.

When the coolers are installed in ships, they will typically consist of 4-6 more or less separate systems. Each system will then be contained in its own box, where the racks are placed. The systems are most likely similar, but they may also be different if they cool separate systems, with different requirements. Each system normally contains 3-5 racks, but can be as few as two or as many as six.⁸

Through conversations with Sperre, the desired water velocity in the pipes are 0,5-1,5 m/s. This is based on internal calculations for obtaining the desired Reynolds number, but is also supported in the literature⁹. The goal is to get the flow to the transition phase from laminar flow to turbulent flow, or in the beginning region of turbulent flow.

1.2.4 System Components

As Figure 5 illustrates, there are many different components in an entire system. The components affecting the internal flow situation of the system is presented in the figure below (Figure 6). The components not included here is the piping to and from every single rack, as this is standard piping, nor manufactured by Sperre.

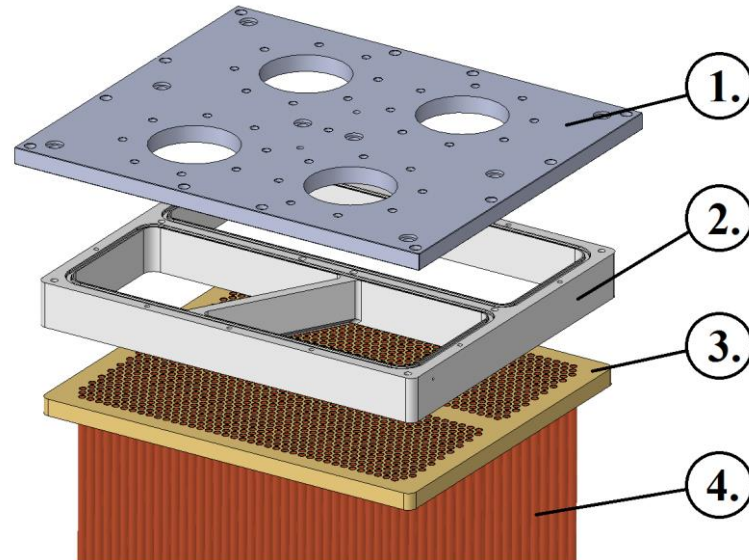


Figure 6: Exploded view of the most vital components of the single rack. 1: Top plate. 2: Flow splitter frame. 3: Pipe holding plate. 4: Pipes.

The top plate (1) is where the main inlet(s) and outlet(s) of the coolant flow through the rack enter/exits. The openings are standard sizes for each of the rack-sizes, ranging from 125 mm to 200 mm in diameter for the ones simulated here. The function of the flow splitter frame (2) is visualized in Figure 7. The pipe holding plate (3) is a plate where all the pipes are fastened, and is a crucial part when it comes to the water tightness of the rack. The pipes (4) are made of 90-10 alloy of copper and nickel, which (according to Sperre) gives the best combination of heat transfer abilities, and corrosion/fouling conditions. Their outer diameter is 12,70 mm, and a wall thickness of 1 mm.

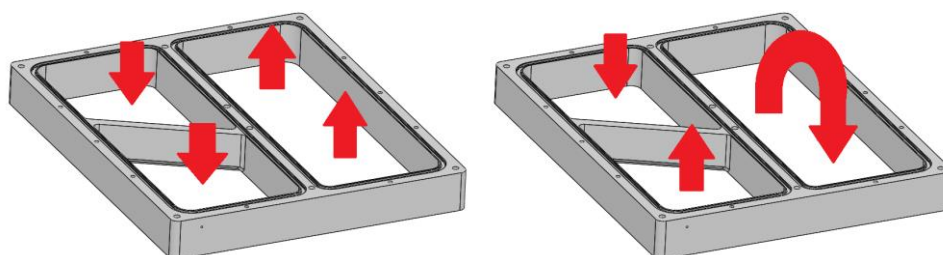


Figure 7: The flow splitter frame, with the red arrows representing the flow direction. To the left is a 2-pass configuration and to the right is a 4-pass configuration.

The flow splitter frame is designed to increase the flexibility of the rack system. It makes it possible to use the rack in two different configurations. The 2-pass configuration is that the water runs through all the pipes once, before exiting the rack. The 4-pass configuration is made such that the water first flows through half of the pipes, before entering the other half of the pipes, to exit the rack on the same side as it entered. The total flow of a 4-pass configuration can be cut in half, to still achieve the same water velocity in the pipes, than the 2-pass. Without the diagonal part of the frame, the 4-pass configuration would not be possible.

1.3 Goals

The main goal and intermediate goals listed below are used as guidelines for making sure the thesis is heading in the right direction, during the process.

1.3.1 Main goal

The main goal for this master thesis is defined accordingly:

Find and compare the pressure drop of coolant fluid through the Sperre Rack Cooler, with the use of experimental testing and computational fluid dynamics, and evaluate the latter method.

1.3.2 Project goals

In order to achieve the main goal for this thesis, there are several intermediate goals to be fulfilled in process.

- Do experimental testing with a fully working Rack Cooler.
- Initiate and optimize the CFD simulations for comparison.
- Compute final CFD simulations to reflect real life pressure drops.
- Adjust configurations and run simulations on other rack cooler sizes.
- Organize and develop easy equations for calculating total coolant pressure drop.

1.3.3 Sperres goal

Sperres goal for collaborating to this master thesis is to get more information of the pressure drop for the coolant circuit of the heat exchanger, to use in internal research and development, as well as in contact with future customers. By having specific numbers of pressure drop, the system requirements are better defined, and the potential advantages



becomes clearer. Methods of determining the pressure drop, for future rack-design, is also one of their goals.

1.4 Limitations

The limitations for this thesis are listed below, and are areas or topics not covered in this report. Some of them are limitations due to lack of time, others because the results created would be of no interest for Sperre.

- The sea water flow conditions.
- Heat transfer from the sea water, and its effect on the coolant fluid temperature, like change in transition region from laminar to turbulent¹⁰.
- All rack sizes not specified in Table 1.
- Larger flows than Sperre specified as the optimal flow spectrum. (0,5-1,5 m/s)
- Connecting pipes to, from and between the racks. This is because these are standard components, not manufactured by Sperre.

Limitations specifically regarding the simulations in SolidWorks Flow Simulation:

- Mesh optimizing of other rack sized than 700-1000S.
- Various setting of fluid turbulence.
- Start-up and stopping conditions, assuming steady state conditions.

2. Methods

The methods used to achieve the main goal are presented in the chapter.

2.1 Experimental testing – system setup

The physical lab testing of the Rack Cooler, is done at Sperre Coolers own test laboratory. This laboratory is mostly used for research and development of products, and is therefore built up with two separate circuits for water circulation. During normal testing, one circuit is used for the sea water side of the heat exchanger (cooling side), with a large tank for storing of seawater to circulate. The fresh water circuits' main component is the heater. With this heater, the technicians can to heat up water to the desired temperature, in order to test the heat transfer between the fluids. In these tests the need for accurate measurements, especially the temperature and flow is essential.

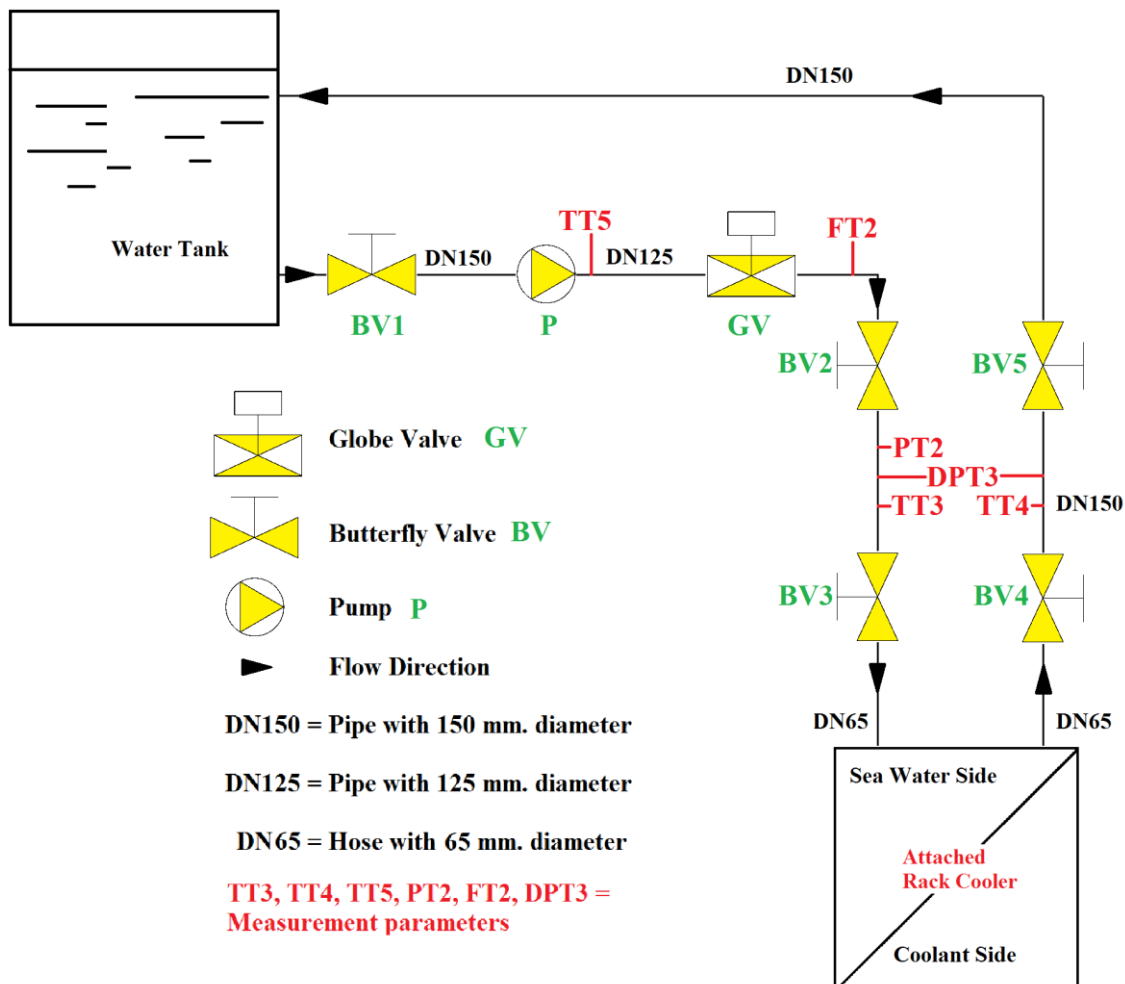


Figure 8: Flow chart with explanations of the experimental testing system.

Table 2: The list of measurement parameters.

Abbreviation	Explanation of parameter
TT3	Inlet temperature of the water [°C]
TT4	Outlet temperature of the water [°C]
TT5	Temperature of water in tank [°C]
PT2	Pressure sensor inlet [Bar]
DPT3	Pressure difference sensor [Bar]
FT2	Flow meter [m ³ /h]

The testing for this thesis focused on the pressure drop through the Rack Cooler, with no regard to the cooling effects or anything else from the designated sea water circuit. The pumps running the system are pumps of a smaller size and capacity than the normal operating conditions Rack Cooler would have. This is mainly because the laboratory is mainly used for smaller models and other types of heat exchangers, with a lower requirement of fluid flow. To be able to get as much flow as possible from the equipment installed, a decision was made to use the sea water circuit. The pump running this system is larger than the heated side system, and the storage tank are also of a much larger capacity. The downside of using this circuit is the ability to set a constant temperature the fluid falls out, but for testing purposes, the increased range of flow are more important. In order to use this circuit the sea water tank needed to be emptied and rinsed, before filling it with fresh water.

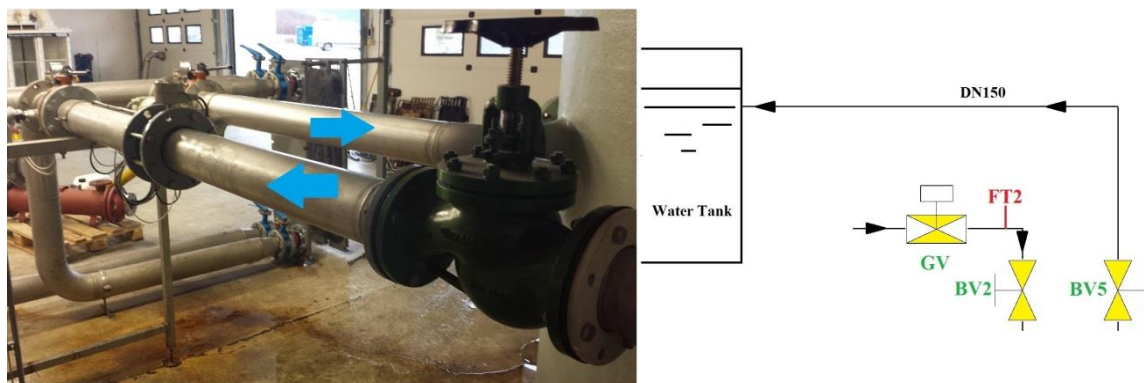


Figure 9: Picture of the piping from the globe valve, and the return to the tank. Blue arrows shows flow direction, and the flow chart to the right represent the same area.

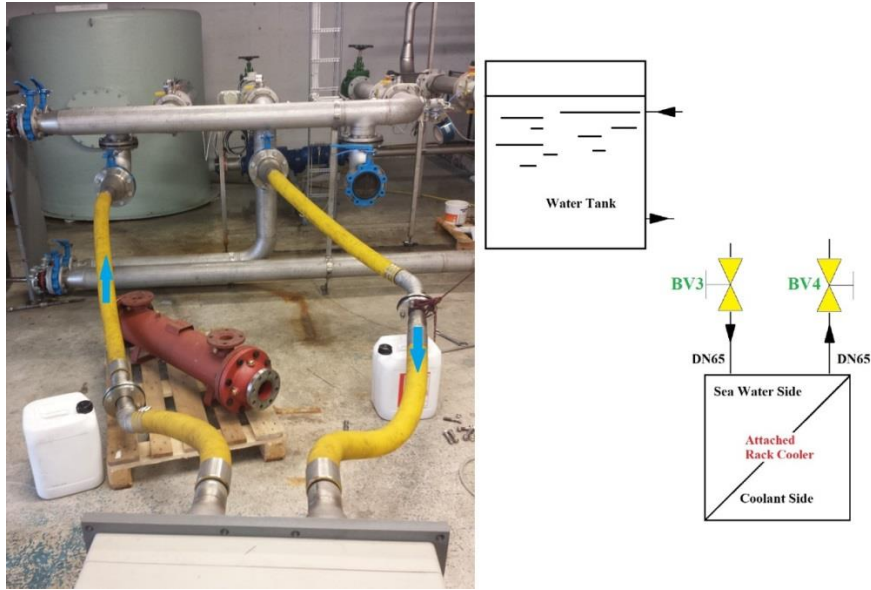


Figure 10: A picture of the entire system, with the connecting hoses in focus and the water tank in the background. The blue arrows are the flow directions, and to the right is the most visual components represented in a flow chart.

The outlet from the storage tank is placed at the bottom side of the tank, and the return inlet is positioned higher up. As the picture shows, there is one butterfly valve before the pump, and a globe valve almost directly afterwards.

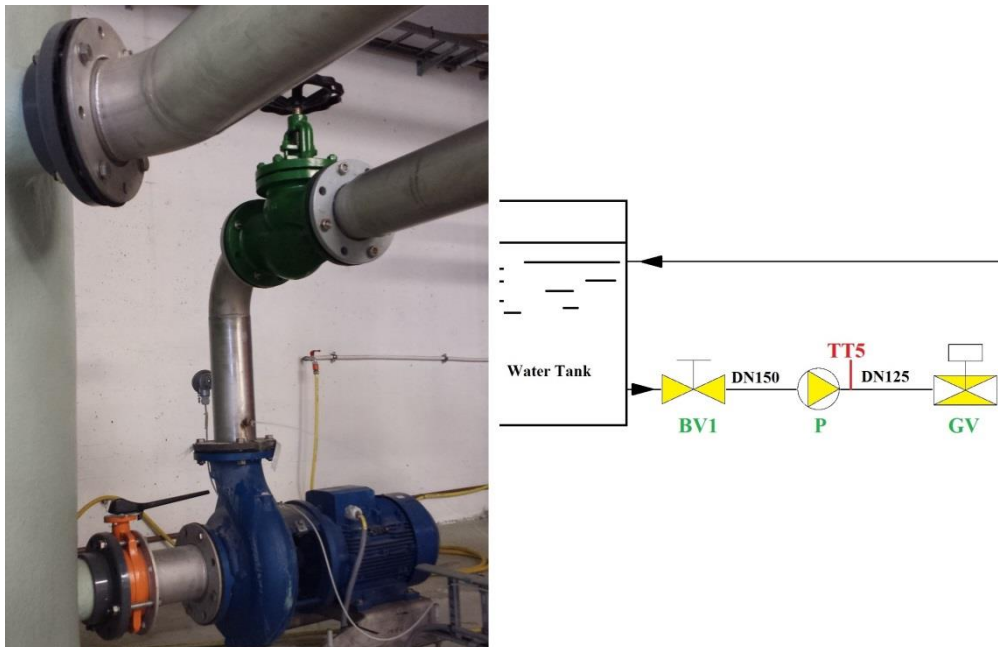


Figure 11: The area of the inlet and outlet of the water tank, with the blue pump and the green globe valve shown. The same area represented in the flow chart to the right.

This globe valve was our only method of regulating the water flow. The pump is a single-stage horizontal centrifugal electro pump (see pump sheet at Appendix II), with a 125 mm

diameter discharge outlet, and 150 mm diameter inlet. The 11 kW, three-phase motor is capable of 1470 rpm with 400 volt, 50 Hz input.

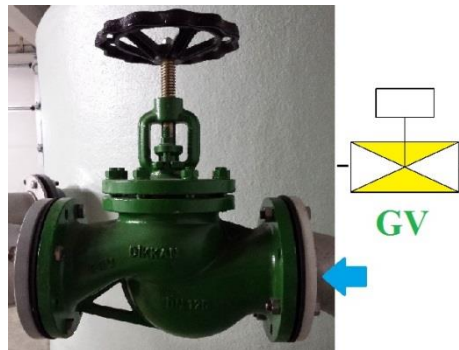


Figure 12: A close up picture of the globe valve, with flow direction arrow in blue and its symbol in the flow chart.

From the 125 mm outlet of the pump, the diameter changes to 150 mm after the valve. All the pressure equipment used to log the readings for this test is taken from this diameter pipe. The flow meter is then placed, as shown in the picture below (Figure 13). This is an electromagnetic flow meter, connected to a live reading display, as well as to the central data logging unit.

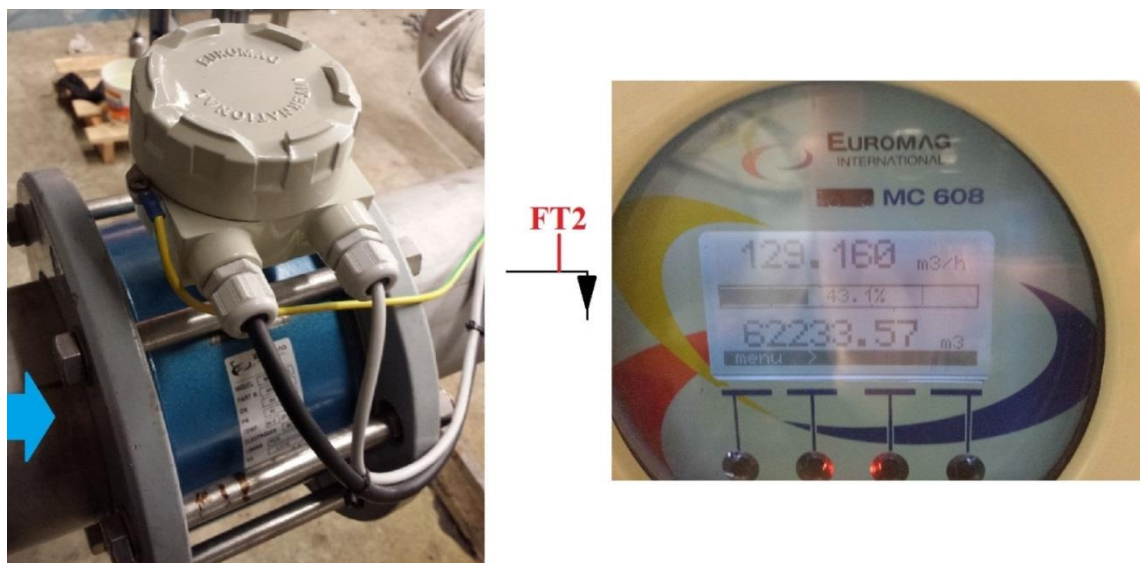


Figure 13: To the left is the flow meter with a blue arrow showing the direction of flow. In the middle is the symbol from the flow chart. To the right is the manual reading window that makes it possible to adjust the flow, without taking a log.



Figure 14: A close up picture of the area where the pressure sensors are fitted, as well as the temperature sensor. The blue arrow represents the flow direction, and to the right are the symbols used in the flow chart.

The two previous pictures show all the different components in the approximate area of where results are extracted. There are two bleeding valves for letting out the pressure after a test, at top and bottom, an analogue temperature gauge, two analogue pressure gauges and a standard butterfly valve. The small blue tube is to pressure transmitter that logs and are used for test results.



Figure 15: The two, small, blue tubes are used for pressure difference readings, and are presented in the flow chart to the right. The blue arrows show the flow direction.



-DPT3-

Figure 16: The pressure transmitter where the two blue tubes from Figure 15 are connected. This is a spare unit. The symbol from the flow chart is to the right.

After this section the flow continues through the last valve before entering the flexible rubber tubing, which is connected to the Rack Cooler. This tubing has an inner diameter of 65 mm, which restricts the flow significantly. In order to have a flexible way of connecting the Rack Cooler, these were the best option of the tubing accessible during testing. In one end of these tubes, there was mounted a normal flange, and in the other end there is a con reducer from 150 mm to 65 mm diameter. The normal mounting flanges are mounted to each other, in order to lengthen the tube sufficiently and to get the correct flange size connected to the Rack Cooler.

With this set up, we were limited to one inlet, and one outlet of the flow. In order to test as many different connections and flow configurations as possible, some changes were done to the rack in certain tests, explained in chapter 2.2.

The return line of the flow is mainly identical to the feeding line, but with the absence of the flow meter, the globe valve and the pump.

2.2 Test setup and configurations

The experimental tests performed at Sperre were done on a “Ready to install”-component. The tests were done on the same rack, for the different configurations, with two of them modified, in a total of five series. Every series of loggings were conducted in the same matter.

The logging system used was set up to take log 59 loggings with an interval of one second between each. These were then exported to Excel, with the original title label on top. The number of different sensors used to log with was thirteen, but many of these are later sorted out from the result, in order to only include relevant results. These are all the

loggings from the part of the system not included in the test. The hour, minute and second of the testing were also logged, in the first three columns, but the internal clock of the instrument were not correct. A picture of the original output file is shown in Appendix III, where all the parameters are displayed.

TT3	TT4	TT5	PT2	DPT3	FT2
-----	-----	-----	-----	------	-----

Figure 17: After removal of the parameters not logged properly, with only relevant information left.

The first logging was with the globe valve entirely open, and with the pump running for a period of time, before initiated. This is to ensure that all air had left the system, and that the flow and system had stabilized. For all configurations the maximum flow achieved was in the range 130 to 140 m³/h. For the second logging the valve was adjusted to achieve as close to 130 m³/h of flow, according to the reading. After every logging, the series was briefly checked to see the average flow and the variation of the loggings. If the average was objectively far away from what aimed for, the valve was adjusted and a new logging started. If the variation in flow was obvious throughout the logging, a new logging was also initiated, in order to ensure steady state condition. By further adjusting the valve, loggings were done in the same matter with a 10 m³/h interval. Between the flow of 10 and 20, a series were logged at 15 m³/h.

2.2.1 No rack



Figure 18: The connecting hoses, connected to each other to create a closed circuit of flow, to measure the systems internal pressure drop.

This test is done to have a basis for the internal pressure drop of the system, without the rack connected. These results include the effects of every component in the system, which is identical to the other tests.

In order to get as similar flow conditions in the yellow connecting hoses, some support was used to make sure there was no sharp bends along its path. The two con reducers at the end of each hose, which is normally connected to the rack, were bolted together.

With a flow coming from a small cross section area, to a large one, and back into another small cross section area, the flow characteristics will not be identical as when connected to the rack, but it will still induce a pressure drop as it would in gradual contraction or expansion.

2.2.2 2-pass half rack

The 2-pass half rack test is done to find the pressure loss in the pipes with the highest possible water velocity. With only two connecting hoses, the best way to find this is by running water through only half of the pipes. This is easily done because of the diagonal



Figure 19: The two con reducers attached to each other.

fluid splitter on one side of the rack. This is possible because the flow cross section area is roughly half of what it would be in a normal 2-pass configuration, and therefore doubling the velocity. The inlet to the rack is set on one side of the splitter, which limits the water to that half of the pipes. For the outlet of the pipes there is no such splitter, so when the system is pressurized, the other half of the pipes will also be filled with water, but it will not flow through them in steady state.



Figure 20: The yellow connecting hoses connected to the rack in a 2-pass half rack configuration. The blue arrows represent the flow directions in the hoses. To the right is the situation represented in flow chart symbols.

The positioning of the rack, on the flow, was done with a fork lift, before connecting the hoses. Even though the position is now optimized according to the length of the hoses, we made sure there were no sharp bends in them. The rack was placed in a lying position, in order to safely transport it, and for easy mounting of hoses and lids.

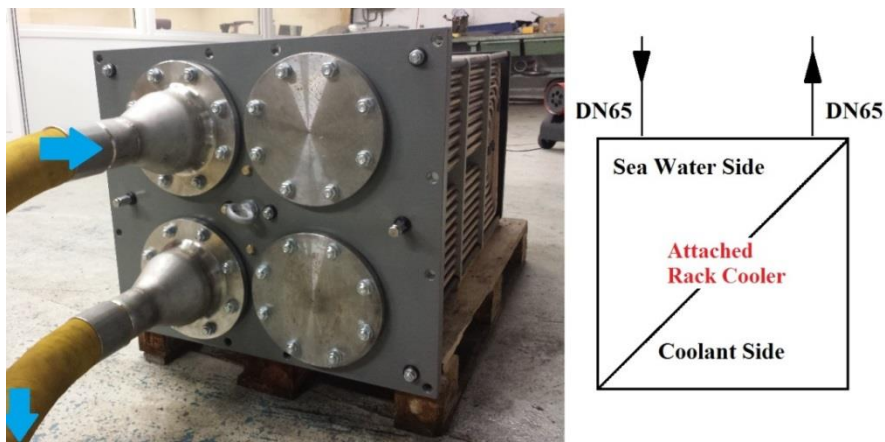


Figure 21: A close up picture of the two hoses connected to the rack, and with the blind flanges installed to water tight the rack. The blue arrows represent flow directions in the hoses, and to the right is the chart symbol of the rack.

This test was done mainly to see the effects of water velocity through the pipe, and is not a configuration the actual product ever would use. It would then have two inlets and two outlets.

2.2.3 2-pass full rack

This test is similar to the 2-pass half rack in the way that the fluid only runs through one set of pipes. The difference here is that the flow in the pipes has half the velocity of the

previous one. This is because the rack is modified with one extra flow splitter frame, inserted the opposite way, which cancels its effect. This test could also been done by manually cutting of the diagonal part of the flow frame, in order to make the fluid accessible to all the pipe, but this includes destructing a flow frame, and due to cost and simplicity we decided to add another frame instead.



Figure 22: The original frame still mounted on the top part which is lifted off, and an extra flow frame is inserted in between.



Figure 23: When looking through two of the holes in the top, we can clearly see that the diagonal splitter in the frame, no longer will restrict the water from filling the total area.

This configuration is the closest to a full 2-pass configuration possible to test.

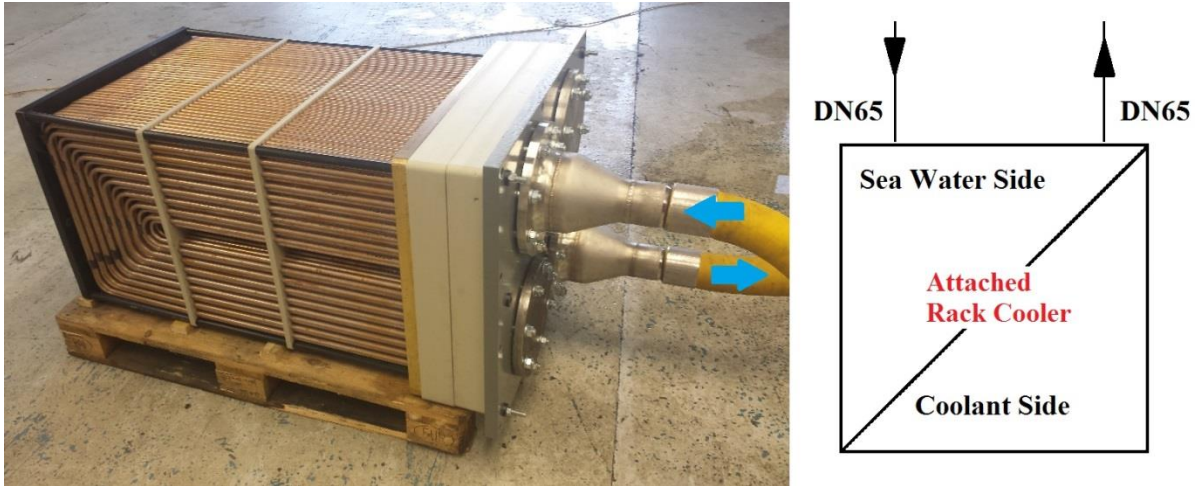


Figure 24: The rack with the extra flow splitter frame installed, and with the hoses connected. The blue arrows represent flow directions in the hoses, and to the right is the picture represented in its flow chart symbol.

2.2.4 4-pass rack

The 4-pass rack configuration is a configuration in which the equipment has a possibility to run during normal operations. This can be used to get the highest water velocity combined with the most passing through the pipes, where the cooling effect appears.



Figure 25: The yellow connecting hoses installed to the rack in a 4-pass configuration. The blue valves are visible at the other end of the hoses, and the arrows represent the flow direction. To the right is the flow chart symbol.

This way of connecting the hoses, are the reason for the diagonal fluid splitter is in place. This enables the fluid to run through only half of the pipes and at their outlet the can continue into a new set of pipes for another two passes.

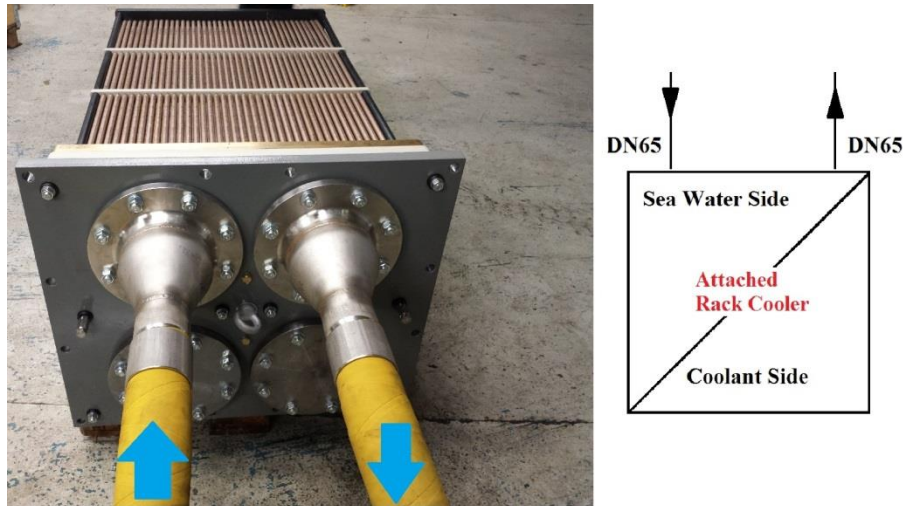


Figure 26: A close up picture of the connected hoses in the 4-pass configuration, where the inlet and outlet is on the same side of the rack. The blue arrows represent flow directions in the hoses, and to the right is the picture represented in its flow chart symbol.

2.3 Computational Fluid Dynamics (CFD)

The Computational Fluid Dynamics, call CFD's are done in the software programme called SolidWorks. The Flow Simulation package is an extended addition to the CAD (Computer-Aided Design) tool of SolidWorks. The method is a form of Finite Element Method (FEM), but with a larger focus on the fluid mechanics, than only the solid mechanics in which FEM is mostly associated with. The two methods are built the same way, with the regard to computational domain, mesh and the actual calculation process, described in 2.3.2, 2.3.3 and 2.3.4.

“Designed by engineers for engineers, Flow Simulation is widely used in many industries and for various applications, where design optimization and performance analysis are extremely important, such as valves and regulators, hydraulic and pneumatic components, heat exchangers, automotive parts, electronics and many others.”

Quote from the SolidWorks help guide. ¹¹

2.3.1 Overview of capabilities

The physical capabilities of the program far exceed the areas of interests in this thesis, but it gives us an indication of the complexity and power of the system. The range of fluid flow and heat transfer phenomena includes ¹²:

- External and internal fluid flows
- Steady-state and time-dependant fluid flows

- Compressible gas and incompressible fluid flows
- Subsonic, transonic, and supersonic gas flows
- Free, forced, and mixed convection
- Fluid flows with boundary layers, including wall roughness effects
- Laminar and turbulent fluid flows
- Multi-species fluids and multi-component solids
- Fluid flows in models with moving/rotating surfaces and/or parts
- Heat conduction in fluid, solid and porous media, with/without conjugate heat transfer and/or contact heat resistance between solids and/or radiation heat transfer between opaque solids (some solids can be considered transparent for radiation), and/or volume (or surface) heat sources.
- Various types of thermal conductivity in solid medium, i.e. isotropic, unidirectional, biaxial/axisymmetrical, and orthotropic
- Fluid flows and heat transfer in porous media
- Flows of non-Newtonian liquids
- Flows of compressible liquids
- Real gases
- Cavitation in incompressible water flows
- Equilibrium volume condensation of water from steam and its influence on fluid flow and heat transfer
- Relative humidity in gases and mixtures of gases
- Two-phase (fluid/particle) flows
- Periodic boundary conditions

The phenomena investigated and used for this cause is:

- Internal fluid flows
- Steady state fluid flows
- No gas flow
- No convection or conduction
- Fluid flows with boundary layers and wall roughness
- Laminar and turbulent fluid flows
- No heat source



What this sums up to is the type of CFD we are interested in, for the purpose of pressure drop and fluid flow patterns. By eliminating as many of the topics as possible, the program will have a lesser amount of data to process, which in turn speeds up the simulation and/or gives us the possibilities of running a more accurate simulation in the wanted topic.

2.3.2 Computational domain:

The computational domain is an automated generated rectangular box, which encloses the solid body in which the simulations are performed. This computational domain can also be adjusted, either manually or automatically if the size or shape of the component is modified. In external analysis the computational domain plays an important role to see the flow characteristics in the aftermath of the solid, but in internal analysis the main concern is to have the inlets and outlets of the flow on the perimeter of the computational domain. The box must also enclose the entire model where the simulation is to be done.

2.3.3 Mesh

The computational mesh is automatically generated inside the computational domain, and is defined on the basis of the total size of it, and the selected level for the mesh refinement. This automated mesh creates cells with identical size, put in layers of the Cartesian axis system. The mesh dictates the accuracy of the simulation and at what point. The cells are of a cubic shape, and have eight corners, which are called nodes, that are shared with up to six other cells. Other programs creates mesh with other sizes, like a mix of hexahedral and tetrahedral shapes¹³, which is a more flexible way of meshing. In the corners the program tries to find an answer for what we are looking for (density, direction of flow etc.). Simplified, this means that with a finer mesh (each cell has a smaller size), the more cells, the more accuracy you gain, but it also demands more processing power and memory. Since the mesh is generated on the basis of the computational domain, it does not take into consideration what areas are solid, and what areas are fluids.

2.3.4 The calculations

For each of the possible topics there are a number of equations the program tries to solve for each individual cell. In the corners of the cell the program tries to find a value for every parameter. It starts out by guessing a value which is either pre-specified, or most often automatically selected as the initial condition. In the area where the conditions changes first, the inlet(s) of these simulation, the values tend to “jump” to a much higher

level than expected, before the conditions starts to stabilize. As an effect of the change at the inlet(s) and/or outlet(s) starts to spread around the model, the value start to even out, in regard to changes. This is because the equations used for solving the parameters in each point, detects less differences. It constantly tries uses many different equation to find the desired value, and when comparing the values, it changes. The hidden algorithms in the program control this entire process and between each corner/node the program interpolates the values.

2.4 Simulation model

The model used for simulation differs from the original model in one main area. The original files are used for a basis of making production drawings, which means they include clearance in holes. In order to run a successful simulation, the model needs to be completely (water)-tight, so this clearance cannot be included. In our model the only area where this is relevant is in the plate where the pipes are fastened. These are manufactured, and therefor drawn 0,1 mm larger than the outer diameter of the pipe inside it. This is because the pipes are fastened by expanding the end of the pipe, enough to be tightly fastened in the plate.

2.4.1 File conversion

The models of the Rack Cooler used for the simulations are mainly provided by Sperre themselves. Internally in Sperre they use another 3D-modelling program called Autodesk Inventor, but by converting their files till .STP-files they could be opened in SolidWorks, and saved as SolidWorks-files. During this conversion process, some of the information in the files is lost:

- The relationship between different parts in an assembly is lost, the “mates”. When opening the assembly every part is in the correct place, but they are locked in that position. This can be solved quickly by “fixing” the assembly and all its parts in its current placement. This works well to the point when something needs to be edited in the assembly.
- The way the parts are built up.

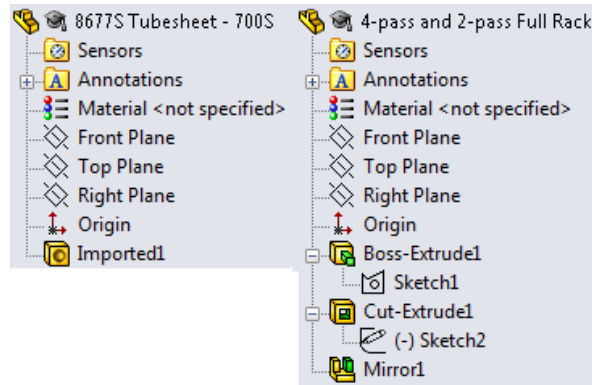


Figure 27: To the left a model converted from STP, and to the right a similar file created in SW

When this is lost, the different features of the part are not displayed. The part will look exactly the same, but when doing measurements on different features the program does not “lock” to the future, only the surface or edge of the part. Generally this is not a problem, as long as the user is aware of how it works. When editing a part, you cannot edit the way the part is built up, only do modifications to the existing part. This is obvious when lengthening a pipe. When building the pipe from scratch in SolidWorks, the way to extend it is to put a different value for the length of the sketch defining the path of the pipe. For editing an imported file, the way to do it is to make a new feature on the part.

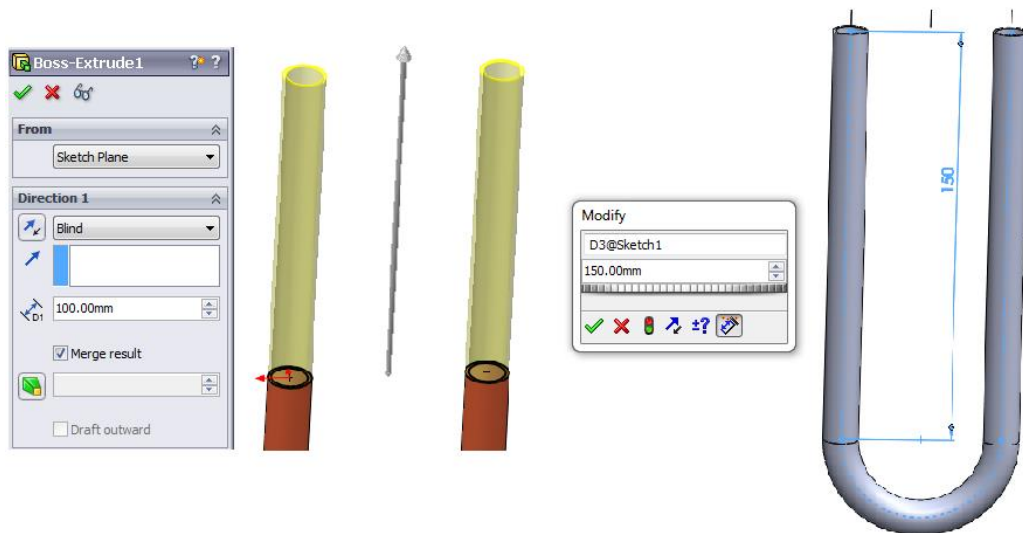


Figure 28: To the left it is shown that you have to make a new feature to build on the existing part to make it long. To the right it is shown that you can edit a value in the original sketch to edit it.

Because of the clearance in the holes for the pipes, and the file conversion differences, the fastest way of building up the part where the pipes are mounted, is from scratch, instead of modifying the original part. This is the only part of the model which is built up from

scratch, and not connected to a file from Sperre. The part was built with the help of internal documents describing the part¹⁴, in addition to the part not used.

Another area in which needed modifications from the original file, is the inlet and outlet of each pipe. After installing them to the plate which holds them, the tip that sticks out is grounded down, and a small chamfer is made in the opening, as shown in Figure 29. This feature is not included in the files, so this was added.



Figure 29: Close up picture of the pipes fastened to the plate holding them.

This feature was added in SolidWorks as shown below (Figure 30).

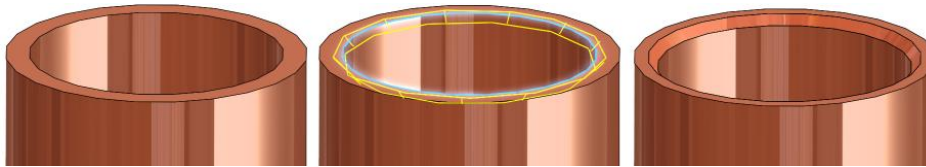


Figure 30: Picture of the original pipe to the left, which is modified with a chamfer in the middle and the finished pipe to the right.

2.4.2 Model simplification

The more unnecessary information there is in a simulation, the more computer power is wasted. By reducing the complexity of the model as much as possible, there is less of this unnecessary information in the model file, and the focus simulation runs easier.

“Less is more”

Andrea del Sarto, 1855, by Robert Browning

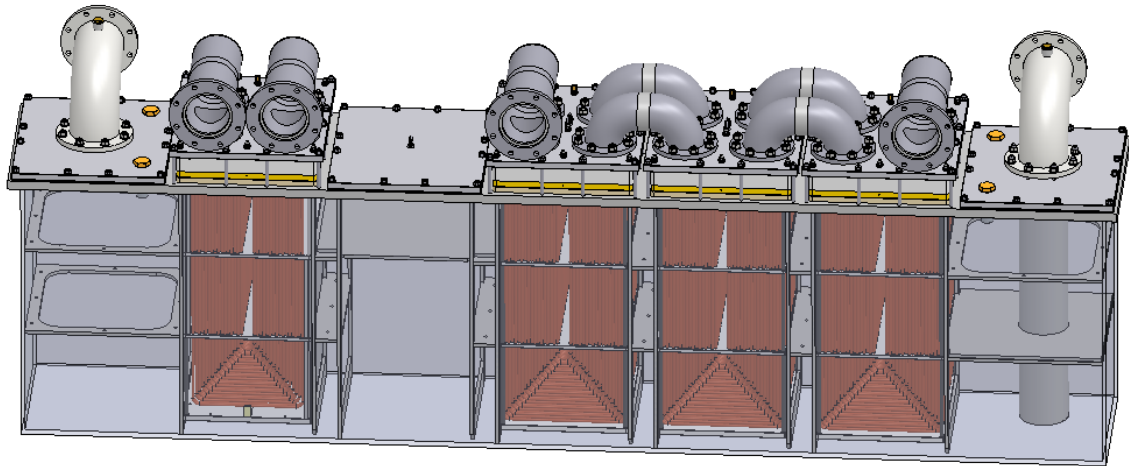


Figure 31: A SolidWorks picture of an assembly of a rack system containing in total four racks, with inlet and outlet piping fitted. The case it is mounted in is transparent.

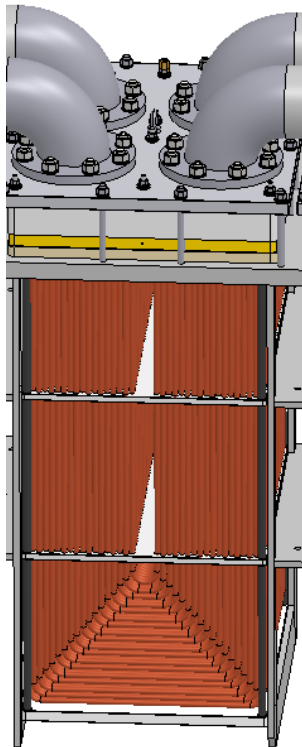


Figure 32: One entire rack, with all its connections.

By starting with the complete assembly of every part in the system, we quickly realize the large potential for simplification. To do a complete simulation of the entire system would create the least amount of post-processing of the results, but the amount of data generated and calculated, would require an out of proportion amount of computer hardware for the purpose. The super computers of today may be sufficient, but the price and access of these makes it unrealistic, in the sense of this thesis.

By focusing on one single rack in the system we have eliminated the calculations of multiple identical parts, in series. What happens in a single rack is the same as the next one, and

the one after that. Also, the number of racks in series is not constant. It depends on the system configuration, which is designed for the customer with based on the space available and the cooling needs. By taking away the box the rack is mounted in, the area for calculation is also automatically reduced.

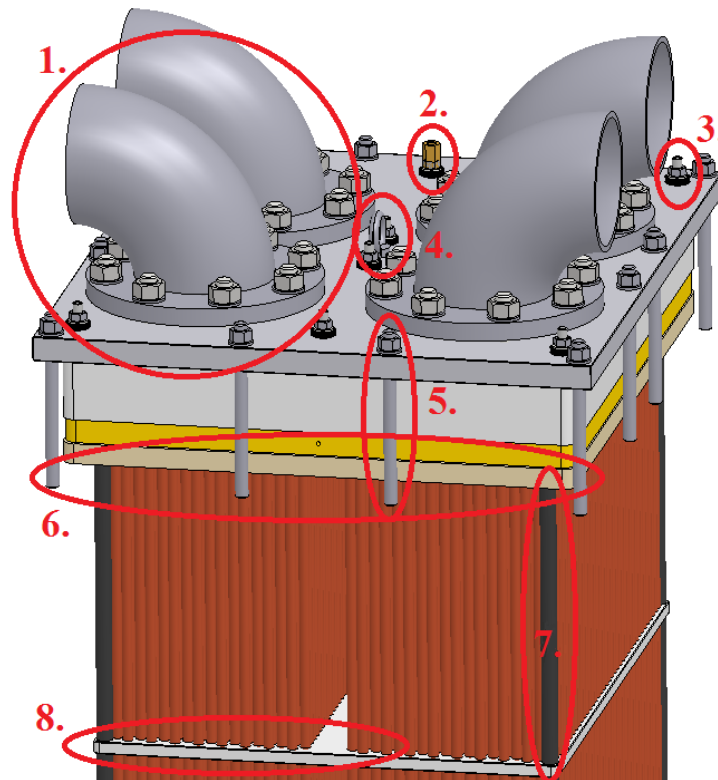


Figure 33: Picture of numbered parts not relevant for simulations.

1. The inlet- and outlet-pipes of the rack is not included, because this area has a well-known pressure drop. The flange and the bolts are also excluded.
2. Ventilation nut for bleeding the system is excluded, because there is no need for ventilation in the simulation.
3. Bolts to hold the top plate (where the inlets are mounted) to the flow frame and the flow plate where the pipes are mounted. These are not necessary because their relation to each other can be locked in the programme.
4. Lifting hook for installation and removal of the rack.
5. Bolt to hold the rack to the frame it is mounted in.
6. Gasket for sealing the rack, so no sea water can escape when flowing around the pipes.
7. Bolts for stabilizing the rack, and the flow plates further down.
8. Flow plate to hold the pipes in place during operations, as well as divide the sea water flow in sections.

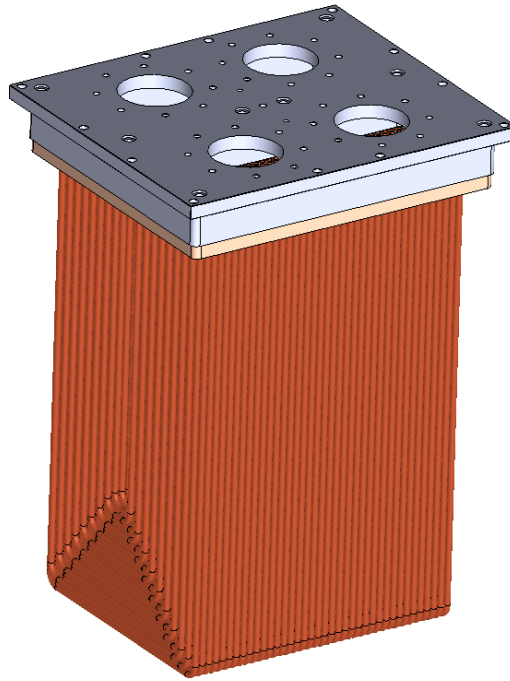


Figure 34: The rack cleared for every part not affecting the flow and pressure drop through it.

After clearing those parts, the rack is as cleared as it can be, without editing the components. Some of the features of the rack can still be optimized in order to further simplify the internal flow analysis. If a simulation of sea water flow, outside the pipes was to be done, this would be as simplified as it could be. The walls of the pipes are the correct 1 mm. thickness and the distance between them is also realistic. These features can use more computer power than necessary, so some further simplifications are done.

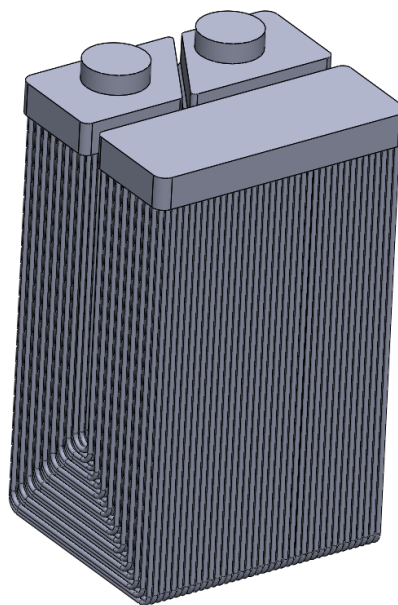


Figure 35: The “Fluid body assembly”, made from where the fluid will be in the model.

In the “Check geometry” function of Flow Simulation, the option of “create fluid body assembly”, creates a part identical to the where the fluid/water exists. This function is used to check for “leakages” in the model, but also to display what areas are filled with fluid. By comparison it is like filling the rack with water, freezing it, and then removing the solid components to reveal the space the fluid occupies. This part is then used with the function of “cavity”, to create a “negative” of the fluid body. A part is created around the entire fluid body, in order to extract the fluid body. The areas of wall thickness and clearance will not be problem, because everything is one solid containing everything but the fluid. This part’s exterior is then only a cube, with inlet/outlet hole(s), so in order to see the inside better some different viewing options are used.



Figure 36: View orientation, front.

This is viewing the part from the front. The picture below (Figure 37) to the left is how the exterior looks, where nothing is visible. The picture in the middle is a section view through the middle of the rack, and we can clearly see the path of the water, which represent the pipes. The picture to the right is a wireframe view, where every set of the pipes is visible.

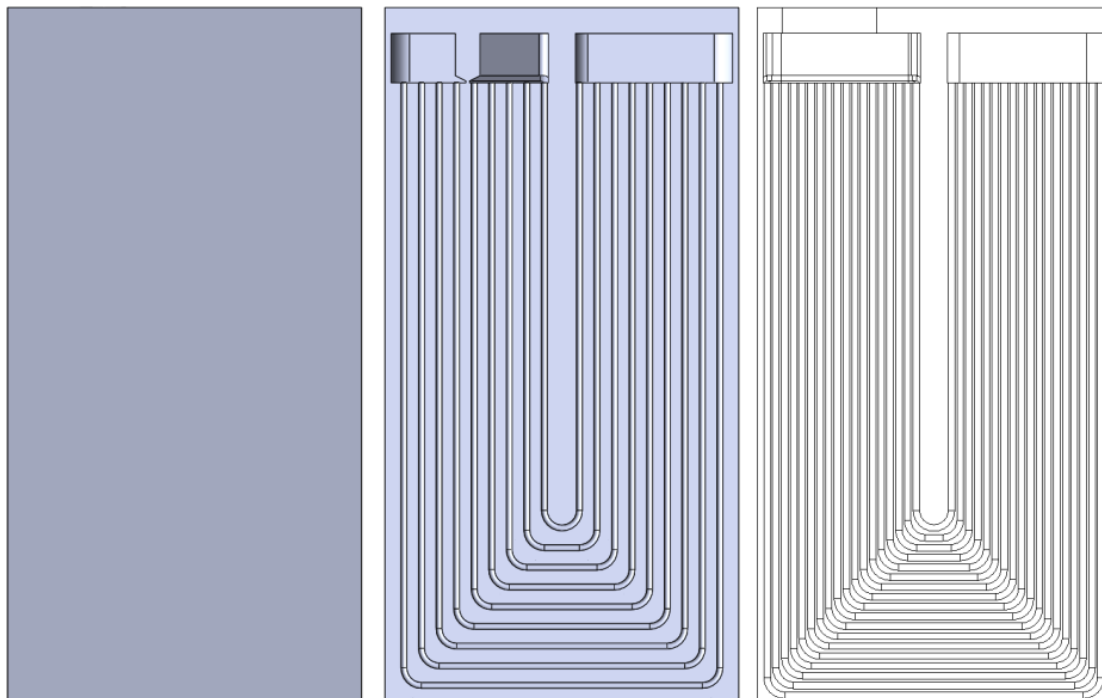


Figure 37: The rack model viewed from the front, in three different display styles.



Figure 38: View orientation, from the left.

This picture is when viewing the rack from the side. The picture below (Figure 39) to the left is again the exterior, where nothing is visible. The middle picture is a section view where the horizontal part of the pipes is visible, in relation to the height of the rack. The picture to the right is wireframe, where this is also visible.

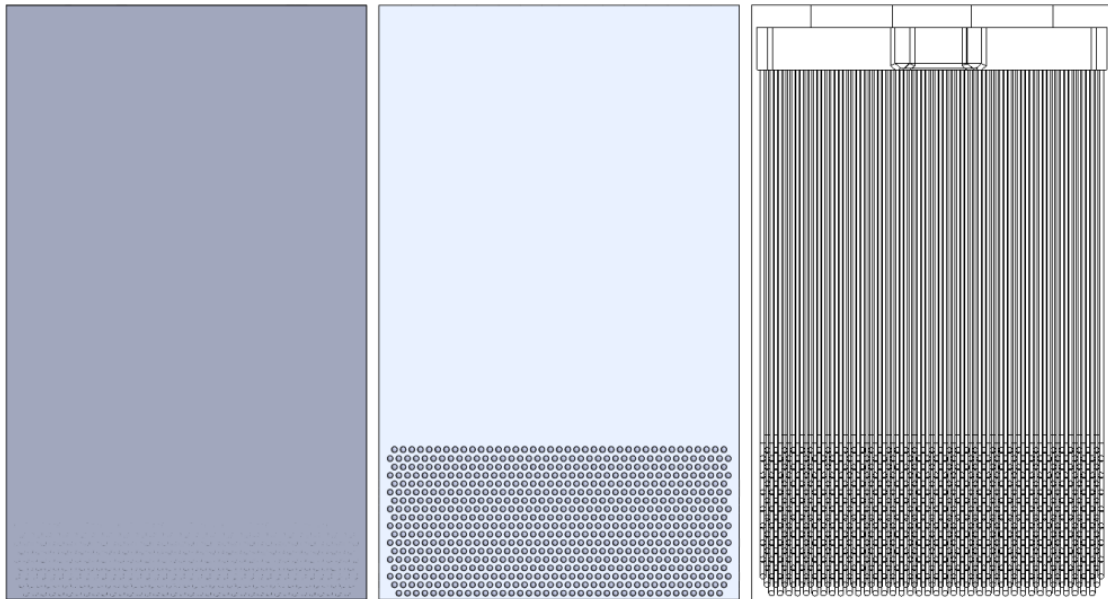


Figure 39: The rack model viewed from the side, in three different display styles.



Figure 40: View orientation, birds view.

When viewing the rack from the top, the inlet(s) and outlet(s) are the only thing shown. In the picture below (Figure 41), the red lines represent at what height of the rack the section view on the right side is taken from. The picture of the upper red line, the diagonal flow splitter is represented clearly. The middle red line's picture shows all the different pipes in its vertical path. The bottom picture is cut through one of the pipes in its horizontal path.

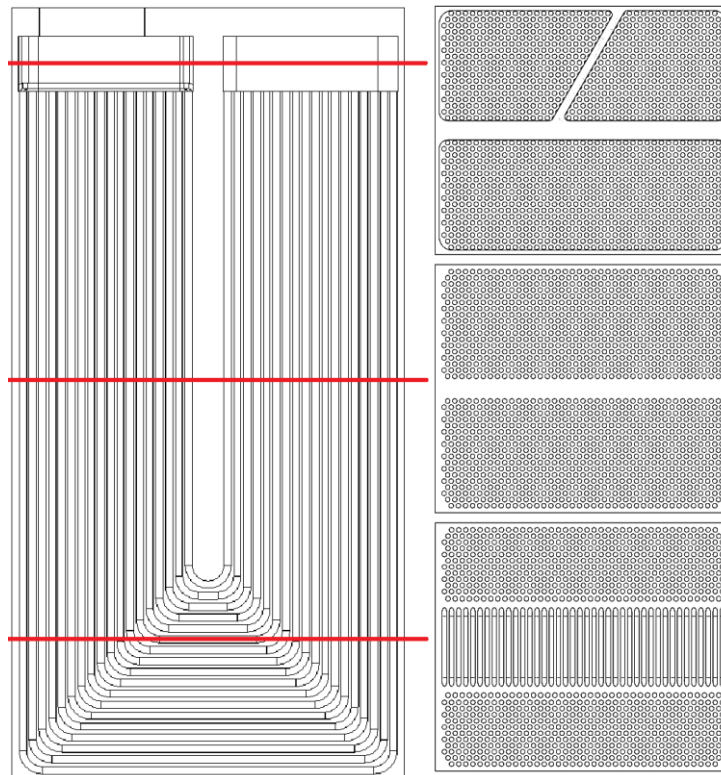


Figure 41: To the left is a wireframe view of the rack, and the red lines represent different heights of where the three other cut view are done.

2.5 Mesh optimization

In order to get the best and most realistic results of the simulations, the mesh plays an important role. The mesh has to be fine enough to reflect the actions and behaviour of the selected feature, but still not too fine for the simulations to be computed. This limit is set by the hardware of the computer used for the simulation. In a pipe simulation where the goal was to find the pressure waves, a large mesh and cell sizes had been used, and proven sufficient¹⁵, but the simulations to be done here, has a larger degree of intricacy, so the cell size plays an more important role.

To find the optimal mesh for the purpose of this project, mesh generations and simulation were done, to see both how the mesh developed with different settings, but also to see how the results, when it comes to pressure drop developed in the model. When obtaining un-logical result, investigations were initiated by the use of different simulation visualization methods, in order to better understand what difficulties the program met. The time each mesh generation demanded, as well the actual calculation process demanded was also an important parameter in what was possibly to do, with the time available. Some meshing configurations was run as a full simulation, some as just the

mesh, and others was aborted when realizing the mesh was either too optimistic (time wise) or too coarse to give realistic results. When obtaining the mesh in which the parameters were optimized, and still within the limits of calculation time available, this mesh was kept constant through most of the different simulation setups. In other words, the mesh settings are not interpreted as a part of the simulation settings, even though it plays an important role.

Table 3: A list of simulations and their mesh done in the process of finding an optimized mesh. DNF is an abbreviation for “Did Not Finish”.

Project name	Model	Cells	Simulation time [hh:mm:ss]
Meshing 100 Test	4-pass Rack	4 049 791	21:32:19
Meshing 100 Local	4-pass Rack	5 359 533	15:37:33
2. Meshing 100 Local	4-pass Rack	8 378 409	DNF
3. Meshing 100 Local	4-pass Rack	5 981 091	12:47:19
Local Mesh 1	4-pass Local Fluid Assembly	64 080	00:20:11
Local Mesh 2	4-pass Local Fluid Assembly	233 382	00:20:19
Local Mesh 3	4-pass Local Fluid Assembly	771 281	01:18:51
Local Mesh 4	4-pass Local Fluid Assembly	763 840	01:18:56
Local Mesh 5	4-pass Local Fluid Assembly	763 840	15:27:28
Local Mesh Extension 100	4-pass Local Fluid Assembly	667 695	04:58:43
4-pass Rack Ex	4-pass Local Fluid Assembly	667 695	01:17:06
4-pass Rack Ex Redone	4-pass Local Fluid Assembly	685 755	01:18:35
4-pass Rack Ex Redone 2	4-pass Local Fluid Assembly	2 552 200	04:32:51
4-pass Fillet	Realistic 4-pass	3 486 777	05:22:44
4-pass RF	Realistic 4-pass	3 621 513	06:31:29

The final mesh was selected because of its balance between the simulation time, and the number of cells. The cells are also positioned in places where they are of good use.

2.5.1 Global mesh

The basic initial mesh is set up using the automatic settings. The “Level of initial mesh” is set to 4, on a scale from 1 to 8. Level 1 and 2 is characterized as a bad and coarse mesh, which should not be used, level 3 is generally an acceptable mesh, while level 4 and up is a finer and better mesh. Because we will specify the regions of relevance for better mesh, this initial mesh is not top priority for the flow situation. The “Optimize thin walls resolution” checkbox is checked, but “minimum gap size”, “minimum wall thickness” and “advanced narrow channel refinement” are not used.

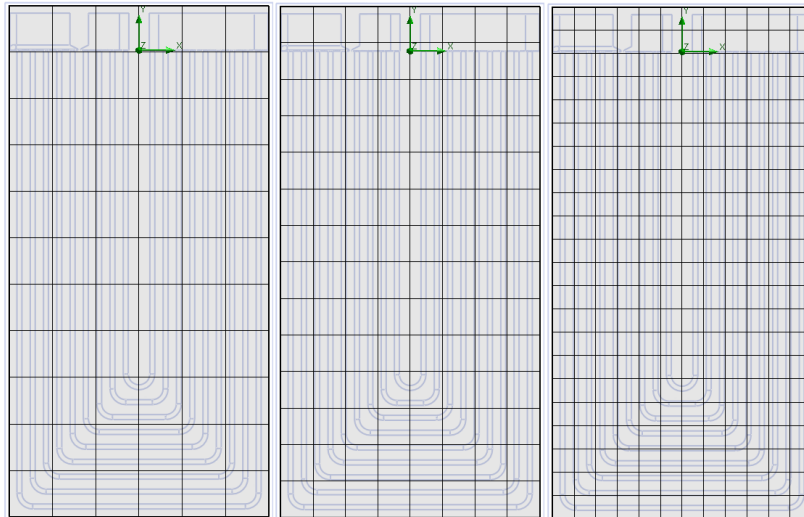


Figure 42: The global mesh grid, in three different levels, level 2, 3 and 4, from left to right.

The more refined mesh shown in Figure 42 is not the only parameter which changes when changing the level. Since the “Optimize thin walls resolution” option is selected, the areas it charges already have a finer mesh, which means these will get even more refined when increasing the level. The other parameters, if selected, will have a smaller default value, with higher global resolution level.

2.5.2 Bend mesh

Finding the pressure drop through a single pipe, has straight forward formulas and equations. This pressure drop counts for a certain amount of the total pressure drop, but the bottom part of the pipe, where there are bends that turns the pipe back upwards, contributes to a large degree of the total pressure drop. A bend in a pipe also has its correlation factors for pressure drop, so it is important that this area of the rack has a better mesh to count for the non-uniform flow.

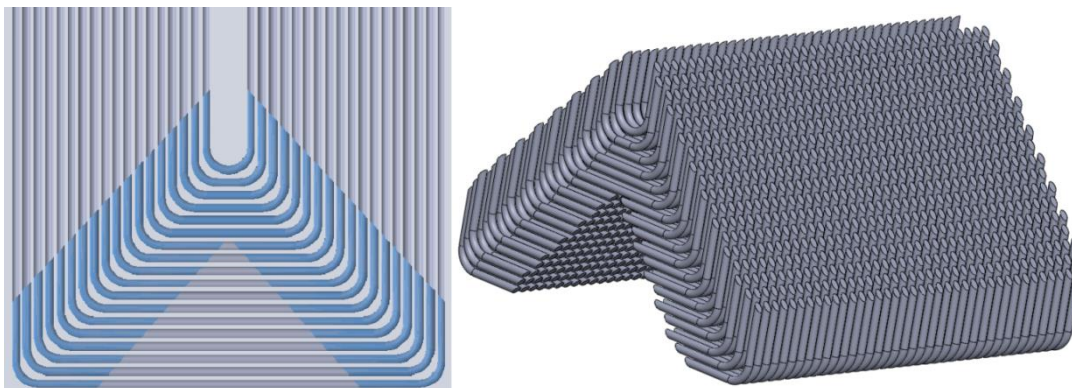


Figure 43: To the left the blue area is where the local mesh is, and to the right is a 3D view of the part inserted to create this local mesh.

In order to create this finer mesh, the fluid body was used. When basing the area for local mesh on the fluid body, the mesh is created in such a manner that it does not improve the mesh in an unnecessary area.

The settings for this mesh were adjusted throughout the process of finding a sufficient mesh. By leaving the “automatic setting” menu, the ability for specifying the mesh more directly is improved.

When leaving the automatic mesh option, three main areas of mesh optimization arrives:

- Solid/Fluid Interface:
 - Small solid feature refinement level: 4 (on a scale from 0 to 9)
 - Curvature refinement level: 3 (on a scale from 0 to 9)
 - Curvature refinement criterion: Default (0,317560429 rad)
 - Tolerance refinement level: 2 (on a scale from 0 to 9)
 - Tolerance refinement criterion: Default (0,144 m)
- Refining Cells
 - Refine all cells: Not checked
 - Refine fluid cells: 4 (on a scale from 0 to 9)
 - Refine partial cells: 3 (on a scale from 0 to 9)
 - Refine solid cells: Not checked
- Narrow Channels
 - Enable narrow channel refinement: Checked
 - Characteristic number of cells across a narrow channel: 10
 - Narrow channel refinement level: 3 (on a scale from 0 to 9)
 - Enable minimum height of narrow channels: Not Checked
 - Enable the maximum height of narrow channels: Not checked

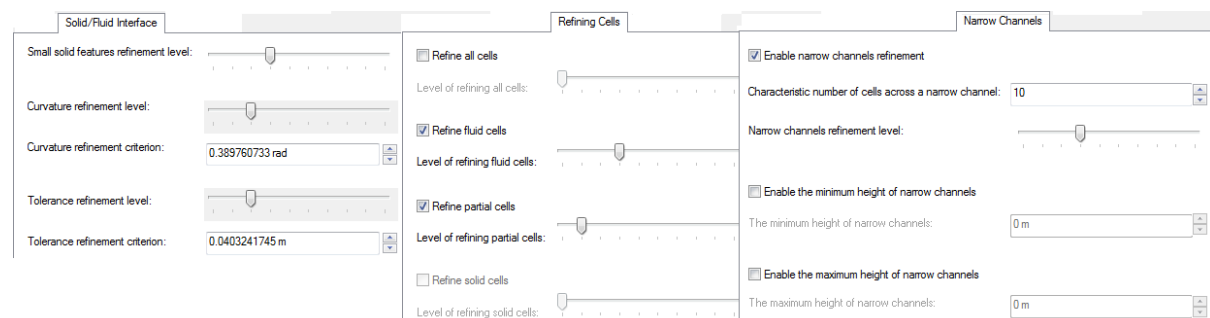


Figure 44: The selection criteria and settings of the local initial mesh, at the bend, as it is viewed.

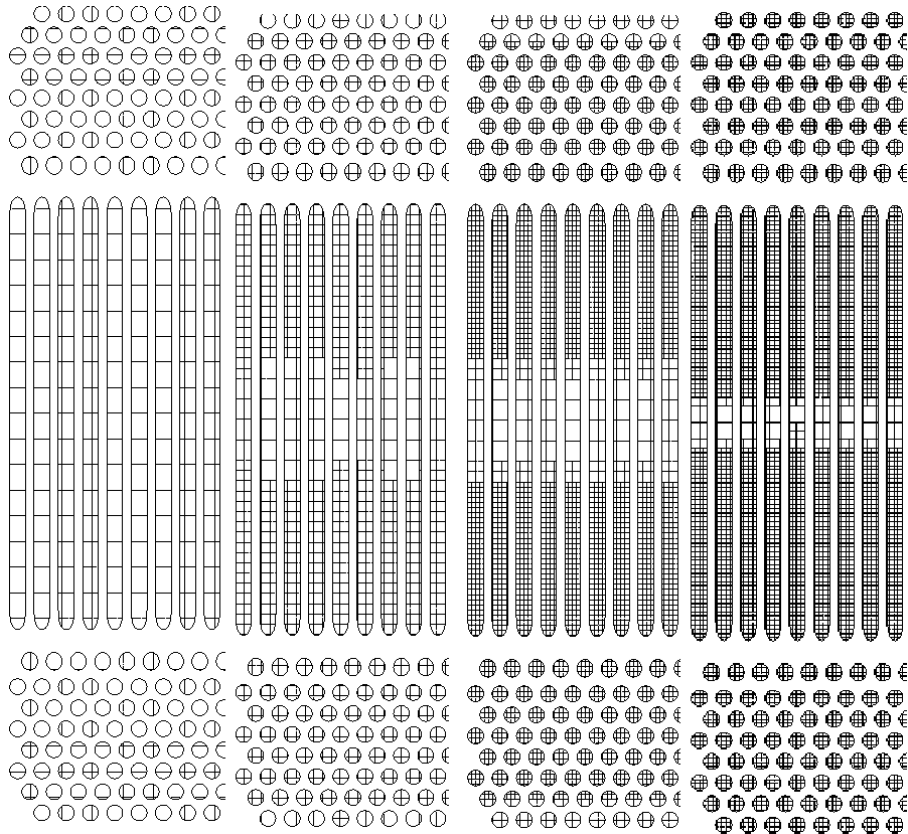


Figure 45: View of the bottom of the pipes, with one pipe cut through the middle. To the left is without a local mesh, the two in the middle this has been added, and the one to the right is the final mesh.

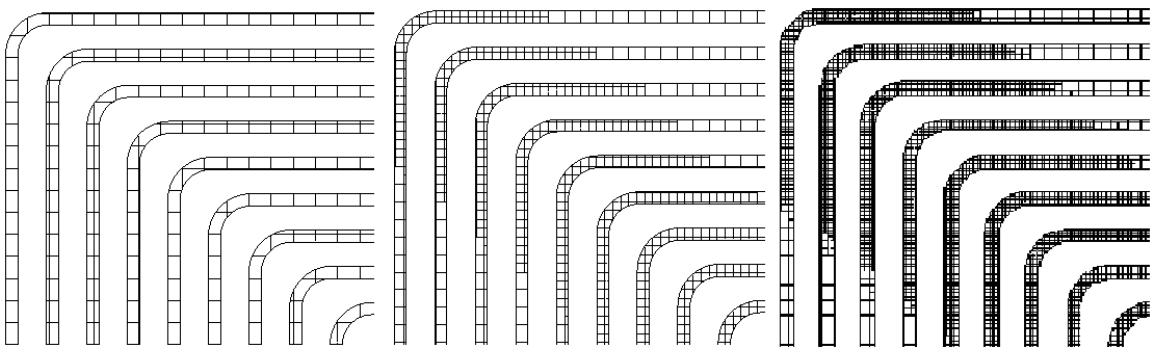


Figure 46: Visualization of the mesh in the bends. To the left is the bend without a local initial mesh, in the middle this has been added, and to the right is the final bend mesh used.

2.5.3 Inlet/outlet mesh

In the area where the pipes are mounted, on the plate, there is a more complex flow situation than in other areas. Before the water enters, or after it leaves the pipes, the water has to find its path, and this “splitting” of flow contributes to turbulence, and non-uniform flow patterns. After the water enters the pipe, it also needs some time for the flow to develop and therefore is the local mesh added into the pipes at a length of ten times the (inner) diameter of the pipe.

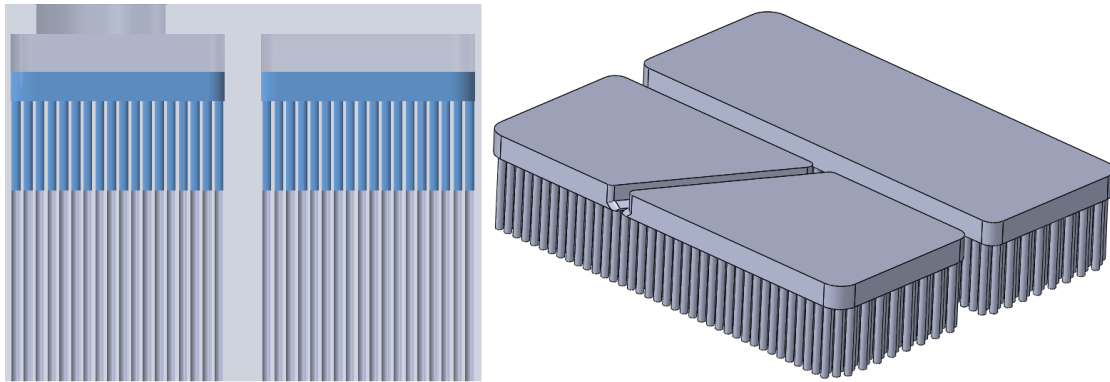


Figure 47: To the left the blue area is where the local mesh is, and to the right is a 3D view of the part inserted to create this local mesh.

The mesh in this region is not derived from the automatic settings, but through investigating different settings, through trial and error. The final setup is as following:

- Solid/Fluid -Interface:
 - Small solid feature refinement level: 3 (on a scale from 0 to 9)
 - Curvature refinement level: 2 (on a scale from 0 to 9)
 - Curvature refinement criterion: Default (0,389760733 rad)
 - Tolerance refinement level: 2 (on a scale from 0 to 9)
 - Tolerance refinement criterion: Default (0,0403241745 m)
- Refining Cells
 - Refine all cells: Not checked
 - Refine fluid cells: 3 (on a scale from 0 to 9)
 - Refine partial cells: 1 (on a scale from 0 to 9)
 - Refine solid cells: Not checked
- Narrow Channels
 - Enable narrow channel refinement: Checked
 - Characteristic number of cells across a narrow channel: 10
 - Narrow channel refinement level: 3 (on a scale from 0 to 9)
 - Enable minimum height of narrow channels: Not Checked
 - Enable the maximum height of narrow channels: Not checked

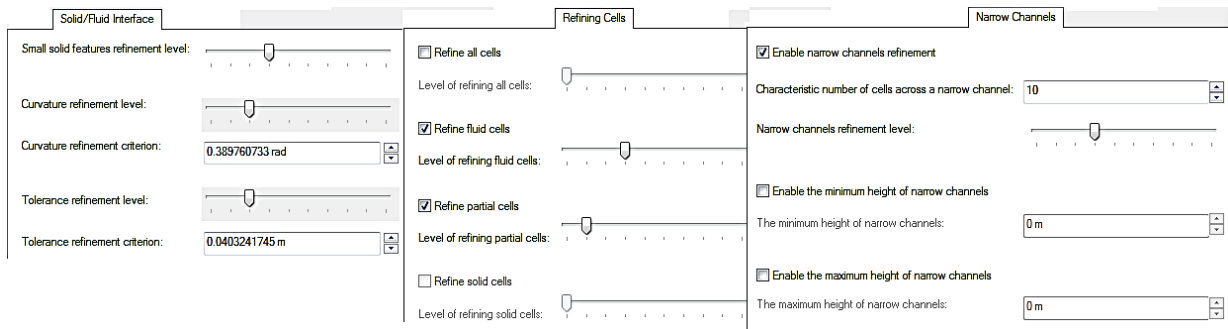


Figure 48: The setup for the local initial mesh of the inlet and outlet region.

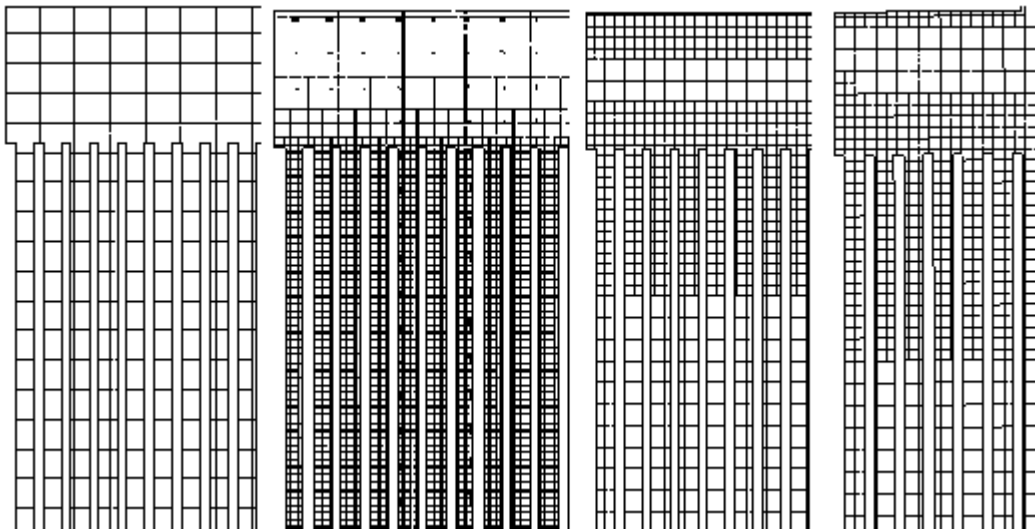


Figure 49: The mesh of the inlet/outlet area. To the left is without a local mesh, the next is a finer mesh, but only inside the pipes. Nr three is a local mesh, and to the right is the final mesh, with its longer area of local mesh, and outside of the pipes as well.

2.6 Rack simulation setup

Many of the settings for the simulations are related to the computational mesh, and are therefore covered in the previous chapter. The rest of the settings are covered in this chapter.

The main settings to control what kind of simulation is going to be performed are defined in the “general settings”. This is initiated the first time by using the “Wizard”-tool when creating a project. During the selections of the general settings (next chapter), if a feature is not included, it will not be possible to insert later. An example is the “Time-dependant” selection, if this is not selected you are not able to get results on the basis of physical time. By including only the conditions necessary, this saves time and computing power to the system.

2.6.1 General settings

The “general settings” are divided in four main topics, and the following are its input:

- Analysis type:
 - Internal
 - Checked: Exclude cavities without flow conditions
 - Physical features
 - Unchecked: Heat conduction in solids
 - Unchecked: Radiation
 - Unchecked: Time-dependent
 - Checked: Gravity
 - Unchecked: Rotation
- Fluids:
 - Liquids
 - Water (pre-defined)
 - Flow Type: Laminar and turbulent (Default)
 - Unchecked: Cavitation
- Wall conditions
 - Default wall thermal condition: Adiabatic wall
 - Roughness: 1,5 micrometer (surface roughness of Cu/Ni piping ¹⁶)
- Initial conditions
 - Thermodynamic Parameters
 - Pressure: 101325 Pa = 1 atm.
 - Checked: Pressure potential
 - Temperature 323,15 K = 50° C
 - Velocity parameter: Default, not outside movement (0 m/s)
 - Turbulence Parameters
 - Parameter: Turbulence intensity and length (Default)
 - Turbulence intensity: 2 % (Default)
 - Turbulence length: 0,00168 m (Default)

2.6.2 Input data

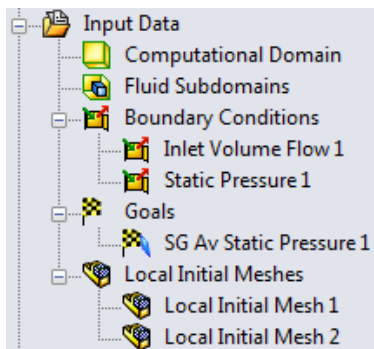


Figure 50: A view of the input data selected in the program, and how it's displayed.

The input data are the actual settings for the specific simulation. The general settings are the same for all the rack simulations, but the input data varies, depending on what flow are simulated, and what configuration the rack has.

The boundary conditions specify mainly what happens at the inlets and outlets. It can also be used to define special walls or wall conditions at specific areas, but in these simulations they are only used for the inlet and outlet lids.

These lids are automated generated parts, which is used to cover an opening, making the part “water tight”. This is a pre requisite for the model before starting the simulation, even though it is not the actual situation. In other words, these lids are imaginary parts which are only used to specify an inlet or outlet condition, and is not it selves included as a component in the simulation.

The “Inlet Volume Flow 1”-tab in the picture above, is the inlet condition of the rack. Its parameters are shown in the picture below (Figure 51).

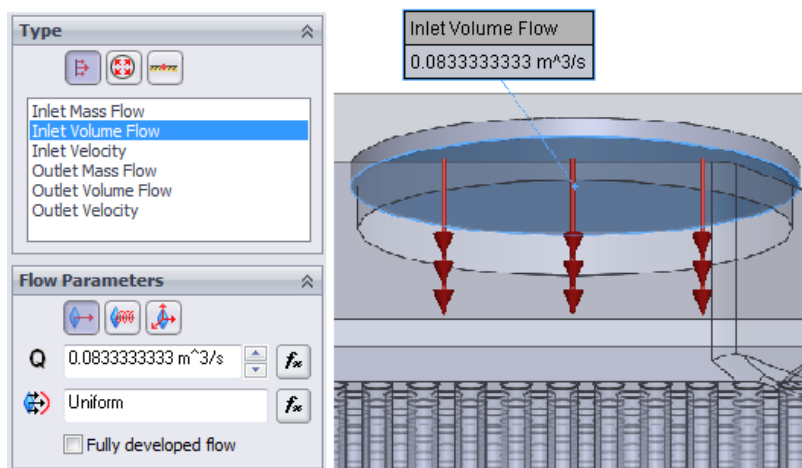


Figure 51: To the left is the inlet flow parameters and to the right is a picture of the inlet face of the lid, a call out window with the specific flow parameter and arrows with the direction of flow. This flow is equal to 300 m³/h.

The inlet flow parameters are independent for each of the simulations. Every configuration of rack is simulated with a range of inlet flow, in order to get results to be used for a specific value. The top icon in the pictures refers to a “flow opening”. The flow

is specified in the units of [m³/s], but it is inserted as [m³/h], in order to get the exact value. It is then converted automatically to the standard SI- units. It is also to specify the mass flow or the inlet velocity of the fluid, but since the desired value of measurement is volume flow, this is selected. For the 4-pass rack configuration there is only one inlet lid, as shown in the picture, but in the 2-pass configuration there are two inlet lids. The setup is identical, with the difference of selecting two lids, the inlet flow selected is divided between the two lids equally. There are three more parameter selection categories available when setting it up, but these are kept as default, as all of them are previously defined in the general settings, and are identical.

The “Static Pressure 1”-tab is the outlet condition.

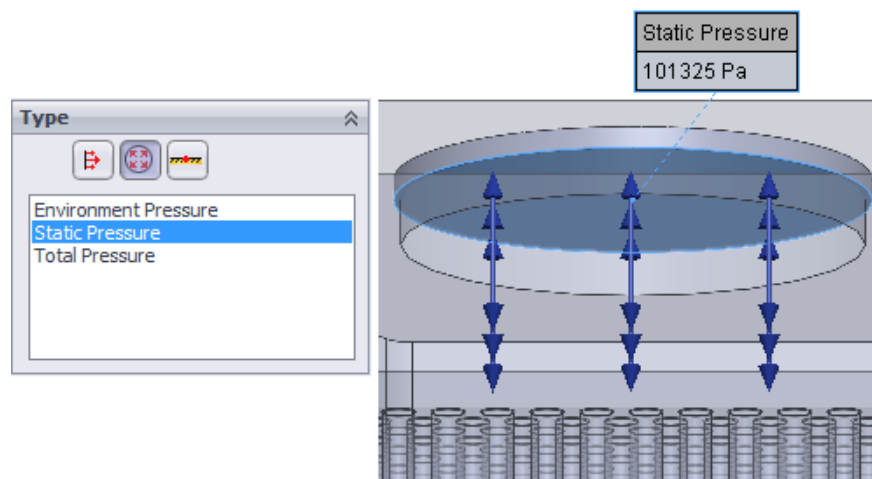


Figure 52: To the left it is shown that the “pressure opening” selection is selected, with a “static pressure” in the opening. To the right the blue arrows indicate this, and the flow can go both ways, it is an opening.

For the outlet of the flow it set a certain pressure at the outlet. This is indicated by the selected icon in the top of the picture and means “pressure opening”. This is to simulate a continuous flow after the opening. The “Environment pressure” has also been selected for some of the 4-pass configurations, because it handles flow vortexes better. This option means the same as an outlet, except for the small differences that it “allows” for vortexes crossing the exit. Here again is the number of lids and openings dependant of the rack configuration, in the same matter as the inlet flow.

In “Figure 50” there is a tab for “goals”. In the picture there is only listed one goal. This goal is the actual goal for the simulation, and is used as the only result for finding the pressure drop. The “SG AV Static Pressure 1” is an abbreviation for “Surface Goal

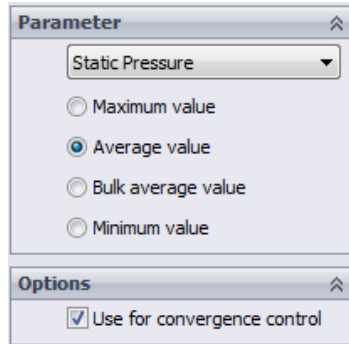


Figure 53: The goal parameter selection window.

Average Static Pressure (1)”. The name of the goal is quite describing for the goal, and as it says, the goal achieved is the average static pressure over a pre-specified surface. The surface(s) in question are the inlet lids, i.e. the same surface as the inlet flow. By finding the pressure of the water at this surface, and subtracting the known pressure at the outlet, the pressure drop through the rack is given. The box checked out in the picture to the left, named “Use for convergence control”, makes an important role in the calculation process.

When this box is check, like it is in these simulations, Flow Simulation has an extra focus for finding a good result on this parameter. It will continue calculating and simulating till this goal reaches convergence. When convergence is reached, Flow Simulation is satisfied and confident that the goal is correct with the selected input data.

2.7 Rack simulation configurations

Each rack-size can be used in two ways, the 2-pass and the 4-pass. Because of the differences in these ways of using the same product, it is also simulated in these two ways.

2.7.1 Experimental test configurations

In order to compare the experimental tests to what is simulated; the configurations used in the experimental testing were simulated in the same matter. These were done only in order to find the relation between the results, and are not used to find the actual pressure drop during operations. These simulations were done in the middle of the process of finding a sufficient mesh for simulations, and therefor will its results have a smaller degree of transferability to real operations, but will act as a confirmation of the experimental data and to certain degree validate that the simulation is working properly.

Setup that is not as described previously:

- Gravity in these simulations is not included. This is partly because they are used for refining the mesh, but also because during the testing the rack was positioned in different matter from what it would during operations.
- Surface roughness is set to 0 micrometer. The effect of this is very limited, according to ¹⁷



- The chamfers in the openings of each single pipe are not included. This was a change done later in the process, after attaining more knowledge in the fabrication process of the rack.
- The local initial mesh may or may not have been included in these simulations.

Configurations:

- 2-pass half rack: This is a configuration not realistic, because only half of the available pipes are enabled.
- 2-pass full rack: This configuration is also not realistic because of the changes done to the rack, in which were done in order to run the experiment.
- 4-pass: Except for the few changed listed previously, this is the same configuration is the same as the realistic one. This is the one used for adjusting the mesh, because this is the one that demands most from the programme, because of its longer flow path.

2.7.2 Real configurations

These configurations are the 2-, and 4-pass configuration of the racks in the way it will be run during normal operations.

- 2-pass: The difference from this one, and the 2-pass half/full from the experimental configurations are that the changes done in the full pass is not done in this one, but in order to run water through the entire rack there is two inlets and two outlet. This is how 2-pass will be set changes.
- 4-pass: This simulation is realistic to the operational scene in a larger degree than the experimental 4-pass, due to the real setup. Except for the difference in these setup-changes, these simulations are similar.

The rack size with the highest focus is the 700-1000S rack. This is the rack the testing up realistically during operations. Another difference in the setup is as described in chapter 2.4 and 2.5, without was done on, but is also one of the more common racks Sperre supplies. For the results to be more universal, some other racks were simulated as well. These were simulated with the same settings as the 700-1000S, and were not mesh optimized for its increased or decreased total size. This means that in a smaller rack, like the 600-1000S, the meshing and the simulations were computed faster than the original 700-1000S.

2.8 Single pipe simulation

The method of simulating one single pipe, and to use the result to extend the other results, is showed in this chapter.

2.8.1 Principle

The single pipe simulations are done to find the difference in pressure drop between different lengths of pipes. These results are used to find the pressure drop of another rack height than what is simulated in its entirety. If comparing a 700-1000S rack to a 700-1200S rack, the flow situation and pressure drop at the inlet(s) and outlet(s) will be identical. The only area where the two racks differ is in the length of the vertical part of the pipes. In turn, this means that the presumed higher pressure drop for the 700-1200S, can only be explained by the difference in pipe lengths.

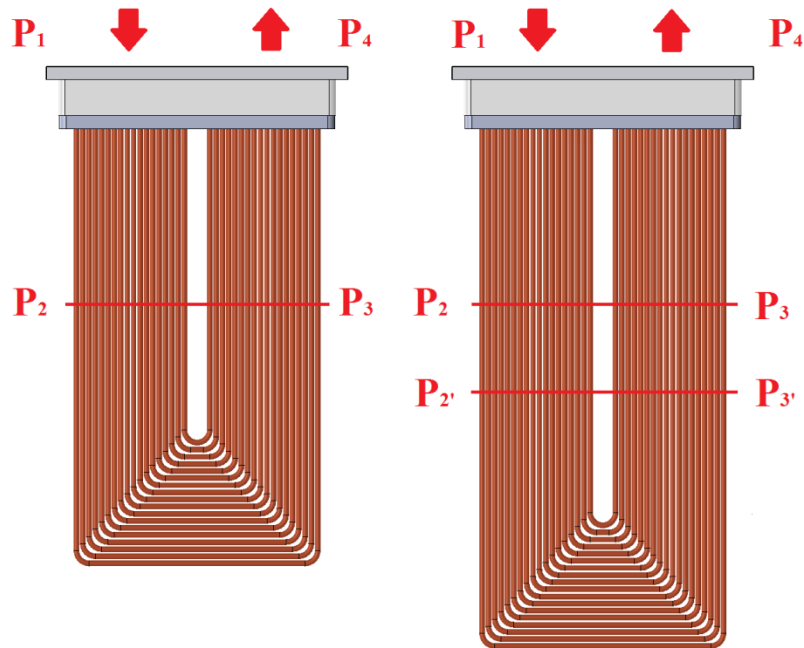


Figure 54: Comparing the 700-1000S rack with the 700-1200S rack and the pressure at different locations.

In Figure 54 the 700-1000S rack is compared with the 700-1200S rack. The pressure drop at both inlets are $P_2 - P_1$, and is identical. In the bottom of each rack, where the pipe bends are located, the pressure drop for the smallest of the two racks are $P_3 - P_2$, and for the larger rack the pressure drop is $P_3' - P_2'$. These two areas are also identical, which means these two pressure drops also have to be identical. For the outlet pressure drop, the situation is the same, $P_4 - P_3$ is the same in both instances. What this means is that the



total pressure drop of the 700-1200S rack, is the pressure drop of the 700-1000S, plus the two pressure drops $P_2 - P_2$ and $P_3 - P_3$.

Because every pipe in a single rack will experience the same pressure drop between its inlet and its outlet¹⁸, the increased pressure drop of a longer pipe can be simulated with the average length pipe and the average water velocity. To be sure this theory is applicable in this situation, the result are compared to the result of two fully simulated racks with different heights. By combining these results, a factor of pressure increase with higher racks can be found.

For these simulations to be as accurate as possible, the pipes for simulation used in each rack, is the pipes in the mid-range, size wise.

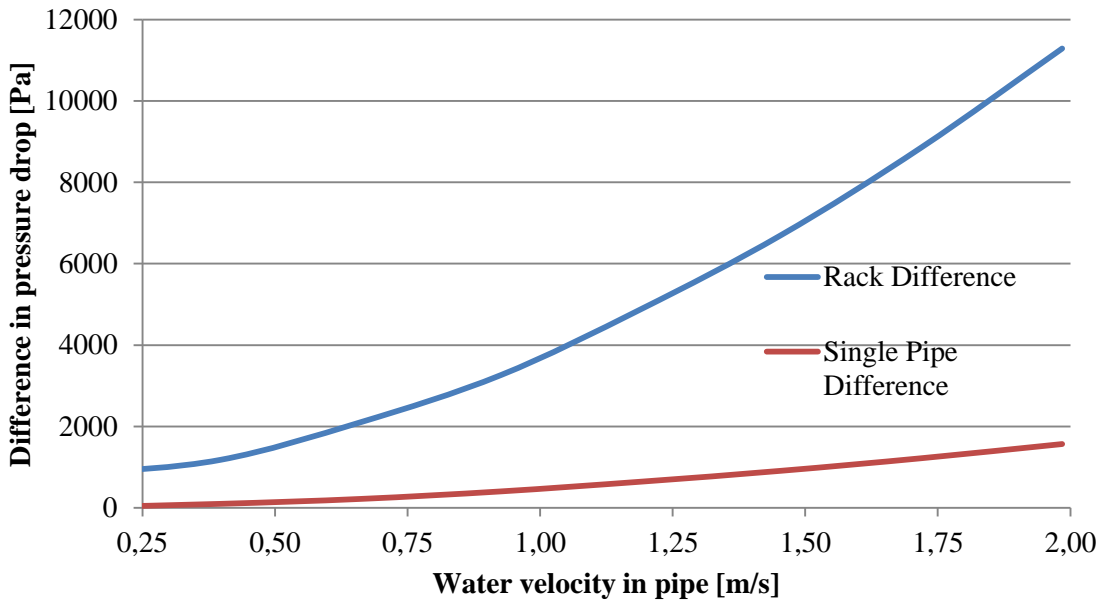
Table 4: List of the different rack sizes considered in the different simulations done for single pipe pressure drop. The selected pipe number, and total pipe numbers are also listed.

Rack models considered	Total number of pipes – Number of different pipes sizes	Pipe number simulated (counted from the shortest)
700-1000S, 700-1200S, 700-1500S	709- 18	10
600-1000S, 600-1200S, 600-1500S	467-14	8
600-1000C, 600-1200C, 600-1500C	367-11	6

The flow of water in the pipes will have to be able to get fully developed in order for this theory to be valid. The entrance region of a pipe opening is considered to be 50 times its diameter¹⁹, which means in our case $10,7 \text{ mm} * 50 = 535 \text{ mm} = 0,535 \text{ meter}$. None of the pipes have a vertical length which is shorter than this. The stability region of a pipes flow after a bend will also have to be long enough for the flow to become fully developed, before exiting the pipe. Some sources claims the flow will not be fully developed for as long as 100 diameters after the bend¹⁸. To be sure this is not the case, graphs of the flow profiles in the pipe are presented in 3.2.1. The pipe these graphs are taken from, is the pipe from the 700-rack. This is because this is the pipe with the shortest height of the three pipes simulated.

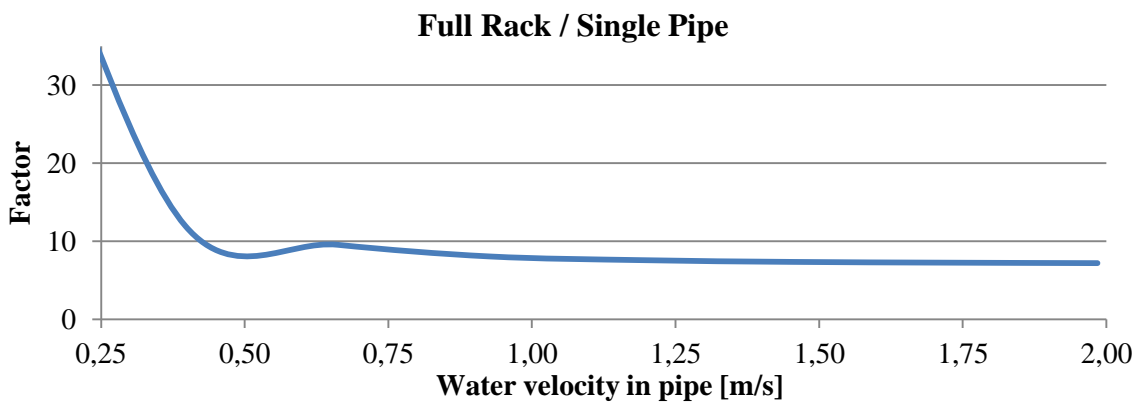
2.8.2 Result treatment

The way the results are treated and incorporated in the results of the full rack configurations, is now to be explained. The difference in pressure drop between a 1000-pipe and a 1200-pipe, from the same rack, needs to be compared to the difference in pressure drop between a fully simulated 1000-rack and a 1200-rack. By comparing these two pressure drops, their relation is found. The selected rack-sizes used here are the 600-1000S and the 600-1200S.



Graph 1: The difference in pressure drop between the 1000-rack and 1200-rack sketched, as well as for the 1000-pipe and 1200-pipe.

Their relation is found by dividing the difference of the rack, with the difference of the single pipe.



Graph 2: When dividing the racks difference in pressure drop with the single pipes difference in pressure drop, for the series of velocities, this graph is drawn.



What Graph 2 shows is that the relation between fully simulated rack and a single pipes difference in pressure drop has an average of about 8, in the area of water velocity relevant. By assuming this average is constant through the series of different racks in question, this relation can be used to find the pressure drop of rack with a longer height than has been simulated in its entirety. This method and the factor of 8 are also used for the 1500-height racks.

The pressure drop of the 4-pass racks are calculated in the same matter, but because the water flow through a pipe twice, the pressure drop of the single pipe is multiplied by two, in addition to be multiplied by the factor of 8.

2.8.3 Result treatment of improved mesh simulations

The increased resolution of the meshing in the added simulation of the 600-1000S 4-pass, and the simulations done of the 600-1000C rack, makes the factor found in the last chapter, uncertain. The basis of this factor lacks for these improved simulations, and therefor there is nothing to support having a factor at all. As shown later in chapter 3.1, the cell size are very different from the simulations used in the last chapter, and the results are as well.

3. Results

All the results of the different tests and simulations from chapter 2, is presented in this chapter.

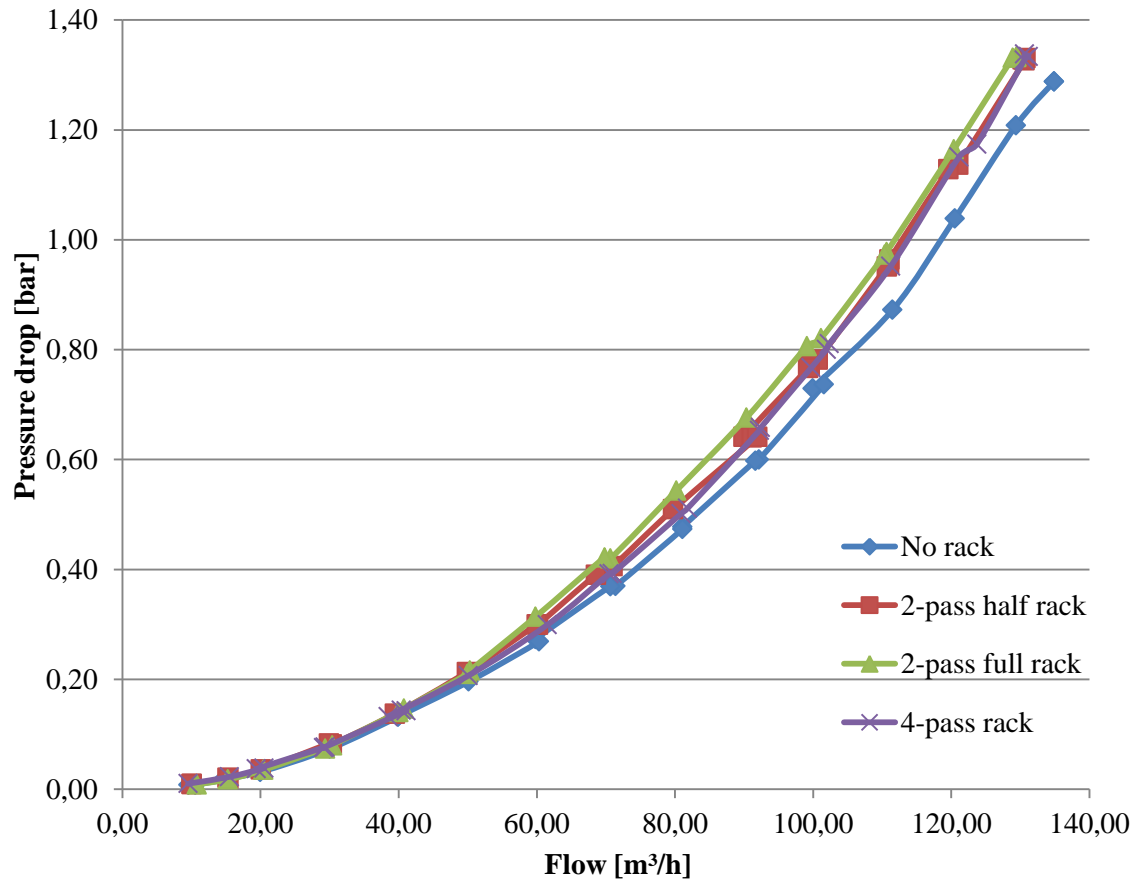
3.1 Experimental test results

The two main parameters from the loggings used for these test are the flow meter reading (FT2) and the pressure difference (DPT3).

3.1.1 Raw results

Table 5: A list of all the relevant results of the experimental testing done at Sperre.

No rack		2-pass half rack		2-pass full rack		4-pass rack	
Flow [m ³ /h]	Pressure Drop	Flow [m ³ /h]	Pressure Drop	Flow [m ³ /h]	Pressure Drop	Flow [m ³ /h]	Pressure Drop
134,91	1,29	130,35	1,33	129,42	1,33	130,61	1,34
134,91	1,29	130,77	1,33	129,47	1,33	131,19	1,33
129,39	1,21	130,65	1,33	128,92	1,33	130,58	1,33
120,52	1,04	121,02	1,14	120,39	1,16	123,71	1,17
111,49	0,87	119,62	1,13	110,64	0,98	121,13	1,15
99,95	0,73	111,06	0,96	110,36	0,97	111,24	0,95
101,58	0,74	111,01	0,96	101,15	0,82	102,35	0,81
92,15	0,60	110,68	0,95	99,09	0,81	101,94	0,80
91,64	0,60	100,71	0,78	90,33	0,68	99,71	0,77
81,09	0,48	99,52	0,77	80,20	0,54	92,39	0,66
81,10	0,47	99,31	0,77	70,67	0,42	92,24	0,65
71,39	0,37	89,96	0,64	69,80	0,42	81,82	0,51
70,64	0,37	91,15	0,64	59,82	0,31	80,88	0,50
59,83	0,27	91,94	0,64	50,32	0,22	70,95	0,39
60,34	0,27	79,75	0,51	49,96	0,21	70,47	0,39
50,14	0,20	70,97	0,41	40,77	0,15	61,54	0,30
39,89	0,13	68,57	0,39	39,99	0,14	50,08	0,21
39,95	0,13	60,17	0,30	29,39	0,07	38,48	0,13
30,02	0,07	59,99	0,30	30,40	0,08	40,41	0,14
19,95	0,03	49,87	0,21	20,43	0,04	41,09	0,14
14,71	0,02	39,44	0,14	15,26	0,02	29,12	0,08
15,57	0,02	30,33	0,08	10,77	0,01	29,36	0,08
10,52	0,01	29,91	0,08			19,41	0,04
9,59	0,01	20,06	0,04			20,50	0,04
		15,23	0,02			15,53	0,02
		15,37	0,02			9,51	0,01
		10,05	0,01				
		10,02	0,01				



Graph 3: All the values from Table 5 plotted on the same graph, to show their relation.

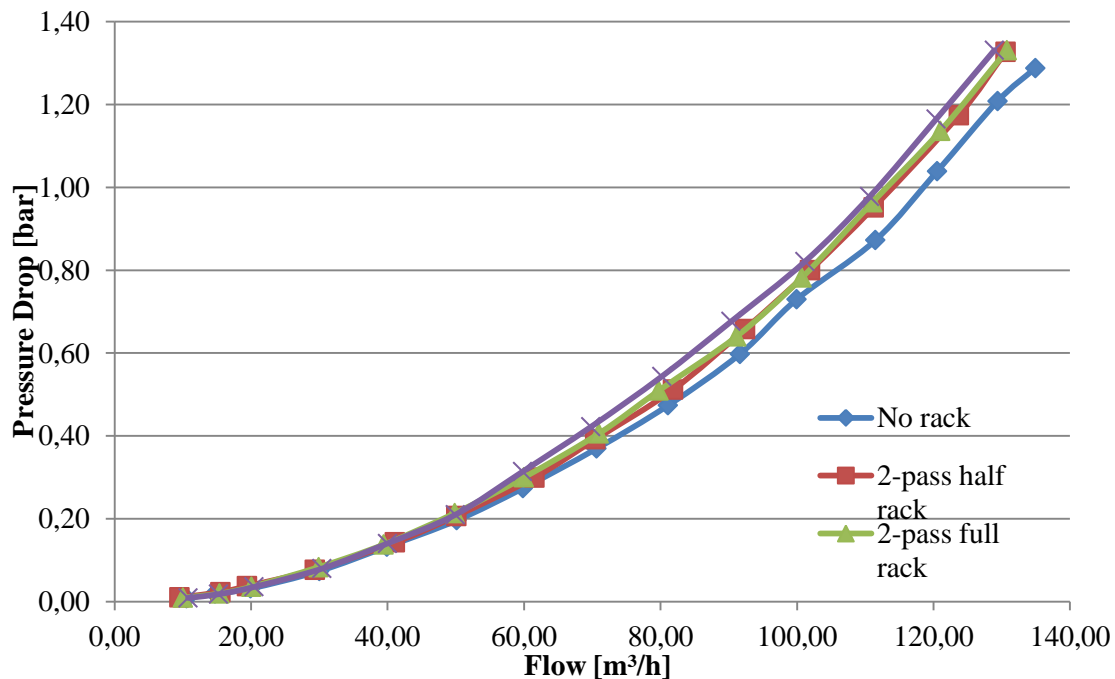
3.1.2 Sorted and ordered results

Since every series of loggings consists of 59 loggings, there is a small spread in the results from each of them. As we can see from the list in the last chapter, some of the series were redone to get a series with a small spread. The next step in sorting the results is to remove the series with the largest spread in loggings, or standard deviation as it is also called. This is done on the basis that the reason for the double set of data, is that a new series was initiated because the system not yet had stabilized. The full list of raw data with standard deviation and relative deviation (%) is inn Appendix III. By doing this, the number of series in each configuration will also become the same, with the exception of the “no rack” configuration which was able to keep a higher flow. This is included to have an as long range as possible in the readings.

Table 6: The selected data for each of the intervals, after removing the ones with the highest relative standard deviation.

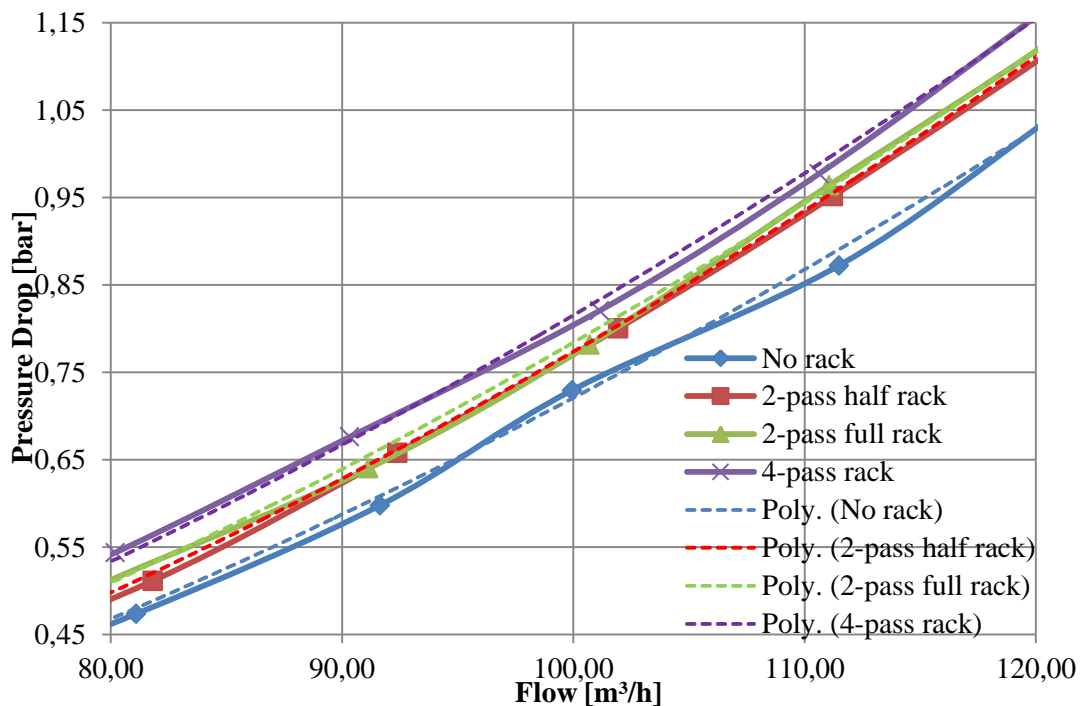
No rack		2-pass half rack		2-pass full rack		4-pass rack	
Flow [m ³ /h]	Drop [bar]	Flow [m ³ /h]	Drop [bar]	Flow [m ³ /h]	Drop [bar]	Flow [m ³ /h]	Drop [bar]
134,91	1,29	-	-	-	-	-	-
129,39	1,21	130,58	1,33	130,77	1,33	128,92	1,33
120,52	1,04	123,71	1,17	121,02	1,14	120,39	1,16
111,49	0,87	111,24	0,95	111,06	0,96	110,64	0,98
99,95	0,73	101,94	0,80	100,71	0,78	101,15	0,82
91,64	0,60	92,39	0,66	91,15	0,64	90,33	0,68
81,10	0,47	81,82	0,51	79,75	0,51	80,20	0,54
70,64	0,37	70,47	0,39	70,97	0,41	69,80	0,42
59,83	0,27	61,54	0,30	59,99	0,30	59,82	0,31
50,14	0,20	50,08	0,21	49,87	0,21	49,96	0,21
39,89	0,13	41,09	0,14	39,44	0,14	39,99	0,14
30,02	0,07	29,36	0,08	29,91	0,08	30,40	0,08
19,95	0,03	19,41	0,04	20,06	0,04	20,43	0,04
14,71	0,02	15,53	0,02	15,37	0,02	15,26	0,02
10,52	0,01	9,51	0,01	10,02	0,01	10,77	0,01

By plotting these series in a graph, they are each represented with an equation. This is done in order to compare the results with the same flow, on a more accurate basis.



Graph 4: All the value from Table 6 plotted on the same graph. These are the sorted results.

When zooming in on an area of the graph, the differences become clearer. The trend line graph is also shown, as a dotted line in the same colour as the original one.



Graph 5: The Graph 4, but zoomed closer to a selected area. The polynomial trend lines are represented in the same colour, but with dotted lines.

The values for each of the trend line shown, is listed below (Table 7). The “x” represents the flow volume selected, and the result will be the pressure drop in bar. The R^2 value is a measurement of how well the trend line fits to the values, and is measured between 0 (no representation) and 1 (represent the exact value).

Table 7: Table of the R^2 values for each of the equations, which is also shown.

	R^2	Equation
No rack	0,9996	$0,00007x^2+0,0004x-0,0003$
2-pass half rack	0,9998	$0,00008x^2-0,00002x+0,0083$
2-pass full rack	0,9997	$0,00007x^2+0,0005x-0,0004$
4-pass rack	0,9997	$0,00007x^2+0,0011x-0,0157$

With these equations the pressure drop in the actual configuration can be easily calculated.

This is the procedure for calculating the pressure drop in a 4-pass configured rack, with the flow of 80 m³/h.

Pressure drop **4-pass** with 80 m³/h – Pressure drop **No rack** with 80 m³/h

$$= (0,00007 * 80^2 + 0,0011 * 80 - 0,0157)$$

$$- (0,00007 * 80^2 + 0,0004 * 80 - 0,0003) = 0,5203 \text{ bar} - 0,4797 \text{ bar}$$

$$= \mathbf{0,0406 \text{ bar}}$$

By subtracting the calculated value, with the value for the “No rack”, its internal pressure drop, without the external system is given. The table below contains these values.

Table 8: The pressure drop of the rack in different configurations. The water velocity in the pipes are also added.

Flow [m ³ /h]	2-pass half rack		2-pass full rack		4-pass rack	
	Velocity water [m/s]	Pressure Drop [bar]	Velocity water [m/s]	Pressure Drop [bar]	Velocity water [m/s]	Pressure Drop [bar]
130	1,13	0,1116	0,57	0,0129	1,13	0,0756
120	1,05	0,0904	0,52	0,0119	1,05	0,0686
110	0,96	0,0712	0,48	0,0109	0,96	0,0616
100	0,87	0,054	0,44	0,0099	0,87	0,0546
90	0,78	0,0388	0,39	0,0089	0,78	0,0476
80	0,70	0,0256	0,35	0,0079	0,70	0,0406
70	0,61	0,0144	0,30	0,0069	0,61	0,0336
60	0,52	0,0052	0,26	0,0059	0,52	0,0266
50	0,44	-0,002	0,22	0,0049	0,44	0,0196
40	0,35	-0,0072	0,17	0,0039	0,35	0,0126
30	0,26	-0,0104	0,13	0,0029	0,26	0,0056
20	0,17	-0,0116	0,09	0,0019	0,17	-0,0014
10	0,09	-0,0108	0,04	0,0009	0,09	-0,0084

As we can see from these values, the internal pressure drops for two of the configurations are calculated to be negative. A negative pressure drop is a pressure gain, which means there has to be some sort of a pump or similar in that area, and it is not. This is obviously due to the method used for obtaining these results, in which there can be several sources for this. The lower the flow is, the higher the relative standard deviation is, which can cause larger miss readings. The pressure drop readings from the low flow area are also more inaccurate because the pressure drop itself is very small.



If setting a lower limit to the validity of our testing at 60 m³/h, the pressure drop will be realistic. This limit is also lower than any of the racks will have during normal operating time.

3.1.3 Adjusted results

Due to the uncertainty in the accuracy of the readings, all the results have been adjusted to find a realistic span where the actual value lies. This is done by adjusting the flow reading from the original series, by a certain degree. By adjusting these, the graph of flow vs. pressure drop will become flatter or steeper. The range of adjustments are done with increments of 2,5 %, to a maximum of 15 %. It has been adjusted both up and down, even though indicators show that the flow meter mainly displayed a higher value than it was supposed to.

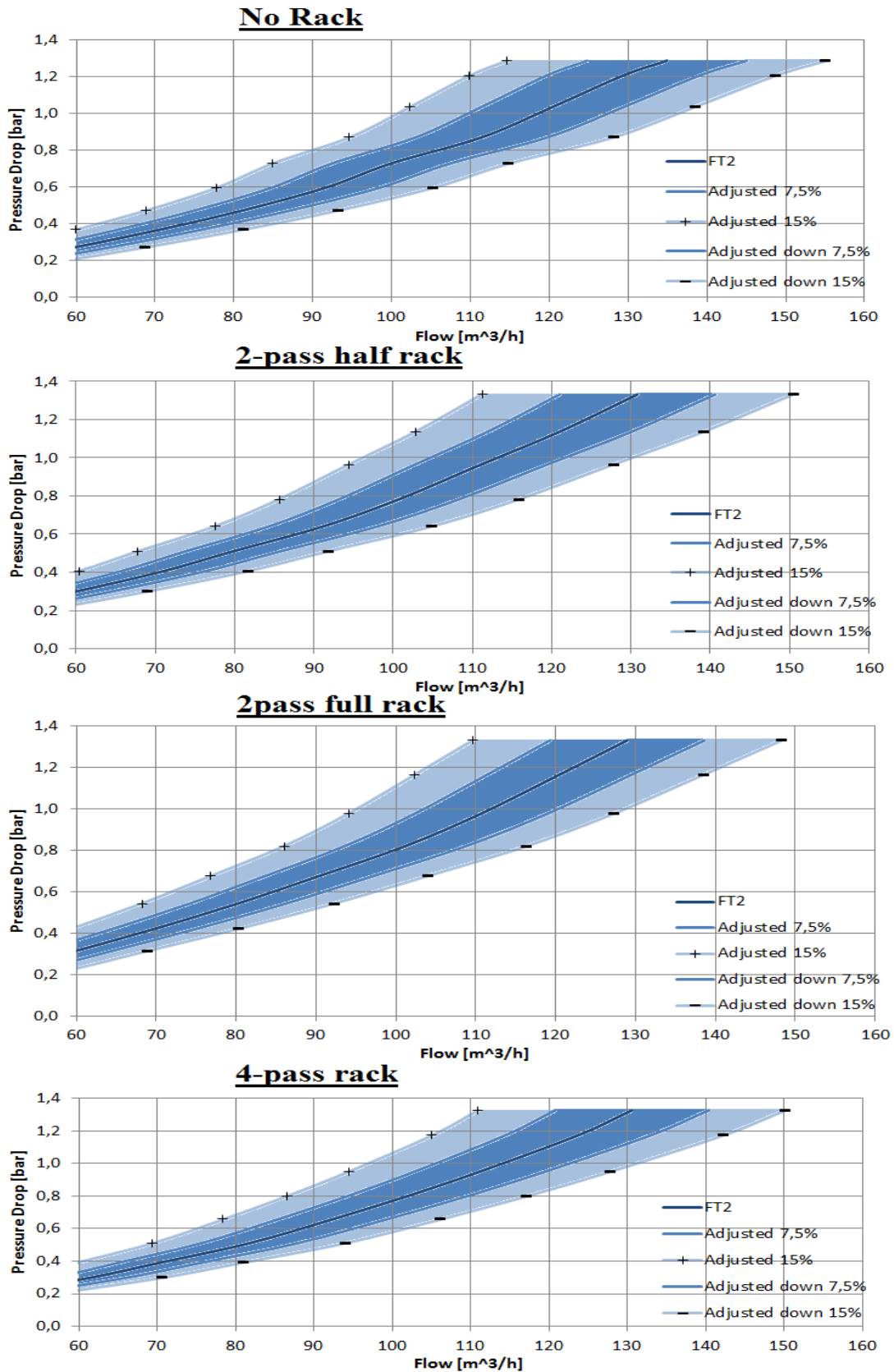


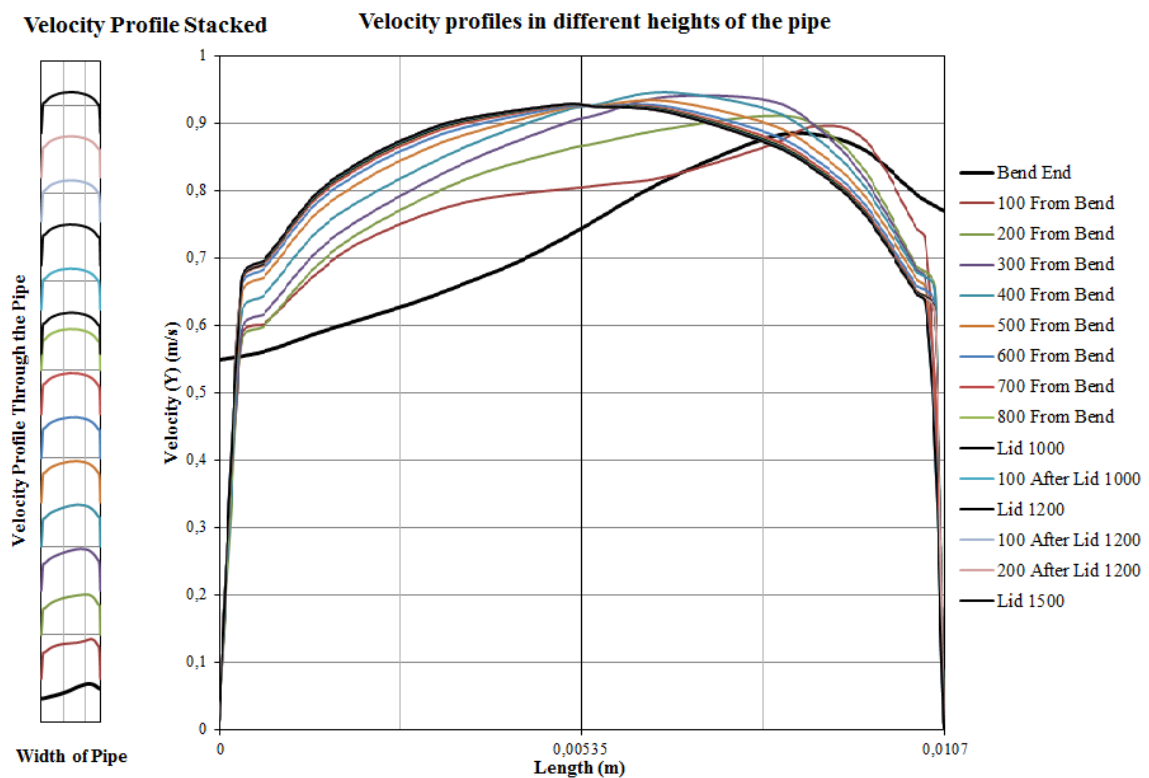
Figure 55: A figure of the four different graphs showing the pressure drop in each of the tests. The dark blue areas are the results adjusted plus/minus 7,5 %, and the light blue is plus/minus 15 %.

3.2 Single pipe simulations

The results of the simulation of one single pipe are presented in this chapter.

3.2.1 Pipe flow profile

The velocity profiles of the water flow in the pipes, is used as a confirmation of the method described in chapter 2.8. As shown in Graph 6, the profile stabilizes at about 600-800mm. after the end of the pipe bend. Those profiles are displayed in blue, light red and light green. Because the light green one (800 mm. from the bend) is not very visible in the large graph, tell us that the profile does not change further.



Graph 6: Velocity profiles of the water flow in the pipe. The different lines represent different heights from the bend, and the areas around each of the three lids. To the left are the profiles stacked according to their placement (width not in scale), and to the right are the same one with one single y-axis.

3.2.2 Pressure results

These are the results derived from the simulations explained in Chapter 2.8.

First are the results from the 700S rack presented. These clearly show the increased pressure drop, with the increased length of pipe.

Table 9: Single pipe simulation result of the selected pipe in the 700 rack. The equivalent flow, and the water velocity in the pipe is shown, as well as the results and the pressure difference to the original 1000 height pipe.

700S Single Pipe						
Equivalent Flow [m³/h]	Velocity in Pipe [m/s]	1000 pipe [Pa]	1200 pipe [Pa]	1500 pipe [Pa]	Diff 1000 VS 1200 [Pa]	Diff 1000 VS 1500 [Pa]
20	0,087	101370	101377	101389	7,7	19,0
60	0,261	101649	101711	101800	61,5	150,5
100	0,436	101935	102044	102210	108,1	274,9
140	0,610	102389	102584	102884	195,7	495,3
180	0,784	102953	103258	103723	305,8	770,5
220	0,959	103586	104003	104653	417,1	1066,7
260	1,133	104343	104929	105790	585,7	1446,9
300	1,307	105223	105973	107098	750,2	1875,7
340	1,481	106083	107020	108407	936,6	2324,1
380	1,656	107082	108241	109933	1158,7	2851,5
420	1,830	108194	109611	111639	1417,2	3445,3
460	2,004	109450	111093	113459	1642,6	4009,0

The results of the 600S- and 600C pipes are listed below (Table 10 and 11), and as we can see, the differences are larger, because the same increase in pipe length, result in a larger per cent increase, because the pipes are originally shorter than the 700S-pipe.

Table 10: Single pipe simulation result of the selected pipe in the 600S rack. The equivalent flow, and the water velocity in the pipe is shown, as well as the results and the pressure difference to the original 1000 height pipe.

600S Single Pipe						
Equivalent Flow [m³/h]	Velocity in Pipe [m/s]	1000 pipe [Pa]	1200 pipe [Pa]	1500 pipe [Pa]	Diff 1000 VS 1200 [Pa]	Diff 1000 VS 1500 [Pa]
20	0,132	101415	101430	101455	15,0	39,4
60	0,397	101866	101965	102109	98,8	242,8
100	0,661	102526	102746	103079	220,5	553,6
140	0,926	103456	103861	104457	405,3	1001,5
180	1,191	104613	105258	106200	644,8	1587,6
220	1,455	105984	106897	108248	912,4	2263,8
260	1,720	107512	108734	110578	1221,5	3065,8
300	1,984	109295	110864	113235	1569,2	3939,9
340	2,249	111564	113552	116438	1988,7	4874,7

Table 11: Single pipe simulation result of the selected pipe in the 600S rack. The equivalent flow, and the water velocity in the pipe is shown, as well as the results and the pressure difference to the original 1000 height pipe.

600C Single Pipe						
Equivalent Flow [m³/h]	Velocity in Pipe [m/s]	1000 pipe [Pa]	1200 pipe [Pa]	1500 pipe [Pa]	Diff 1000 VS 1200 [Pa]	Diff 1000 VS 1500 [Pa]
20	0,168	101458	101489	101519	30,3	60,7
60	0,505	102074	102220	102434	145,8	359,5
100	0,842	103136	103483	104007	346,9	870,3
140	1,178	104545	105152	106094	606,2	1549,1
180	1,515	106309	107254	108670	945,3	2361,6
220	1,852	108438	109796	111819	1358,6	3381,5
260	2,189	110957	112825	115682	1867,7	4724,7

3.3 Rack Simulation Results

The 700-1000S rack is the rack where the mesh is optimized according to its physical features, and the computing capacity available. The first two sets of results are of this rack. The outlet pressure of every simulation is set to 101325 Pa = 1 atm. In Appendix V is a picture of the result file created from SolidWorks, in which the following results are extracted. The pressure shown is the static pressure.

Table 12: The 700-1000S 2-pass rack simulation with the inlet pressure with coloured background being the results. Its main flow parameters are flow, water velocity in pipe, outlet pressure, and pressure difference in two units, with the one in bar being the main desired unit of results.

700-1000S 2-pass				
Flow [m³/h]	Water Velocity [m/s]	Inlet Pressure [Pa]	Pressure Drop [Pa]	Pressure Drop [bar]
20	0,087	100547	-778	-0,008
60	0,261	101502	177	0,002
100	0,436	103717	2392	0,024
140	0,610	107253	5928	0,059
180	0,784	111755	10430	0,104
220	0,959	117163	15838	0,158
260	1,133	123506	22181	0,222
300	1,307	130774	29449	0,294
340	1,481	138985	37660	0,377
380	1,656	148075	46750	0,467
420	1,830	158057	56732	0,567

Table 13: The 700-1000S 4-pass rack simulation with the inlet pressure with coloured background being the results. Its main flow parameters are flow, water velocity in pipe, outlet pressure, and pressure difference in two units, with the one in bar being the main desired unit of results.

700-1000S 4-pass				
Flow [m³/h]	Water Velocity [m/s]	Inlet Pressure [Pa]	Pressure Drop [Pa]	Pressure Drop [bar]
20	0,174	101387	62	0,001
60	0,523	109925	8600	0,086
100	0,871	127310	25985	0,260
140	1,220	151817	50492	0,505
180	1,569	183427	82102	0,821
220	1,917	221938	120613	1,206
260	2,266	267210	165885	1,659
300	2,614	319072	217747	2,177

The next rack configuration being simulated in its fully content is the 600-1000S rack.

Table 14: The 600-1000S 2-pass rack simulation with the inlet pressure with coloured background being the results. Its main flow parameters are flow, water velocity in pipe, outlet pressure, and pressure difference in two units, with the one in bar being the main desired unit of results.

600-1000S 2-pass				
Flow [m³/h]	Water Velocity [m/s]	Inlet Pressure [Pa]	Pressure Drop [Pa]	Pressure Drop [bar]
20	0,132	100685	-640	-0,006
60	0,397	103042	1717	0,017
100	0,661	108350	7025	0,070
140	0,926	116041	14716	0,147
180	1,191	125774	24449	0,244
220	1,455	137400	36075	0,361
260	1,720	150972	49647	0,496
300	1,984	166511	65186	0,652
340	2,249	184031	82706	0,827
380	2,514	203491	102166	1,022

To compare two different heights of racks, the 600S-rack has also been simulated with the 1200 length, in its 2-pass flow configuration. These are results to be used in comparison with the results gained from the results of chapter 1.1, presented in chapter 3.2.2.

Table 15: The 600-1200S 4-pass rack simulation with the inlet pressure with coloured background being the results. Its main flow parameters are flow, water velocity in pipe, outlet pressure, and pressure difference in two units, with the one in bar being the main desired unit of results.

600-1200S 2-pass				
Flow [m³/h]	Water Velocity [m/s]	Inlet Pressure [Pa]	Pressure Drop [Pa]	Pressure Drop [bar]
20	0,132	101510	185	0,002
60	0,397	104222	2897	0,029
100	0,661	110455	9130	0,091
140	0,926	119305	17980	0,180
180	1,191	130660	29335	0,293
220	1,455	144109	42784	0,428
260	1,720	159836	58511	0,585
300	1,984	177799	76474	0,765

Table 16: The 600-1000S 4-pass rack simulation with the inlet pressure with coloured background being the results. Its main flow parameters are flow, water velocity in pipe, outlet pressure, and pressure difference in two units, with the one in bar being the main desired unit of results.

600-1000S 4-pass				
Flow [m³/h]	Water Velocity [m/s]	Inlet Pressure [Pa]	Pressure Drop [Pa]	Pressure Drop [bar]
20	0,265	103483	2158	0,022
60	0,794	124357	23032	0,230
100	1,323	163196	61871	0,619
140	1,852	217444	116119	1,161
180	2,381	287356	186031	1,860
220	2,911	372596	271271	2,713
260	3,440	472750	371425	3,714

Since the 600-rack is physically smaller than the mesh optimized 700-rack, an attempt of simulating the 600-1000S 4-pass with a finer mesh, was conducted, in the of the simulation period. The number of pipes, which is the area of largest influence on pressure drop and meshing, has been reduced by over 30 % compared to the 700-rack, so the initial global mesh refinement was increased from level 4, to level 5, to see if the computer handled it, without taking too long. The increment intervals of the simulation has been reduced to 20 m³/h, and the maximum simulated flow reduced to fit the water velocity span selected as 2,0 m/s.

Table 17: The 600-1000S 4-pass rack simulation with the improved mesh settings. The inlet pressure with coloured background is the results. Its main flow parameters are flow, water velocity in pipe, outlet pressure, and pressure difference in two units, with the one in bar being the main desired unit of results.

600-1000S 4-pass (Improved Mesh)				
Flow [m³/h]	Water Velocity [m/s]	Inlet Pressure [Pa]	Pressure Drop [Pa]	Pressure Drop [bar]
20	0,265	102609	1284	0,013
40	0,529	105726	4401	0,044
60	0,794	110478	9153	0,092
80	1,058	116790	15465	0,155
100	1,323	124619	23294	0,233
120	1,588	133929	32604	0,326
140	1,852	144608	43283	0,433
160	2,117	156774	55449	0,554

The radically reduced pressure drop of the rack, will need further investigation and has been given its own chapter. Chapter 4 will go further into the results, and compare them, to find the reason of the differences.

The 600C-rack has even fewer pipes than the 600S-rack, and there for its simulation is also done with the improved mesh refinement level of 5.

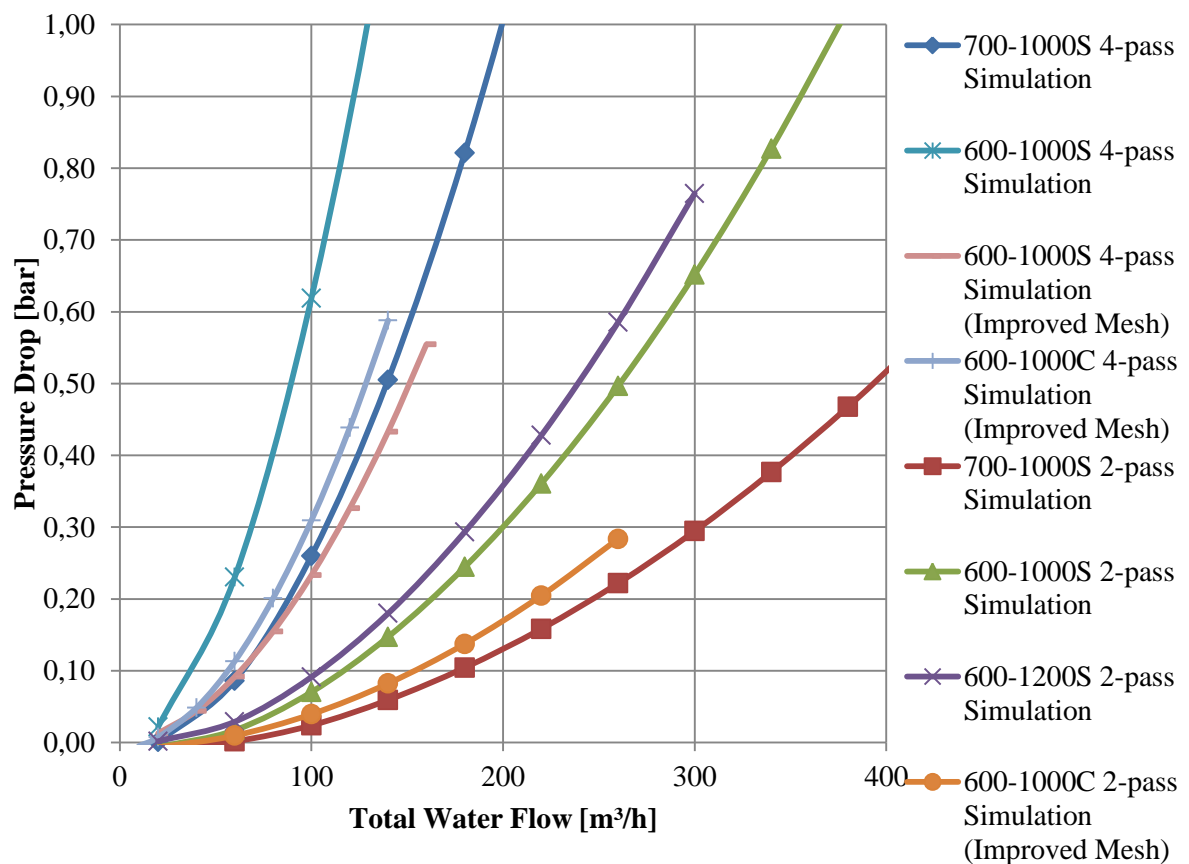
Table 18: The 600-1000C 2-pass rack simulation with the improved mesh settings. The inlet pressure with coloured background is the results. Its main flow parameters are flow, water velocity in pipe, outlet pressure, and pressure difference in two units, with the one in bar being the main desired unit of results.

600-1000C 2-pass (Improved Mesh)				
Flow [m³/h]	Water Velocity [m/s]	Inlet Pressure [Pa]	Pressure Drop [Pa]	Pressure Drop [bar]
20	0,168	100641	-684	-0,007
60	0,505	102295	970	0,010
100	0,842	105274	3949	0,039
140	1,178	109551	8226	0,082
180	1,515	115065	13740	0,137
220	1,852	121789	20464	0,205
260	2,189	129689	28364	0,284

Table 19: The 600-1000C 4-pass rack simulation with the improved mesh settings. The inlet pressure with coloured background is the results. Its main flow parameters are flow, water velocity in pipe, outlet pressure, and pressure difference in two units, with the one in bar being the main desired unit of results.

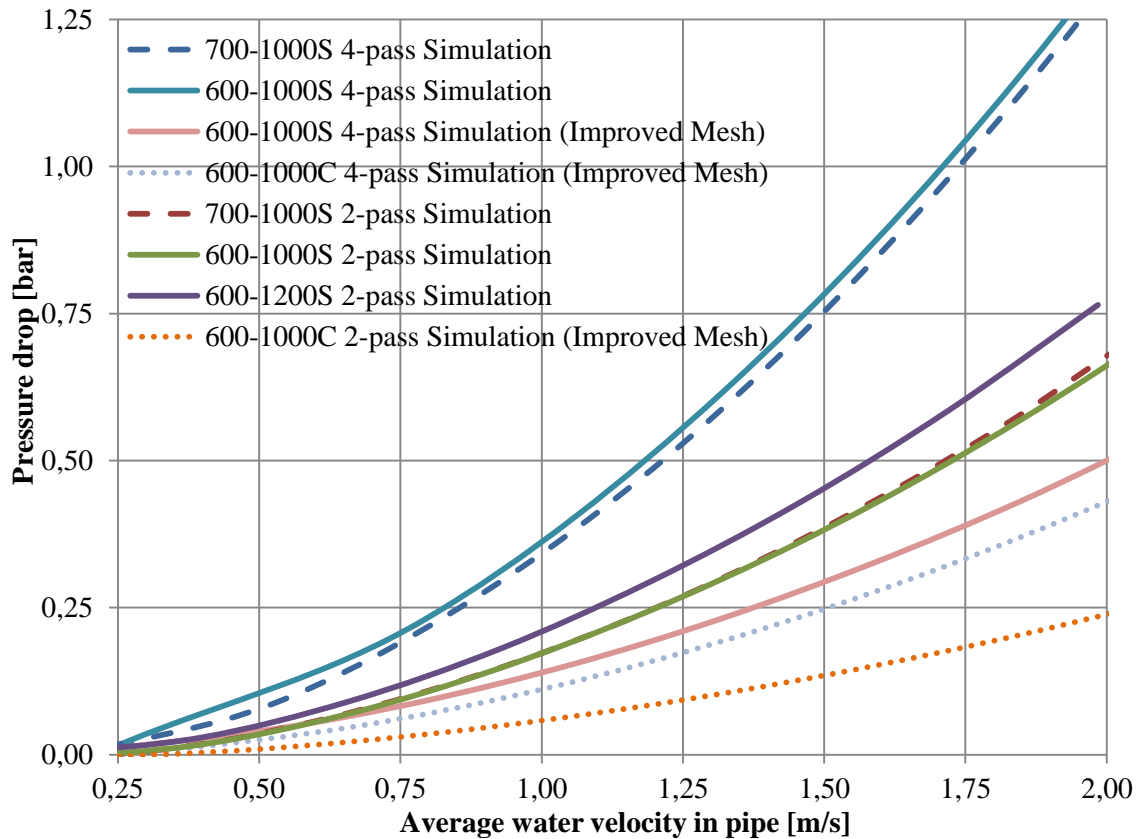
600-1000C 4-pass (Improved Mesh)				
Flow [m ³ /h]	Water Velocity [m/s]	Inlet Pressure [Pa]	Pressure Drop [Pa]	Pressure Drop [bar]
10	0,168	100847	-478	-0,005
20	0,337	102060	735	0,007
40	0,673	106163	4838	0,048
60	1,010	112643	11318	0,113
80	1,347	121406	20081	0,201
100	1,683	132255	30930	0,309
120	2,020	145177	43852	0,439
140	2,357	160125	58800	0,588

All results are plotted in the graph below (Graph 7), to see their relations to each other and the total volume flow in m³/h.



Graph 7: A graph showing the pressure drop simulated in all the simulations described in this chapter. The x-axis displays total water flow up till 400 m³/h and the y-axis displays pressure drop up till 1 bar.

A better way to display the results is in regards of the average velocity of the water in the pipes. By doing this, the differences in pipe numbers and flow configuration does not make natural effects of the slope.



Graph 8: The graph displays the pressure drop (y-axis) and the average water velocity in the pipes (x-axis), based on the simulations done.

The three lines with the lowest pressure drop in Graph 8 are the simulations with the improved meshing. The 700-1000S rack and the 600-1000S rack's results follow each other closely, both in the 2-pass configuration, and the 4-pass configuration. This is not the case with the 600-1000S rack with the improved meshing, which gives a result less than half of the first one. This is further discussed in chapter 4. The other observation is universal for all racks, even with the improved mesh, and that is that the pressure drop when running a 2-pass configuration is very close to half, of the pressure drop when running a 4-pass configuration.

3.4 Combined results

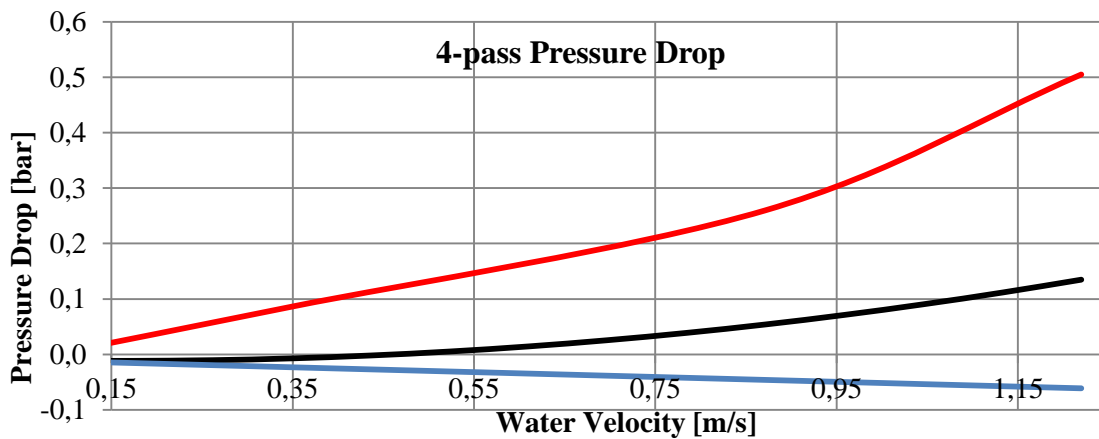
By combining result from different tests and simulations, they results become more clear.

3.4.1 Experimental combined results

The results of the experimental physical testing are here shown in the context of its comparable result from the simulations.

3.4.1.1 4-pass Rack

The 4-pass testing results are the results presented in 3.1.3 where the “no pass” results has been subtracted from the “4-pass rack” results, to give the result of only the pressure drop through the rack. Since both of these results has been adjusted both upwards and downwards, the results presented are the maximum- and minimum-lines, which represent the span within the + or – 15%. The simulation results presented are the same ones shown in 3.3.

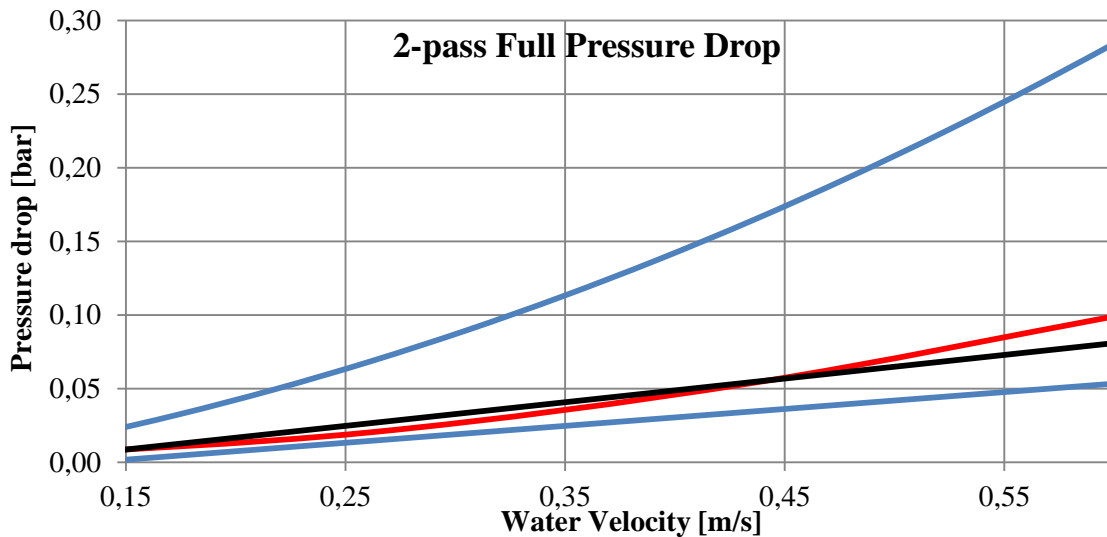


Graph 9: The blue line is the experimental minimum pressure drop of the 4-pass, the black line is the measured value and maximum. The red line is the simulated pressure drop of the 4-pass.

After adjusting the test results, the minimum value of pressure drop, becomes negative. This is not realistic, so the area in which the value can lie, is between zero and the measured black line. The simulated results are much higher.

3.4.1.2 2-pass Full Rack

The 2-pass full rack testing data is taking from the same chapter as the previous one, and calculated in the same way. The simulation results are not presented previously, because this is not a kind of simulation with a high priority. Normal 2-pass simulations consist of two inlets and two outlets, but as explained in 2.2.3, there were only one of each in the testing, with an extra flow splitter frame installed, to eliminate the effect of only one. Therefor there was done a separate simulation, with only one of each, but the results will not be used for anything more than comparing with the experimental testing data.

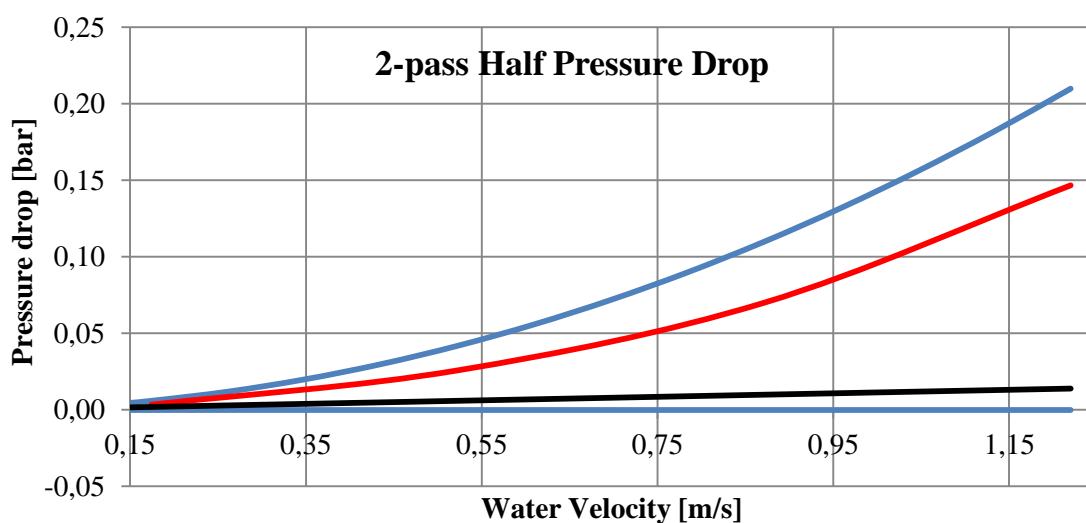


Graph 10: The black line is the test result, the two blue lines represent the maximum and minimum values of the testing results, and the red one is the simulated result.

The graph shows that the simulation result is consistent with experimental results, in the span of the data. The shape of the curve is not as consistent, so if extrapolating the results, the consistency would be lost.

3.4.1.3 2-pass Half Rack

The test results for these results are the results from the same chapter as previously, and calculated the same way. The simulation results are not presented previously, because this is only half the pipes of a regular 2-pass configuration, and it has been conducted an own simulation for it.



Graph 11: The experimental testing result with a black line, its maximum and minimum values represented in blue lines, and the simulation results in red.

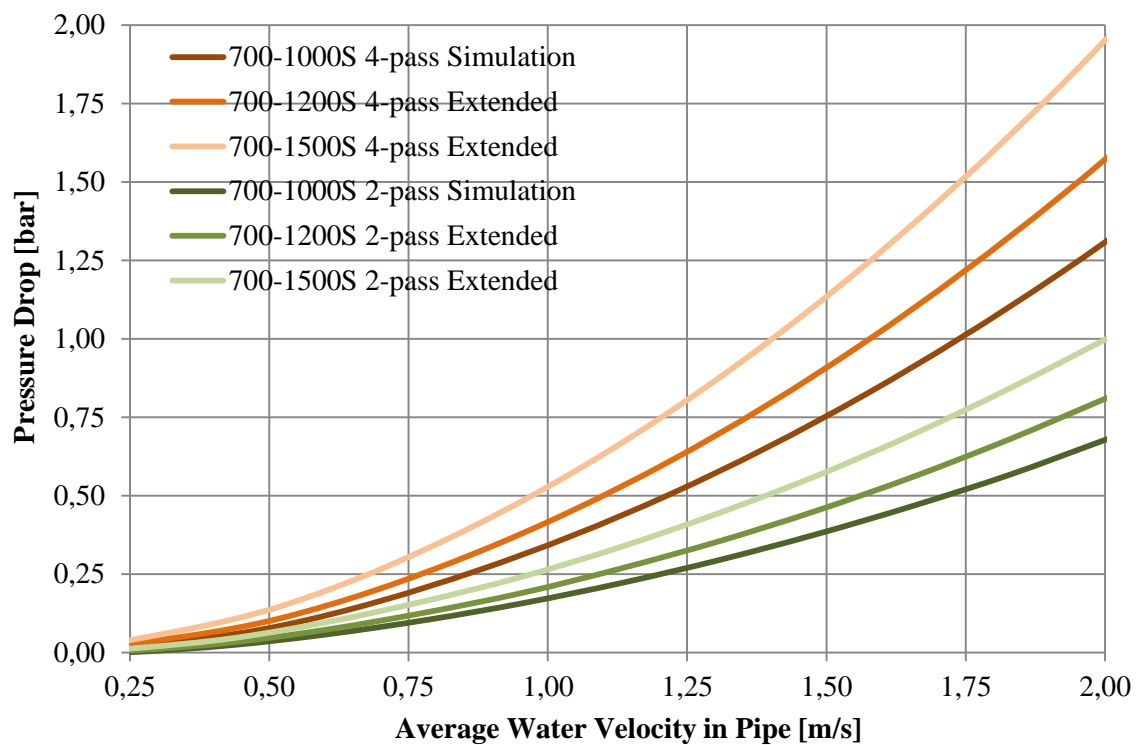
The simulated results presented are consisted with the experimental data's adjusted values.

3.4.2 Rack simulation results

The results presented here, is the results of the rack-simulations presented in chapter 3.3, combined with the results of the single pipe simulation presented in chapter 3.2.2.

3.4.2.1 700S-rack

In all the extended results presented for the 700S-rack, the factor of eight has been used, as described in chapter 2.8.2.



Graph 12: The combined results of the six different configurations of the 700S-rack.

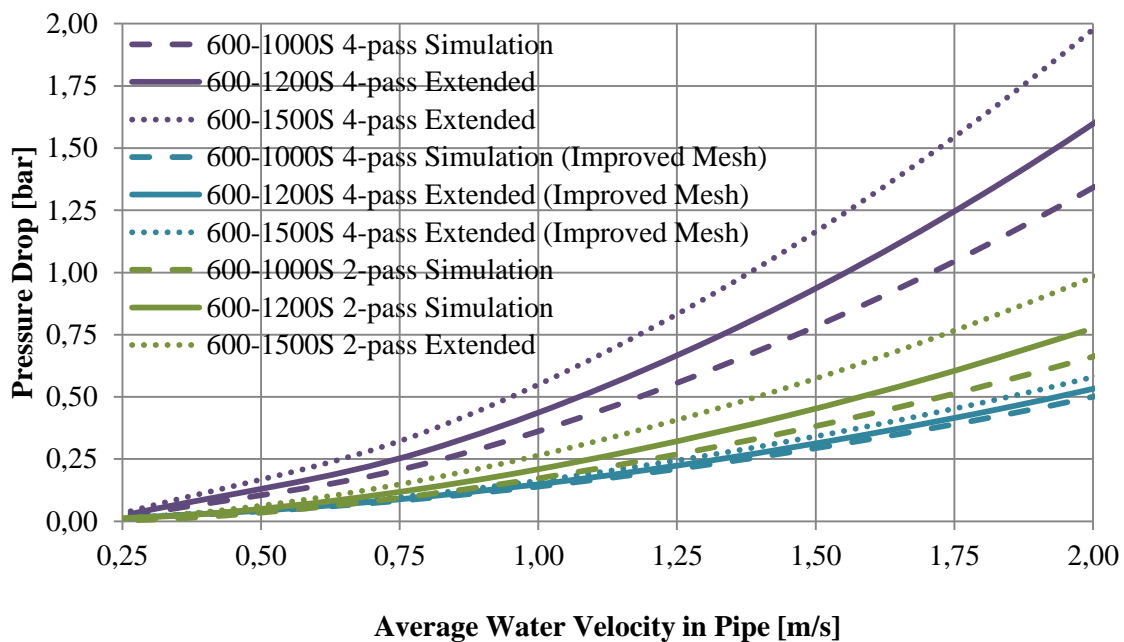
When adding a polynomial trend line (regression line) to every line in the graph, the formula of each graph can be displayed. With these equations the pressure drop at any optional value of water velocity can be easily calculated.

Table 20: A table of Graph 12 presented as an equation with the average water velocity as the X, to calculate the pressure drop. The three last columns is the pressure drop at 0,5 m/s, 1 m/s and 1,5 m/s.

Rack-Config.	Result Source	Equation [X= Water Velocity]	Pressure Drop [bar]		
			At 0,5 m/s	At 1,0 m/s	At 1,5 m/s
700-1000S 2-pass	Simulation	$0,1599*X^2+0,0265*X-0,0147$	0,04	0,17	0,38
700-1200S 2-pass	Extended	$0,1888*X^2+0,0346*X-0,0147$	0,05	0,21	0,46
700-1500S 2-pass	Extended	$0,2269*X^2+0,0539*X-0,0161$	0,07	0,26	0,58
700-1000S 4-pass	Simulation	$0,2922*X^2+0,082*X-0,0294$	0,08	0,34	0,75
700-1200S 4-pass	Extended	$0,3501*X^2+0,0981*X-0,0293$	0,11	0,42	0,91
700-1500S 4-pass	Extended	$0,4263*X^2+0,1368*X-0,0321$	0,14	0,53	1,13

3.4.2.2 600S-rack

The extended results presented for the 600S-rack, are both derived from the original mesh settings, as well as the improved mesh settings. The ones from the original settings have utilized the factor of eight, but the other ones do not, as explained in chapter 2.8.3. The large difference in results of the 600-1000S results are further discussed and investigated in chapter 4.



Graph 13: The combined results of the six different configurations of the 600S-rack, plus the simulation and extended result of the improved mesh configuration.

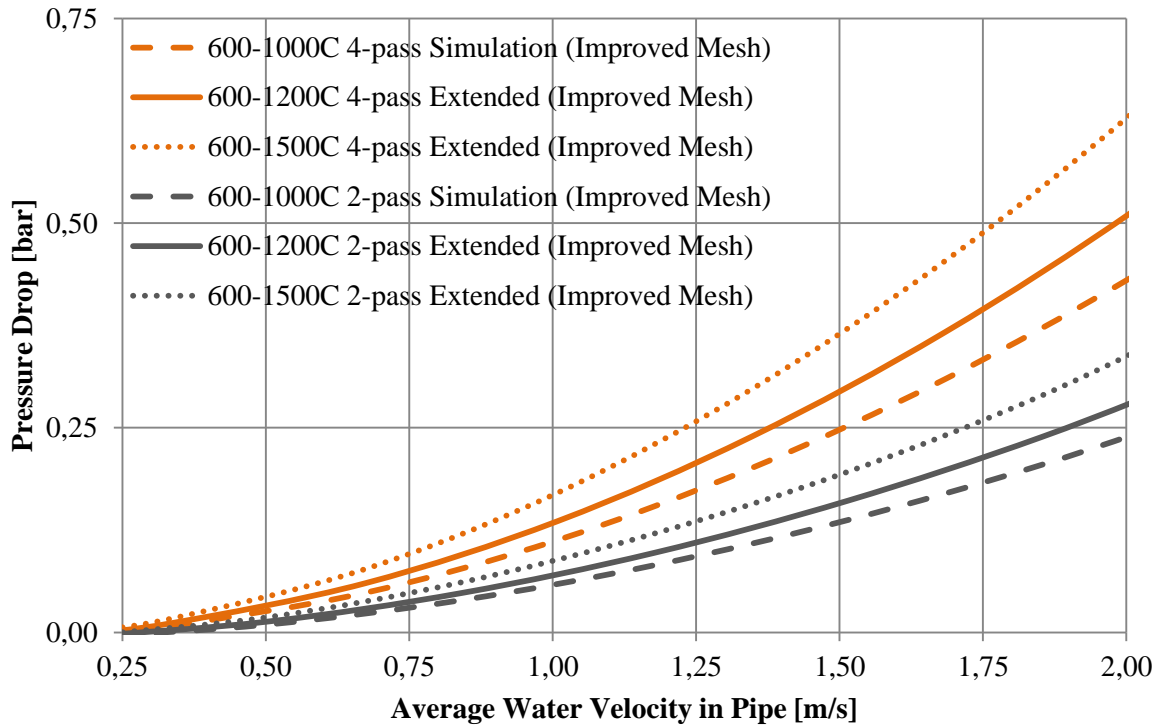
The equation of the regression line for each of the graphs is listed below. The pressure drop with three different water velocities are shown, based on the equation.

Table 21: A table of Graph 13 presented as an equation with the average water velocity as the X, to calculate the pressure drop. The three last columns is the pressure drop at 0,5 m/s, 1 m/s and 1,5 m/s.

Rack-Config.	Result Source	Equation [X= Water Velocity]	Pressure Drop [bar]		
			At 0,5 m/s	At 1,0 m/s	At 1,5 m/s
600-1000S 2-pass	Simulation	$0,1464 * X^2 + 0,0477 * X - 0,0208$	0,04	0,17	0,38
600-1200S 2-pass	Simulation	$0,1749 * X^2 + 0,0457 * X - 0,0119$	0,05	0,21	0,45
600-1500S 2-pass	Extended	$0,2111 * X^2 + 0,0794 * X - 0,0241$	0,07	0,27	0,57
600-1000S 4-pass	Simulation	$0,2805 * X^2 + 0,1276 * X - 0,0384$	0,10	0,37	0,78
600-1200S 4-pass	Extended	$0,3323 * X^2 + 0,1535 * X - 0,0412$	0,12	0,44	0,94
600-1500S 4-pass	Extended	$0,4057 * X^2 + 0,1993 * X - 0,0476$	0,15	0,56	1,16
600-1000S 4-pass	Simulation (Improved Mesh)	$0,1069 * X^2 + 0,0386 * X - 0,0057$	0,04	0,14	0,29
600-1200S 4-pass	Extended (Improved Mesh)	$0,1134 * X^2 + 0,0419 * X - 0,006$	0,04	0,15	0,31
600-1500S 4-pass	Extended (Improved Mesh)	$0,1226 * X^2 + 0,0476 * X - 0,0068$	0,05	0,16	0,34

3.4.2.3 600C-rack

All the results presented here is a direct combination of the rack-simulation, and the single pipe simulation, like explained in chapter 2.8.3. First, the results are plotted in Graph 14, before the equation of their regression line is listed in Table 22.



Graph 14: The combined results of the six different configurations of the 600C-rack, all of them which have an improved mesh than the original mesh. Notice the y-axis scale, compared to the two previous graphs.

Table 22: A table of Graph 14 presented as an equation with the average water velocity as the X, to calculate the pressure drop. The three last columns is the pressure drop at 0,5 m/s, 1 m/s and 1,5 m/s.

Rack-Config.	Result Source	Equation [X= Water Velocity]	Pressure Drop [bar]		
			At 0,5 m/s	At 1,0 m/s	At 1,5 m/s
600-1000C 2-pass	Simulation (Improved Mesh)	$0,0551 \cdot X^2 + 0,0144 \cdot X - 0,0112$	0,01	0,06	0,13
600-1200C 2-pass	Extended (Improved Mesh)	$0,0634 \cdot X^2 + 0,0173 \cdot X - 0,0111$	0,01	0,07	0,16
600-1500C 2-pass	Extended (Improved Mesh)	$0,0762 \cdot X^2 + 0,0218 \cdot X - 0,0112$	0,02	0,09	0,19
600-1000C 4-pass	Simulation (Improved Mesh)	$0,0952 \cdot X^2 + 0,0321 \cdot X - 0,0153$	0,02	0,11	0,25
600-1200C 4-pass	Extended (Improved Mesh)	$0,1128 \cdot X^2 + 0,0352 \cdot X - 0,0133$	0,03	0,13	0,29
600-1500C 4-pass	Extended (Improved Mesh)	$0,1385 \cdot X^2 + 0,0441 \cdot X - 0,0135$	0,04	0,17	0,36

4 Discussion and investigation of 600-1000S rack results

In this chapter, the two simulations of the 600-1000S, with different mesh settings, are investigated to find their differences and reason for them.

4.1 Result summary comparison

To see if the lowered pressure drop of the rack with the better mesh, might be evident of something different than only a better mesh, the total report summaries for each simulation is investigated. These full reports can be found as Appendix VI and Appendix VII but the differences between them are listed in the table below (Table 23), and the maximum/minimum table is separate as Table 24.

Table 23: A list of differences of the two simulations, with the criteria listed first.

Criteria		Poor mesh simulation	Improved mesh simulation
INPUT DATA			
Result resolution level (initial mesh setting):		4	5
RESULTS			
Iterations (one travel):		273	366
Meshing time:		Not displayed	Not displayed
Preparation for simulation [time]:		1:43	3:44
Convergence achieved [time]:		3:28:53	11:13:24
Calculation finished [time]:		3:13	8:05
Warning:		None	A vortex crosses the pressure opening
Basic mesh dimensions (see chapter 4.3)	Calculation Mesh		
	Number of cells in X	10	14
	Number of cells in Y	24	34
	Number of cells in Z	12	18
	Number Of Cells		
	Total cells	2 535 865	6 109 796
	Fluid cells	363 175	1 471 876
	Solid cells	779 580	1 749 960
	Partial cells	1 393 110	2 887 960
Goals			
Value [Pa]		124 357	110 478
Delta		42	21
Criteria		531	81

As a confirmation of what the goal for the second simulation was, to only change one single input parameter, the effect is obvious, and the number of cells has over doubled. Table 23 also shows that the result resolution level is in fact the only changed parameter.

4.1.1 Results

In the results part of Table 23, the number of iterations done before convergence is the same as the number of iterations needed to do one travel. This means that from “starting the flow” in the first iteration, by the last iteration this “particle” has reached the outlet. Because of the larger number of total cells, the iterations needed to do one travel, has changed. Both simulations are set up to not stop, until one travel is finished, and has reached convergence. The time it took for the mesh is not displayed, as the simulation has been done as a batch run, with the mesh copied from the first simulation. By doing this the mesh generation part only needs to be done one time for each rack configuration, instead of before every single simulation. As shown, the time each of the other steps of the simulation took, the improved mesh simulation used 2-3 time the time in every step, with the actual simulation before convergence being the one with the largest impact of time-usage. With this climbing from about 3,5 hours to over 11 hours, the total time for doing a series of simulation on one rack, triples.

The warning which appears in the pressure opening of the improved mesh, can be tracked back to the design of the inner space where the outlet lid is, but is not a real problem, because the flow would continue in a pipe in real operations.

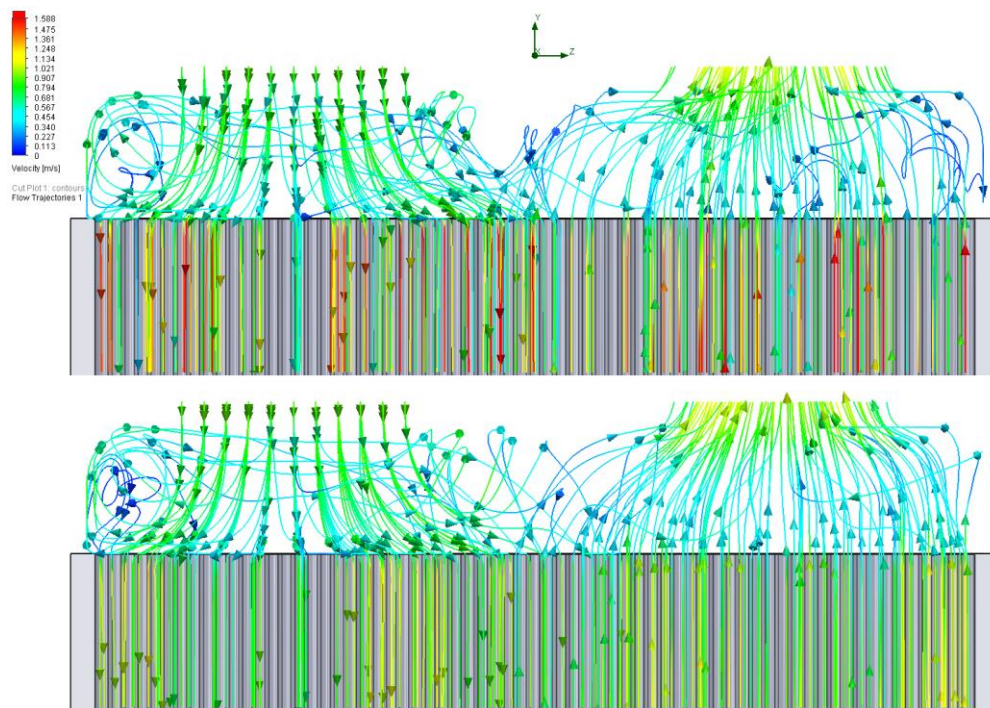


Figure 56: The flow trajectories at the inlet and outlet. The top one is the first simulation, and the bottom one is the one with improved mesh. The scale is water velocity and maximum is 1,588 m/s and minimum is 0 m/s. The calculated average water velocity is 0,794 m/s.



The flow trajectories of the two simulations do not differ significantly. At the exit the trajectories are somewhat more sorted, and it shows less turbulence towards the exit. To the left of the inlet, a vortex is very visible in both simulations, without any improvement in the latter simulation, which most likely means it is a realistic feature.

The calculation mesh and the number of cells are the next topics listed in the Table 23, and are commented and discussed in detail in chapter 4.3.

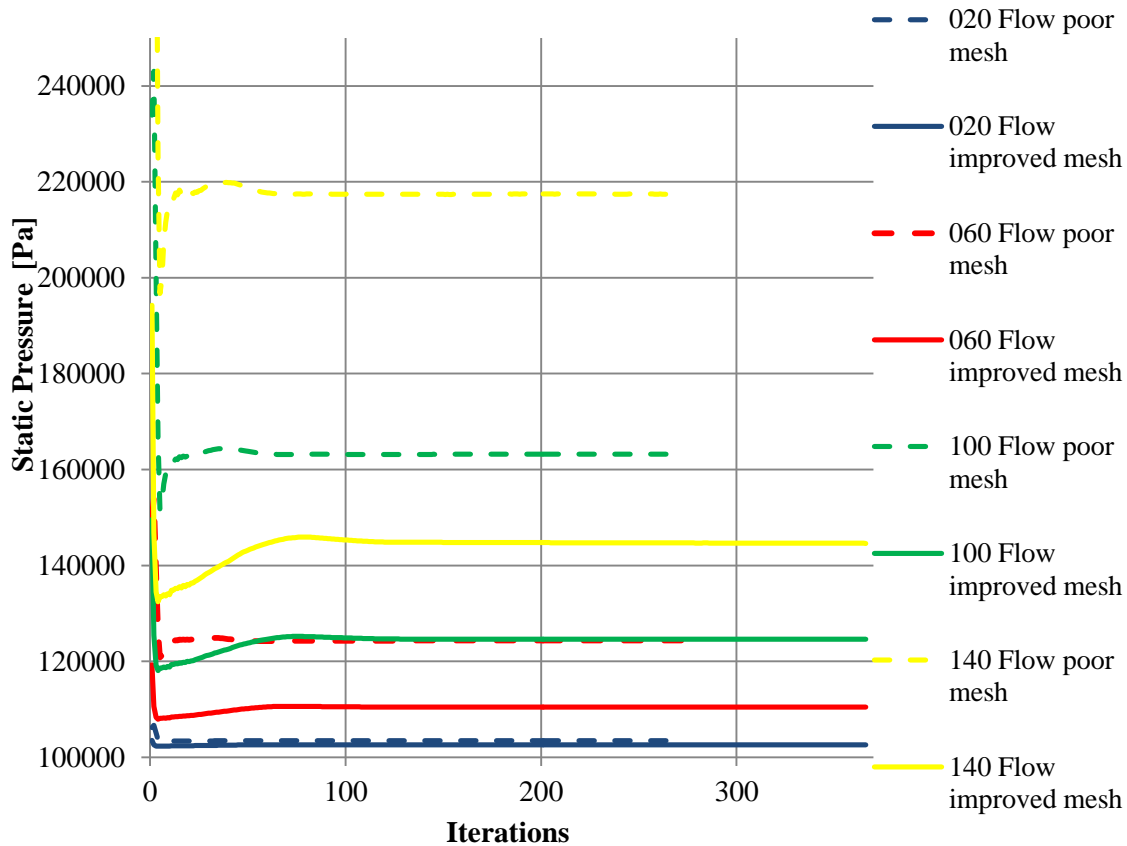
4.1.2 Goals and convergence

The bottom part of Table 23 gives information of the convergence of the result goals of each simulation. The values are, as discussed previously very different, but so is the delta and the criteria. The delta is the dispersion of the goal, in a range selected automatically. This range is continually being updated to look for convergence, but when finished, the differences in this range will still give a good indication of the stability of the results. To see that this delta is cut in half in the improved simulation, gives the results more validity.

If the simulation has done one travel, and the goal not converged, the simulation will continue until the delta drops below the criteria value. This value can be selected manually, but is here selected automatically by the program, and gives a good indication of how strict the program will be, for the result to converge. Since this is done automatically it reflects the program's view of the model and simulation, in regard to the result. Since the criterion of the improved mesh simulation is only 15% of the value for the first simulation, it gives a reason to think that the program is more satisfied with the model and its mesh.

When exporting the result file as an Excel file, the results are not only given as a value and its average, maximum and minimum value, but the entire list of value of each iteration is given in a list, and as a plot. The next graph (Graph 15) is of the goal, also the pressure and at what iteration. The plots shown are only of the comparable simulations done, with the same flow, for easier comparing them.

Convergence plot simulation



Graph 15: On the x-axis is the iteration of the simulation, and on the y-axis is the pressure at the inlet. As the pressure at the outlet is set to 1 atm. (101325 Pa), the plot can give an indication of the convergence. The solid lines are the simulation with improved mesh, and the dotted line is the first simulations with poor mesh.

By doing this the convergence of the results will be shown, to be sure the simulation ended successfully or if the results are evident of some understandable bug in the program, or of any other no logical incident in the calculations. In the result file for each simulation the goal is plotted according to iteration, and is also a source of information.

4.1.3 Minimum and maximum

The difference in the minimum and maximum values of the table below (Table 24) is very different. In the poor mesh simulation, almost every single parameter has a more extreme value, than in the improved mesh simulation. This translates to more uncertainties in the values, because its interpretation of the model creates these extreme values.

Table 24: Further information from the full simulation reports, the maximum and minimum values of selected parameters.

Name	Poor mesh simulation		Improved mesh simulation	
	Min	Max	Min	Max
Pressure [Pa]	101113.50	134488.17	101073.64	119559.18
Velocity [m/s]	0	3.062	0	1.657
Velocity (X) [m/s]	-3.061	2.928	-1.512	1.494
Velocity (Y) [m/s]	-3.046	3.019	-1.657	1.478
Velocity (Z) [m/s]	-0.964	1.310	-1.061	1.297
Vorticity [1/s]	3.443e-006	2342.688	8.537e-005	1091.239
Shear Stress [Pa]	0	75.61	0	19.37
Relative Pressure [Pa]	-211.50	33163.17	-251.36	18234.18

4.2 Cut plot comparison

To better understand and see the differences of the two simulations, cut plots of the flow velocity and pressure, in addition to the mesh, are used. By comparing the same areas, with the same flow, differences appear because of differences in the interpretation of the rack in the two simulations. Every figure shown in this chapter is divided in three different plots of the same area. The ones to the left is from the first simulation of the 600-1000S rack, with its scale set automatically according to what SolidWorks means is favourable. These scales are then copied to the plots in the middle, but these are from the second and improved simulation. By being sure the scale is identical, the plots are directly comparable. The plots to the right have their own scale, and this is the automatic scale for the improved simulation, which the plots also illustrate. The plots are created with the two main parameters shown, the pressure and the water velocity, and the top and bottom values of the plots are given in the figure caption.

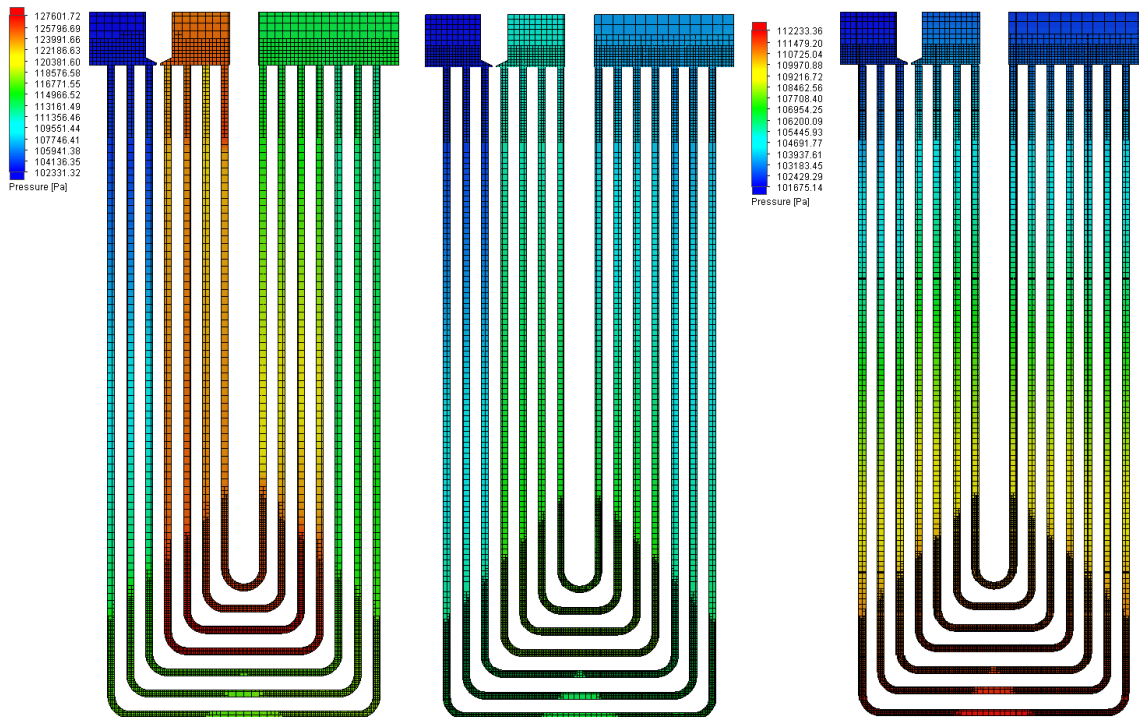


Figure 57: Pressure plot cut through the middle of the rack. The coarse simulations value: Maximum: 127601,72 Pa, Minimum: 102331,32 Pa. The improved simulations values: Maximum: 112233,36 Pa, Minimum: 101675,14 Pa.

Straight away it is obvious that the difference of the pressure is smaller in the improved simulation, which is also evident in the result. By looking at the improved simulation plots with automatic mesh, the distribution of the pressure is also a lot more logical, in the sense that the highest pressure will be in the bottom of the rack, due to gravity. In the top left corner of each of the plots, is the pressure at the inlet and the outlet. The outlet is in every plot dark blue, because the pressure in that region is the lowest. On the other side of the flow splitting frame, the white area without water, the pressure is naturally much higher, and indicates the inlet pressure. In the first plot, this area is very close to the maximum value of pressure (orange VS red), but in the plot to the right, the pressure in the area is not close to the maximum pressure on its scale. In comparison, the pressure here is visualized with just a slightly lighter blue, which is far from the maximum pressure of the rack, which is in the bottom of the pipes. The reason for this is that the pressure difference due to height has a larger degree of significance in the rack with the lowest total pressure drop, like the improved mesh simulation.

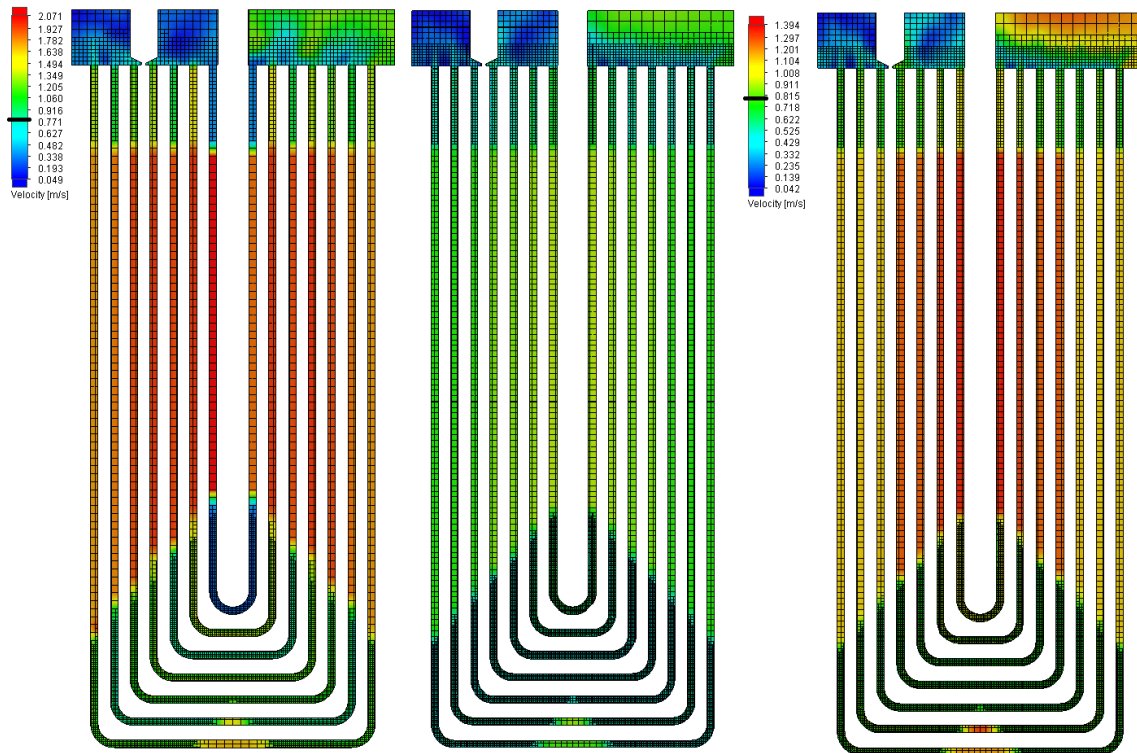


Figure 58: Velocity plot cut through the middle of the rack. The coarse simulations value: Maximum: 2,071 m/s, Minimum: 0,049 m/s. The improved simulations values: Maximum: 1,394 m/s, Minimum: 0,042 m/s. The average water velocity in the pipe is calculated to 0,794 m/s, and its approximate value is marked on the scale.

For the velocity plots, the differences in water velocity from the fine mesh areas to the coarse mesh areas are clearly shown, in both simulations. In the coarse mesh simulation the velocity goes from about 1,2 m/s in the inlets, to about 1,9 m/s in the straight pipes with poor meshing. For the improved simulation, these numbers are about 0,8 m/s to 1,1-1,3 m/s, which is a significant smaller span. Still, the calculated average velocity in the pipes should be 0,794 m/s, so the inlet and outlet areas are quite close, while the straight pipe part is far off. When comparing the velocity difference in the top areas of the rack, to the straight pipes, this difference is smaller in the improved mesh simulation. In the coarse simulation the colour changes from blue and green to red, but in the improved one it changes from blue and yellow to yellow and red.

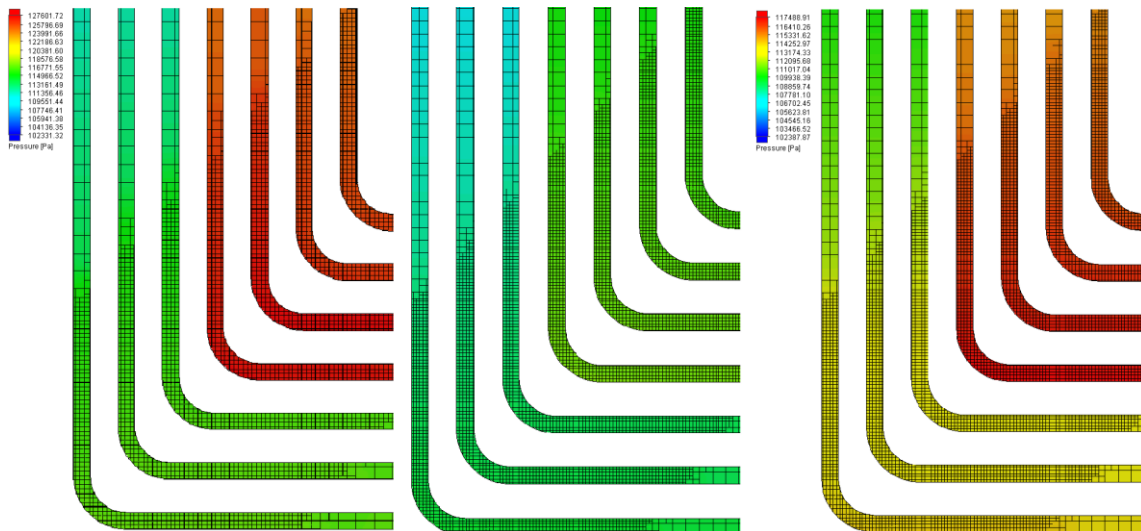


Figure 59: Pressure plot cut through the middle of the rack, zoomed in to the bend area. The coarse simulations value: Maximum: 127601,72 Pa, Minimum: 102331,32 Pa. The improved simulations values: Maximum: 117488,91 Pa, Minimum: 102387,87 Pa.

The close up pressure plots of the bend area does not tell us much more about the results. It is clear in all three plots that in the four visible inner pipes, the pressure is significantly higher than in the other three. This is because these pipes are the pipes the flow enters first, before it exits them and enters the other pipes. These pipes will then experience a higher pressure, which is clear in both cases.

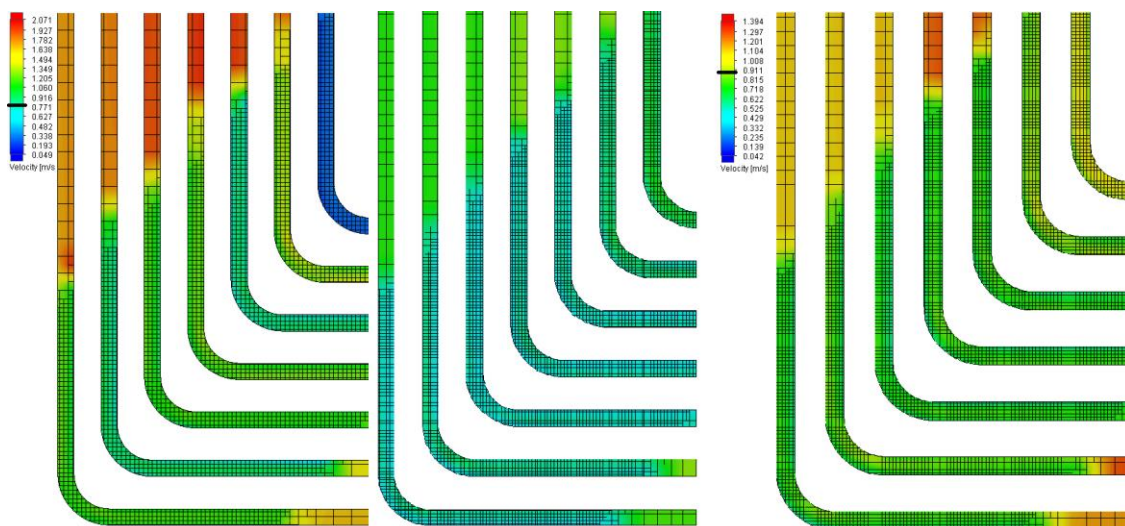


Figure 60: Velocity plot cut through the middle of the rack. The coarse simulations value: Maximum: 2,071 m/s, Minimum: 0,049 m/s. The improved simulations values: Maximum: 1,394 m/s, Minimum: 0,042 m/s. The average water velocity in the pipe is calculated to 0,794 m/s, and its approximate value is marked on the scale.

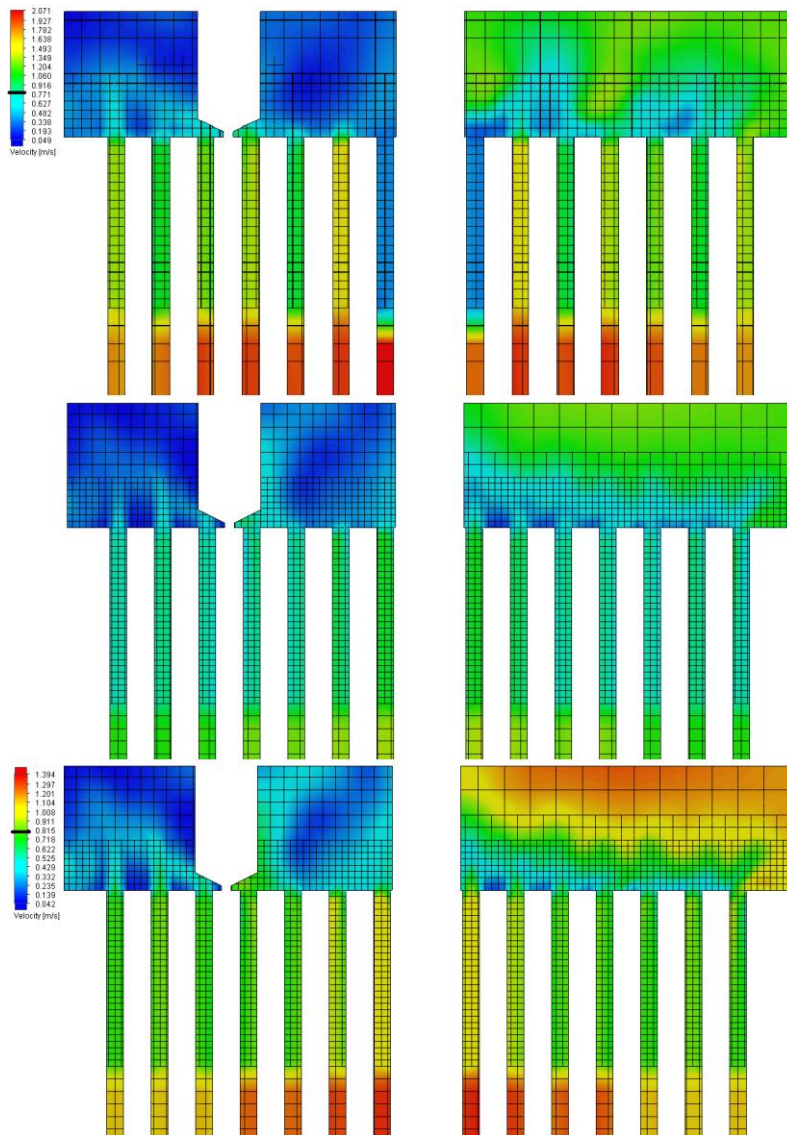


Figure 61: Velocity plot cut through the middle of the rack. The coarse simulations value: Maximum: 2,071 m/s, Minimum: 0,049 m/s. The improved simulations values: Maximum: 1,394 m/s, Minimum: 0,042 m/s. The average water velocity in the pipe is calculated to 0,794 m/s, and its approximate value is marked on the scale.

When zooming in to the bend area, and plotting the velocity, another special feature is clearly shown. The most inner pipe has, in the coarse mesh simulation, almost no flow through it. The velocity of the water in this pipe is close to zero, but when comparing to the improved simulation this un-logical feature disappears. There are also two other pipes, in the coarse plot, which stand out for no apparent reason, and this is also not evident in the improved one. The velocity is more

uniform in the different pipes, with a small but steady, increase towards the inner pipes.

This supports the theory

from chapter 2.8.1 because the shorter the pipe, the higher velocity it needs, to experience the same pressure drop.

The plots to the left are zoomed in plots of the area of water inlet and outlet of the pipes. The main visual difference is the spread of water velocity in the pipes of the first (top) simulation, compared to the improved one. The contours of the velocity out of the pipes on the right hand side, are clearer in the improved one as well. The sudden increase of velocity when the water enters the poor mesh regions, in every pipe, is evident of challenges faced with the mesh in those areas.

4.3 Cell size and amount of cells

The cell size and the amount of cells in the two simulations are here compared and discussed, as well as compared to recommended values.

4.3.1 Total amount of cells

When comparing the two simulations of the 600-1000S rack, the only settings which differs between the two, are the automatic mesh settings. To further investigate the differences created by this setting, the tab of “automatic settings” was unselected, to see the number of cells in each plane-direction. By comparing these numbers with the total size of the computational domain, its size is easily calculated.

Table 25: The connection between the size of the computational domain, and the number of cells in all three directions of the two simulated cases. The amount of cells created automatically is highlighted, its volume and its size, as well as the total number of cells. Extracted from Table 23.

	Computation domain [cm]	Level 4 refinement [cells] (total)	Level 5 refinement [cells] (total)
X-direction	46,6	10	14
Y-direction	111,1	24	34
Z-direction	56,8	12	18
Multiplied=	294068,4	2880 (2 535 865)	8568 (6 109 796)
Cell volume [cm ³]	Volume divided on nr. of cells=	102,11	34,32
Size (L,H,W) [cm]	Cube root of volume=	4,67	3,25

The reason that the total number of cells in both cases differs from the total number of cells in the computed simulations, is partly due to the setting selected called “Optimize thin wall resolution”, which will increase the mesh in certain areas. The two local meshes added contribute to most of the added cells, but in this chapter the focus is on the automated global mesh setting.

Since most of the computational domain of the rack simulation consists of single pipes, the dimension of the cells has a major impact on the accuracy of the calculations through the pipe. When decreasing the cell wall lengths from 4,67 cm to a smaller 3,25 cm, the difference in what Flow Simulation calculated is obvious from the results. Still, the improvement in cells size makes the cells still over three times as large as the diameter of the pipe (from barely 4,4 times). If continuing to improve the mesh, by decreasing the cell size, the results are most likely to continue to change. In a previous simulation of flow

outside of some pipes in a heat exchanger, the cell size used was 0,3-0,5 mm, with pipe dimensions of 5-14 mm²⁰, which is 10-45 cells the diameter. As shown in chapter 2.5.2 and 2.5.3 there is a selection in the manual mesh generation called “Characteristic number of cells across narrow channel”, which is of special importance. The pipe in this case has an inner diameter of 1,07 cm, and compared to the total volume of the rack and in the computational domain, it can very well be defined as a narrow channel. In the default automatic resolution level, this selection is set at 5, and at the resolution level of 5, this number is set at 10. What this indicates is that, if selected, the mesh will try to be refined to the level of having 5 or 10 cells across the diameter of the pipe. Compared to what has been simulated, where the cell is actually over three times as large as the diameter, not 0,2 or 0,1 times the diameter, it can be said it has an dramatic effect of the accuracy. In the previously mentioned simulations done with a mix of hexahedral and tetrahedral shaped cells, the number of cells across was for reference 4-5 cells, but gave good results due to the cell size¹³. Below (Table 26) is a table showing the required number of cells, in total, to get close to the mesh size recommended by the program.

Table 26: The first two rows shows the cell size and numbers from the simulation, and the rest is the size and numbers of cells to safsifye different number of cells across the pipe.

Number of cells across	Size (L,H,W,) [mm]	Cell volume [mm ³]	Total number of cells
0,23 (first simulation)	46,74	102107	2 880 (2 535 865)
0,33 (improved simulation)	32,5	34321	8 568 (6 109 796)
0,5	21,4	9800	30 006
1	10,7	1225	240 047
2	5,35	153	1 920 379
5 (default recommended)	2,14	9,8	30 005 923
10 (improved recommended)	1,07	1,23	240 047 384

If following one of the two recommended cell sizes from the table above, no further cell refinement would be needed, and none of the selections in the mesh generation process would have to be selected. The mesh would then end up being overly fine in the areas of the main inlets and outlets. Many cells would also be fully solid cells, without any fluid contact, which the program would not consider in the calculations. As shown, by using

the default value of numbers of cells across the pipe, the total amount would be almost five times larger than the improved simulation. Taking into account the time the mesh generation of the improved simulation took, which was around 72 hours, the need for greater computer power is obvious. If using ten cells across the pipe, with almost forty times the total number of cells, the requirements increase many fold.

4.3.2 Types of cells

The type of cells in a simulation, can tell us much about how the program has interpreted the model, as well as how the mesh generation and refinement is done. Each cell can be defined as one of five categories; fluid-, solid-, partial-, irregular- or trimmed-cells. Neither of the simulations has created cells in the two latter categories, but the three other ones are listed below, as well as the extent of them.

Table 27: A list of the types of cells in each of the two simulations. The numbers are extracted from Table 23, but with the percentage of each of them added.

Number Of Cells	Poor mesh simulation		Improved mesh simulation	
	Amount	%	Amount	%
Total cells	2 535 865	100	6 109 796	100
Fluid cells	363 175	14	1 471 876	24
Solid cells	779 580	31	1 749 960	29
Partial cells	1 393 110	55	2 887 960	47

The increase of the percentage of fluid cells in the improved simulation, reflects that the mesh is finer, as well as the increase of cells fully enclosed by water. These are the cells where the water will be able to flow freely, in whatever direction it needs, and wants. Because the simulations done in this project does not take into account heat transfer or any other phenomena where solid cells has an effect, the need of them are greatly restricted. The solid cells are fully enclosed by the solid restricting the water, but most of the interaction between the water and solid, will be in the partial cells, which in turn plays a very important role. The increase of percentage of the fluid cells can be explained by the refining in the areas of this interaction, where it has resulted in a larger decrease of the partial cells, than of the solid cells.

4.3.3 Simple pipe comparison

By finding the pressure drop of a single, short section of a pipe, with different methods, the errors between simulations and calculations can be found. The simple pipe is a pipe

with the inner diameter of 10 mm, length of 100 mm, and with the average water velocity of 1 m/s at 50°C.

4.3.3.1 Phenomenological equation

The dimensions used in the calculations are listed below (Table 28), and all values are specific for these calculations.

Table 28: A list of the parameters used the following calculations. Its symbol and units are shown, as well as its value, if given.

Name	Symbol	Value	Unit
Hydraulic diameter-inner diameter	D	0,01	m
Length of pipe	L	0,1	m
Average velocity of water	\bar{V}	1	m/s
Darcy friction factor (Colebrook equation)	f		-
Roughness of pipe	ε	$1,5 \cdot 10^{-6}$	m
Density	ρ	988,1	kg/m ³ -Pa*s
Dynamic viscosity	μ	$0,547 \cdot 10^{-3}$	kg/m*s
Head loss due to friction-Pressure drop	h_f		Pa
Reynolds number	Re		-

The equations used are taken from the book “Heat and Mass Transfer”¹⁶.

Reynolds Number:

$$Re = \frac{\rho * \bar{V} * D}{\mu} = \frac{988,1 \text{ kg/m}^3 * 1 \text{ m/s} * 0,01 \text{ m}}{0,547 * 10^{-3} \text{ kg/m} * \text{s}} = \mathbf{18064} \Rightarrow \text{Fully turbulent}$$

Colebrook equation for Darcy friction factor (can be found in a Moody chart, but with possibilities of reading error:

$$\frac{1}{\sqrt{f}} = -2,0 \log \left(\frac{\varepsilon/D}{3,7} + \frac{2,51}{Re\sqrt{f}} \right)$$

$$\frac{1}{\sqrt{f}} = -2,0 \log \left(\frac{1,5 * 10^{-6} \text{ m} / 0,01 \text{ m}}{3,7} + \frac{2,51}{18064 * \sqrt{f}} \right)$$

$$f = 0,0268509$$

The Darcy-Weisbach equation states:

$$h_f = f * \frac{L}{D} * \frac{\rho \bar{V}^2}{2}$$

$$h_f = 0,0268509 * \frac{0,1 \text{ m}}{0,01 \text{ m}} * \frac{988,1 \text{ kg/m}^3 * 1 \text{ m/s}^2}{2} = 132,66 \text{ Pa}$$

4.3.3.2 Simulations

There have been done simulations of seven different amounts of numbers across the channel, to compare the results to the other equations, and see how they differ from each other. In the mesh generation for the simulation, all selections of mesh refinement have been unselected, to only make single size cells with equal distribution. They are made of a manual input in the different directions. The program was not able to calculate the pressure drop in this model, with less than 2 cells across the diameter, so this is lowest number simulated.

Table 29: Different number of cells across the pipe diameter of the simulations, their dimensions and the total number of the cells.

Number of Cells across	Cell Size (L,H,W) [mm]	Cell volume [mm ³]	Total number of cells
2	5	125	80
5	2	8	1 250
10	1	1	10 000
15	0,67	0,296	33 750
20	0,5	0,125	80 000
30	0,33	0,037	270 000
50	0,2	0,008	1 250 000

In Table 29 the total number of cells is only total volume of the computational domain, divided on the cell volume. In the two next figures, the mesh is shown clearly.

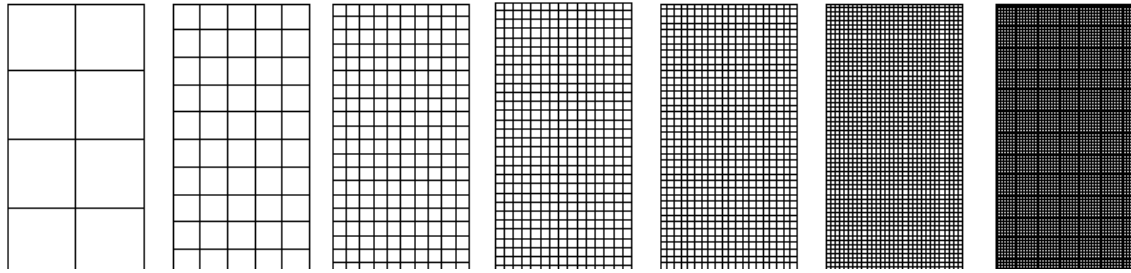


Figure 62: Mesh visualization of the seven different amounts of cells across the pipe diameter, viewed from the front.

If viewing the cells front the top, and through the pipe, it is easy to see how the number of cells across the diameter is made. When adding colour to each cell, with different colour for each of the cell types, this is even more emphasized.

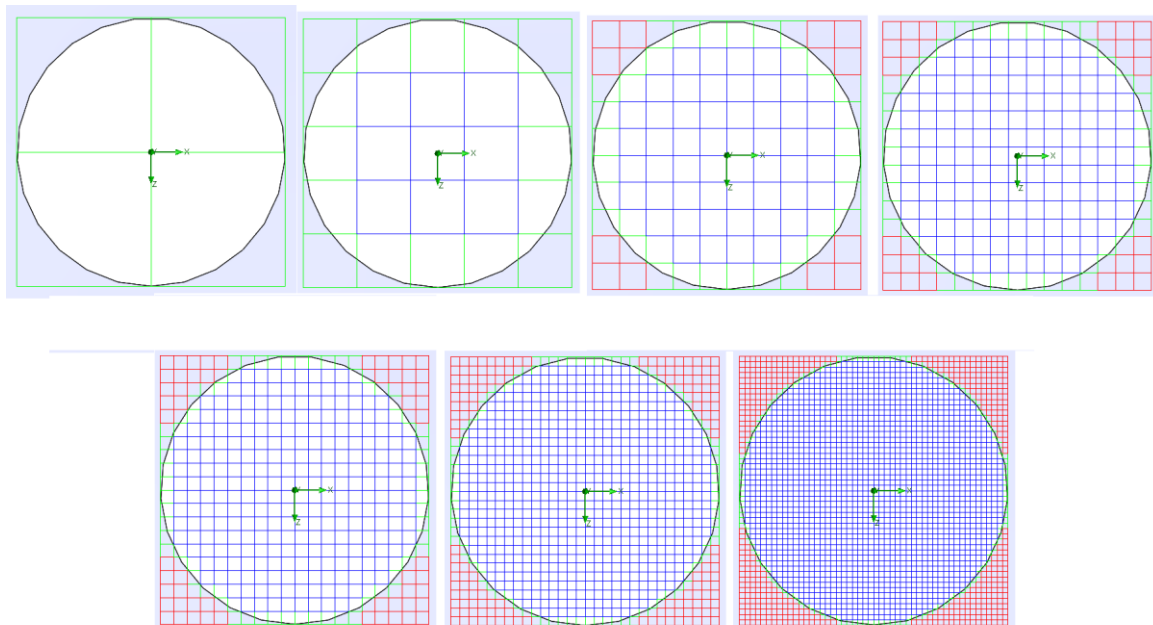


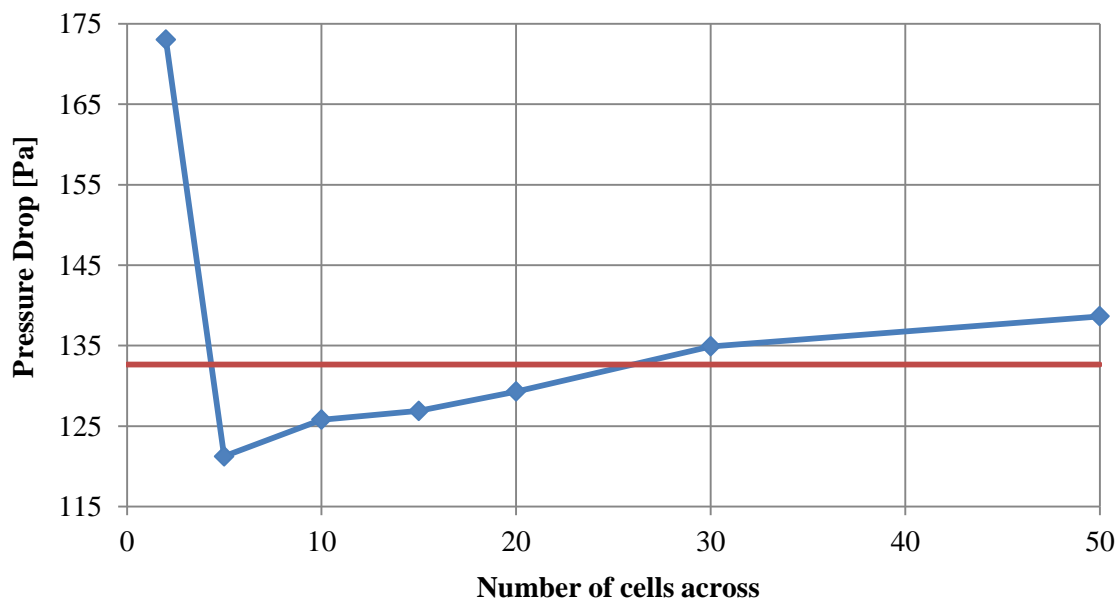
Figure 63: Mesh visualization of the mesh in the seven different simulations, with a birds-view. The green cells are partial cells, the blue are fluid cells, and the red cells are solid cells.

In the next table (Table 30) the results of the simulations done with the different number of cells and cell sizes are listed. Its convergence values are listed as well, and (except for the first one) the simulation with 30 cells across is the one with the lowest values of delta and criteria.

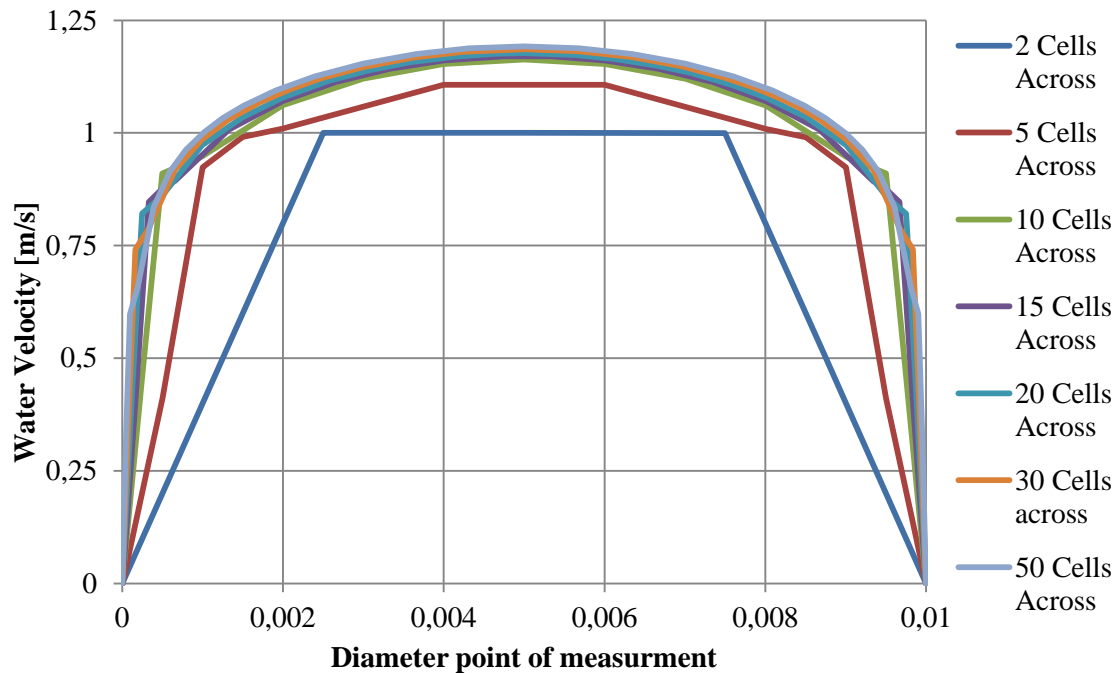
Table 30: The results of the simulations with different number of cells across the pipe diameter. Its pressure drop is showed, as well as its value relative to the calculated pressure drop. The delta and criteria for each simulation are the two last parameters.

Number of Cells across	Pressure Drop [Pa]	Relative to calculation	Delta [Pa]	Criteria [Pa]
2	173,05	30,4 %	0,0002	0,053
5	121,24	-8,6 %	7,922	8,136
10	125,80	-5,2 %	4,955	6,132
15	126,89	-4,3 %	2,134	2,213
20	129,30	-2,5 %	2,034	2,091
30	134,91	1,7 %	1,801	1,987
50	138,64	4,5 %	2,255	3,645

The simulation giving the result closest to the calculation is the simulation with 30 cells across the pipe diameter. Even though the result of the first simulation has, by far, the two lowest values of delta and criteria, the result itself is over 30 % higher than the calculated value, which makes it rule itself out. The simulation with the highest number of cells seems to experience more difficulties in making the result converge, than with fewer cells. This can be explained by the large amount of cells needed to be calculated with very little difference between them.



Graph 16: The blue line represent the simulated pressure drop of the different simulations, and the red line is the calculated value for reference.



Graph 17: A graph of the water velocity flow profiles through the pipe, with the different amount of cells across the diameter. With increasing cells, the turbulent flow profile is very clear.

When seeing the water velocity flow profiles from the different simulations, we understand better why the two first simulations, with the least amount of cells, give results that are over 5% of the calculated value. It is also evident that when reaching 10 cells and more across the diameter, the profile does not change significantly when adding more cells. Its profile is clearly turbulent²¹, as expected.

What this simple simulation shows us, when compared to the calculations, is the effect of the mesh. With the number of cells across a narrow channel like a pipe, even when following the recommendations of SolidWorks Flow Simulation, can be upwards as much as 10 % different from the equations based on consistent theory and empirical observations. It also tells us that the goal does not have to be to get the maximum number of cells into a simulation, because this will complicate the simulation, as well as be a waste of time and computing power.

5 Discussion

In this chapter the methods and results are discussed.

5.1 The experimental testing

The experimental testing setup and result handling are discussed in this chapter.

5.1.1 Factors of influence

When analysing the entire system for experimental testing, several uncertainties appear who can and will influence the reliability and accuracy of the tests.

5.1.1.1 Flow meter accuracy

The flow meter for the experimental tests is previously mentioned, and is an electromagnetic flow meter, by the manufacturer EuroMag, and model MUT1000EL²², with a MC608 converter²³. According to their web site, the accuracy of the sensor is 0,2 % with flow down to 0,5 m/s, which in our case equals to 31,8 m³/h. The converter is listed with an accuracy of 0,2-0,4 %. These numbers indicates a large accuracy in the readings, but there are several other factors which can affect the results.

The installation and setup of the flow meter can be a source of miss readings for the sensors According to²⁴ the optimal way of installing an electromagnetic flow meter is in a vertical position, with upwards flow.

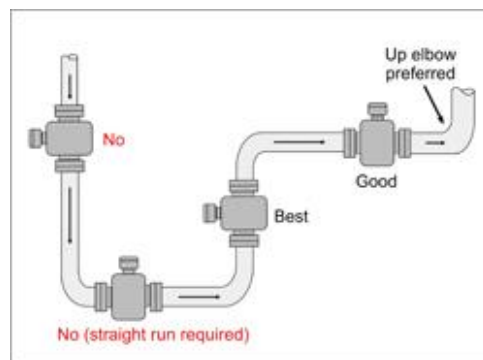


Figure 64: Different positioning of the flow meter will great different degrees of results.²⁴

The maximum operating temperature for the equipment is not likely to have been exceeded, due to the fact that for this part of the system, the water is never preheated (as is not the case for the flow meter in the other part of the system, which we did not use during these test, as described earlier).

The subject of flow meter accuracy was discussed thoroughly with Sperre before the testing started. They were aware of the possibility for relative large errors in readings, so they called for an electrician to come and do some tests where they compared flow with a clamp on, ultrasonic flow meter. As a result from these tests, they initiated further investigation of the errors, in order to give me more accurate numbers for what the flow actually was. These results are also listed in the same chapter. With a potentially large error in the flow, the results from the experimental testing will be devalued.

5.1.1.2 Placement of the pressure difference sensors

The placement of the pressure difference sensor in a system should be sufficiently far away from any bends or cross section area changes, so that the flow is as developed as possible.¹⁸ Because of the centrifugal effects there will be an increased pressure along the outer wall of the bend and a decreased pressure along the inner wall of the bend. This distorted flow pattern is what makes the pressure drop in the bend, but it will also affect the flow further down the line, after the bend is over. In some cases the velocity profile will not become normal with as much as 100 times the diameter down the line. Other sources¹⁹ say the effect of the bend will last up to 50 times the diameter downstream.

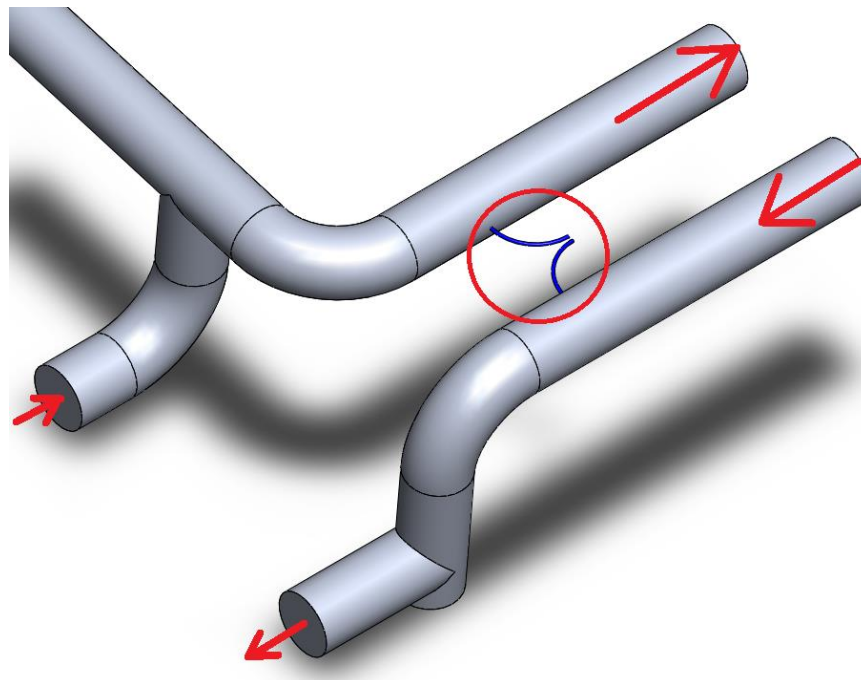


Figure 65: A simplified visual model of the piping system around the pressure sensors, in blue. The flow directions are marked with red arrows.



Figure 66: The small, blue pipelines are connector to the pressure transmitter in the middle, and to the main piping to the left and right.

As we can see from the picture, the inlets flow comes from a straight pipe for several diameters, but on the outlet line there is a bend in close proximity of the sensors.

5.1.1.3 Cross section area

In order to find the most accurate pressure drop in the component we are testing, the pressure drop in the system alone plays an important role. The more complex, in a flow pattern sense, the system is, the larger its internal pressure drop will be. As described previously the cross section area of the flow is mainly between 150 mm diameter and 125 mm diameter, but it is also reduced to 65 mm diameter in the connecting hoses to the rack. What this does is increase the pressure drop because of the velocity and turbulence of the water increases many folds. The difference of a 150 mm diameter to a 65 mm diameter in regard to the cross section area is $(75\text{mm}^2 / 32,5\text{mm}^2) = 5,33$. This means that the area is 5,33 times larger in the large pipes. The velocity of the water will then also have to increase by the same factor. The inlets and outlets of the rack are all 150 mm diameter and the minimum flow area for the water through the pipes in the rack is $(354 \text{ pipes} * \pi * (10,7\text{mm}^2/4)) = 31831,8 \text{ mm}^2$, but the small hoses is only $(\pi * (65\text{mm}^2/4)) = 3318,3 \text{ mm}^2$. This is barely ten per cent of the total cross section area inside the rack.

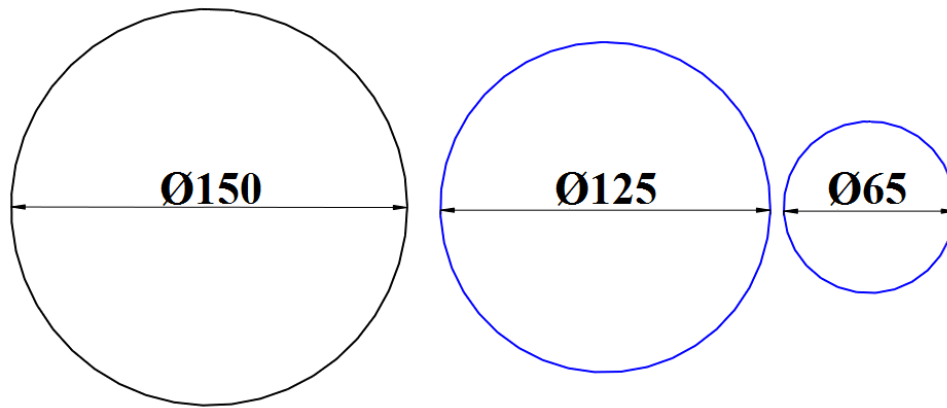


Figure 67: The three pipe diameters used in the system, in scale with each other. The black one is the one used for the main piping, and the one to the right is the inside diameter of the connecting hoses.

This adds up to a large pressure drop in the system, and that the effect of having a rack installed under testing is very small. By comparison it is like finding the height difference of water when adding one more bucket of water, into an already filled up bathtub.

5.1.1.4 Temperature difference

These tests were done in a partly closed loop of water. A large tank was filled about half ways with water over night, but it was continually filled during the time of testing. This is due to the loss of water during changing the piping connections. The water filling the tank was taken from a normal household water hose, at approximately 4,85°C. The initial test was then done with this temperature, but during the test the water became warmer. This is due to the convection from the heated air in the testing facility, as well as the motion of the water which creates internal sheer stress and higher temperature. The tests were done during three days, and during the night the temperature decreases again. One of the days the weather was cold, so we used heaters to heat the facility, which means that in some of the series of tests the temperature increased by 1,5°, and some only by 0,2°. The total span of the water temperature the testing were done with was 4,23° to 6,98°. This difference of 2,75° is not significant, but two parameters this affects is the density and the dynamic viscosity. The change in density is negligible, but the dynamic viscosities change is 7,7%, and affects the Reynolds number equation shown in 4.3.3.1. Still, the total change is pressure drop due to temperature difference, is within the accuracy of the readings.

5.1.2 Result adjustment

The amount the results are adjusted, to compensate for reading errors in the instrument, and other uncertainties, cannot be supported by any exact measurements. Since all experimental data are taken in the same system, with the same instruments, there are no other results they can be compared with, to confirm the numbers. The way the results were adjusted, were by only adjusting the flow parameter in the results. The adjustment could also have been done by adjusting the pressure drop, to the original flow rate, which might have given another result.

5.2 The simulations

The simulations of the rack and its part are discussed here.

5.2.1 Inlet conditions

The inlet flow condition of every simulation is a uniform distribution of the flow. This is very seldom the case of flow in a pipe. The options available in the programme were to set the flow as fully developed. A fully developed flow in a circular pipe has a velocity profiled as the one to the right in Figure 68, and will not be the case straight after a bend, entrance or cross section change.

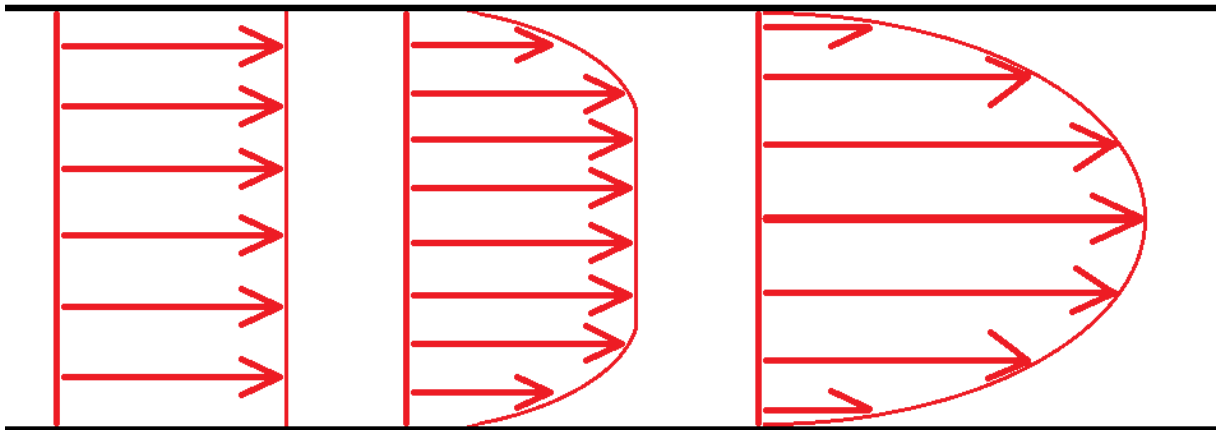


Figure 68: Flow profile of the velocity in a pipe. To the left is the inlet profile used in the simulations. In the middle profile, the flow has started to develop, and the one to the right is a fully developed laminar flow profile.



5.2.2 Mesh

As described in chapter 2.3.3 and 4.3, the mesh of the model in Flow Simulation is of great importance to the results. This is thoroughly discussed previously.

5.2.3 Computer capabilities

The computer's capabilities to do complex and demanding simulations are mainly set by its CPU and RAM.

CPU is the "Central Processing Unit" of the computer, and can be called its brain. This is the place where most of the processing and therefor calculations are done, and its limits are loosely set by their clock rate and the amount CPU's or CPU-cores working. The clock rate is the CPU's "rate of instruction", is measured in hertz. The higher amount of CPU's working together in parallel, the most instructions it can do at the same amount of time as well.

Ram is the "Random-access Memory" of the computer, and is also hardware. As the name says, it is a storage unit of the computers data, most often short term. It has to receive the data produced by the CPU. As the memory of the RAM available decrease, it also has to send data to the hard drive of the computer for storage.

From the full reports created by SolidWorks, the system information is shown. When comparing the computers used for the rack-simulation, to a normal laptop, it is evident that those computers are in fact more powerful, and suited to compute the amount of information needed in a large simulation.

Table 31: System information of a software upgraded 5 year old laptop.

Product	Flow Simulation 2013 SP3.0. Build: 2339
Computer name	SJEF-PC
User name	Sjef
Processors	Intel(R) Core(TM)2 Duo CPU T6500 @ 2.10GHz
Memory	4090 MB / 8388607 MB
Operating system	Windows 7 Service Pack 1 (Build 7601)
CAD version	SolidWorks 2013 SP3.0
CPU speed	2100 MHz

Table 32: System information of one of the three identical computers used for simulations.

Product	Flow Simulation 2013 SP4.0. Build: 2401
Computer name	TFFL4-04
User name	lassis
Processors	Intel(R) Xeon(R) CPU E3-1230 v3 @ 3.30GHz
Memory	16297 MB / 8388607 MB
Operating system	Windows 7 Service Pack 1 (Build 7601)
CAD version	SolidWorks 2013 SP4.0
CPU speed	3301 MHz

5.3 Results

The method of simulating one single pipe, and finding a correlation factor to a full rack, is a method of simplifying and extrapolating results in which could be investigated further. The reason for this extrapolation comes down to, once again, computer power and time available. To more confidently simulate the entire range of rack-sizes, all of them needs to, individually be mesh optimized and simulated, or at least each series. If using the method used in chapter 2.8, this could be confirmed better, by comparing to a fully simulated rack.

6 Conclusion

This chapter is divided in four sections. By concluding the two methods individually, their strengths and weaknesses are emphasized better. The results are then concluded, before the recommendations for future testing and simulations are listed.

6.1 Experimental testing

The use of experimental testing for finding the pressure drop can be an exact method, if the system used for the testing are built specifically for the task. The system used for the testing presented here, is not built for the task of testing a heat exchanger of this size. A Rack Cooler of a smaller configuration (like the 600C-serier) would be more suitable, in order to achieve the desired water velocity inside the pipes. The pressure drop of such a configuration would also differ more from the systems internal pressure drop, and would therefor also be more exact. Since the system were built up with only one inlet and out outlet, it was impossible to replicate one of the two flow configuration exactly (2-pass).

The flow meter was not calibrated, and this introduced an uncertainty in what the flow actually was, during testing, especially since there were technicians doing measurements on arrival to the test facility.

One of the reasons the experimental testing can be the desired way of finding the pressure drop, is that the testing can be done on a fully functional and finished product, like done here. The challenges of change in component design and building the model correctly in a software programme, is not an issue when doing physical testing. The drawback is that the rack has to be physically built before they can achieve applicable results.

6.2 CFD simulations

The main drawback using computational fluid dynamic software for a large and complex model as the Rack Cooler, are the uncertainties during simulations. As mentioned in chapter 3.3, an attempt of simulating an already simulated configuration, but with one higher level of mesh refinement, resulted in a very different result, and an investigation of why. For this method to be reliable, the mesh has to be refined to a much larger degree than what was possible with the recourses available. This proves that the computing power available was not sufficient to get the results desired, because the mesh had to be a lot more coarse than it should have been.

The method described in depth in chapter 2.8, with the use of one single pipe simulation to see the difference in pressure drop when changing the pipe length, is a method which might not have been exact enough. The factor used for correlation (8), is quite exact for the situation it derived from, but may not be as transferable as it has been used.

The flow patterns in the areas of inlet(s) and outlet(s) derived from the simulations are results with the most certainty to. These are in areas where there is a sufficient mesh to see where the water goes. These results can be used for optimizing the area for reducing the vortexes and lowering the pressure drop.

All the parts drawn in the 3D-program were drawn to be used as manufacturing processes, and not CFD simulations. This made it necessary to do adjustments in tolerances, because in the simulations the whole model needs to be water tight, which in the original model was not. This is because the tolerance it is manufactured with is used for inserting the pipes, and then expanded that area of the pipe for making it a tight and fastened connection.

6.3 Results

The most unambiguously result, which is supported both of the testing and all the simulations, are that the pressure drop in a 2-pass configuration is more or less half of the pressure drop in a 4-pass configuration.

6.4 Future work

The recommendations for further work are split in two sections. The first one is for the physical testing of the Rack Cooler, in order to achieve more precise, valuable, consequent and reliable results. Section two gives recommendations for the use of computation fluid dynamic software, to simulate the pressure drop.

6.4.1 Experimental testing

The existing test system should be rebuilt and upgraded to better accommodate testing of Sperre's Rack Cooler. Below is a list of these changes, necessary for pressure drop testing:

- Calibrate and/or upgrade the flow meters installed
- Increase the pumps capacity to be able to reach the flows the racks are designed for.



- Move pressure difference sensor outlets to areas of more/fully developed flow profile.
- Install adjustable piping or flexible hoses for connection to the rack, with the same diameters as the openings in the rack. Because these openings have different dimension according to which size rack it is, there should be a selection of connections. These must be installed in a matter where both inlets and outlets can be utilized.
- The temperature of the water during testing should be as close to the temperature of the situation it is trying to replicate.

If upgrading the system to use its full potential, e.g. large racks with flow both inside and outside the rack, these upgrades must be done to the entire system. These tests would then be used to test its heat transfer abilities, and upgrading both the water tank and the water heat (for the circuit not used for the testing presented here), might be a necessity.

6.4.2 CFD simulations

The first and most important step towards being able to simulate the pressure drop, and/or the entire rack system, with heat transfer, is being sure the computer used are capable of such demanding simulations. I recommend consulting computer experts, to find the specific needs for a computer suitable. As shown, a normal, brand new workstation is not enough. The possibility to rent computer power in an off location computer centre, should be investigated and considered, if found applicable.

The recommendation from the program of “number of cells across narrow channel” should be strictly used as a minimum value. This is tested in chapter 4.3.3, and the results show that, in these cases, 30 cells should be used across the pipe.

7 Reference List

1. Agency, I. E. (2013). *World Energy Outlook 2013: Executive Summary*. London. 15 pp.
2. marketsandmarkets.com. (2014). *Subsea Production & Processing Systems: Market by Technology/Components, Types & Geography - Global Trends & Forecasts to 2018*. *Markets and Markets*: 249.
3. marketsandmarkets.com. (2013). *Offshore Support Vessel Market: Global Trends & Forecasts To 2018*. *Markets and Markets*: 246.
4. *GEA Bloksma Box Coolers K-type*. (2013). gea-heatexchangers. Available at: <http://www.gea-heatexchangers.com/products/shell-tube-heat-exchangers/machine-cooling-systems/> (accessed: 12.10).
5. *Rack calculator*. (2012). Internal Sperre. Unpublished manuscript.
6. *Range oversikt*. (2014). Sperre Coolers AS. Unpublished manuscript.
7. *Sperre Rack Coolers References*. (2014). Sperre Coolers Web Site: Sperre.
8. Isaksen, L. F. (2013). TIP300 - Concept and product realization Phase 1: Flow optimizing of heat exchanger. UMB (NMBU): IMT. 84 pp.
9. Abraham, J. P., Sparrow, E. M. & Tong, J. C. K. (2009). Heat transfer in all pipe flow regimes: laminar, transitional/intermittent, and turbulent. *International Journal of Heat and Mass Transfer*, 52 (3–4): 557-563.
10. Chang, W., Pu-zhen, G., Zhan-wei, W. & Si-chao, T. (2012). Experimental study of transition from laminar to turbulent flow in vertical narrow channel. *Annals of Nuclear Energy*, 47: 85-90.
11. SolidWorks. *Flow Simulation 2013 Online User's Guide*.
12. TechnicalReference. *SolidWorks Flow Simulation technical reference PDF*.
13. Gandhi, M. S., Ganguli, A. A., Joshi, J. B. & Vijayan, P. K. (2012). CFD simulation for steam distribution in header and tube assemblies. *Chemical Engineering Research and Design*, 90 (4): 496.
14. Døving, R. (2014). *Oversikt rørplater Rack*. Sperre Coolers AS. 1 pp. Unpublished manuscript.

15. Corli, A., Gasser, I., Lukáčová-Medvid'ová, M., Roggensack, A. & Teschke, U. (2012). A multiscale approach to liquid flows in pipes I: The single pipe. *Applied Mathematics and Computation*, 219 (3): 866 and 871.
16. Çengel, Y. A., Ghajar, A. J. & Kanoğlu, M. (2011). *Heat and mass transfer: fundamentals and applications*. Singapore: McGraw-Hill. XXI, 902 s. : ill. pp.
17. Dai, B., Li, M. & Ma, Y. (2014). Effect of surface roughness on liquid friction and transition characteristics in micro- and mini-channels. *Applied Thermal Engineering*, 67 (1–2): 288-289.
18. Finnemore, E. J., Franzini, J. B. & Daugherty, R. L. (2002). *Fluid mechanics with engineering applications*. Boston: McGraw-Hill. 312-313 pp.
19. Biswas, P. G. & Som, P. S. K. Fluid Machinery. Available at: http://nptel.ac.in/courses/Webcourse-contents/IIT-KANPUR/FLUID-MECHANICS/lecture-37/37-2_losses_pipe_bends.htm (accessed: 11.04.2014).
20. Tan, X.-h., Zhu, D.-s., Zhou, G.-y. & Yang, L. (2013). 3D numerical simulation on the shell side heat transfer and pressure drop performances of twisted oval tube heat exchanger. *International Journal of Heat and Mass Transfer*, 65: 244-253.
21. FlowControl. *Flow Profile Theory & Practice*. Available at: <http://www.flowcontrolnetwork.com/articles/flow-profile-theory-practice> (accessed: 10.05).
22. MUT1000EL electromagnetic flow meter. (MUT1000EL). In *Euromag International*. Available at: <http://www.euromag.com/en/mut1000el> (accessed: 11.04.2014).
23. MC608 A/B/R Converter. (MC608 A/B/R). In *Euromag International*. Available at: <http://www.euromag.com/en/converters> (accessed: 11.04.2014).
24. Livelli, G. (2010). Flowmeter Piping Requirements. *How Much Straight Run Is Enough?* Available at: <http://www.flowcontrolnetwork.com/articles/flowmeter-piping-requirements> (accessed: 11.04.2014).

Appendix I List of current available rack-sizes⁶

Type	Frames	Tanktop	Antall rør	Surface (m ²)	Deling (mm)
500-0800-S	500	800	301	19,2	500
500-1000-S	500	1000	301	24,0	500
500-1200-S	500	1200	301	28,8	500
600-0800-C	600	800	367	23,4	500
600-1000-C	600	1000	367	29,3	500
600-1200-C	600	1200	367	35,1	500
600-1500-C	600	1500	367	43,9	500
600-0800-S	600	800	467	29,8	600
600-1000-S	600	1000	467	37,2	600
600-1200-S	600	1200	467	44,7	600
600-1500-S	600	1500	467	55,9	600
700-0800-C	700	800	551	35,2	600
700-1000-C	700	1000	551	43,9	600
700-1200-C	700	1200	551	52,7	600
700-1500-C	700	1500	551	65,9	600
700-1000-S	700	1000	709	56,5	700
700-1200-S	700	1200	709	67,9	700
700-1500-S	700	1500	709	84,8	700
800-1000-C	800	1000	817	65,2	700
800-1200-C	800	1200	817	78,2	700
800-1500-C	800	1500	817	97,7	700
800-1800-C	800	1800	817	117,3	700
800-1500-C	800	2100	817	136,8	700
800-1800-C	800	2500	817	162,9	700
800-1200-S	800	1200	932	89,2	800
800-1500-S	800	1500	932	111,5	800
800-1800-S	800	1800	932	133,8	800
800-2100-S	800	2100	932	156,1	800
800-2500-S	800	2500	932	185,8	800

Appendix II Pump sheet

	BOMBAS ITUR, S.A.	Technical Data	Quotation no. Project normabloc pumps Date 2004-09-21 Page																																						
Customer no. Customer		Delivery time: General																																							
		Requested data Fluid <i>Water, clean</i> 100 % Temp: 20 °C <i>Dens: 0,9983 kg/dm³ Visc: 1,005 cSt</i> Flow 0 m³/h Head 0 m																																							
		Pump data Type N4-125/250B Design Monobloc D Impeller type Closed Impeller size Ø 271 mm Outlet width 37 mm																																							
		Hydraulic data (according to ISO 9906-2A) Flow m³/h Head m Speed 1470 rpm Efficiency % Shaft power kW																																							
DNs Suction side DIN DN 150 PN 10 		DNd Discharge side DIN DN 125 PN 10 																																							
Motor data Rated power P2 11 kW Speed 1470 rpm 50 Hz Rated voltage 400 V Rated current 21 A Protection IP 55 Insulation class F Temperature class B		Execution: 1003 Pump housing Bronze (RG-5) Pump cover Bronze (RG-5) Impeller Bronze (SN-10) Pump shaft Stainless Steel (AISI-316L) Wear rings Bronze (RG-7) Shaft sleeve Stainless Steel (AISI-316L)																																							
Shaft seal Type CierreSimpleDIN Materials / Shaft seal ITUR DIN K CS/GR-NI		Three-phase IP-55 Rated power P2 11 kW Speed 1470 rpm 50 Hz Rated voltage 400 V Rated current 21 A Protection IP 55 Insulation class F Temperature class B																																							
		<table border="1" style="width:100%; border-collapse: collapse;"> <thead> <tr> <th colspan="2">Dimensions in mm</th> </tr> </thead> <tbody> <tr><td>a</td><td>140</td></tr> <tr><td>b</td><td>64</td></tr> <tr><td>c</td><td>22</td></tr> <tr><td>d</td><td>234</td></tr> <tr><td>DNd</td><td>125</td></tr> <tr><td>DNs</td><td>150</td></tr> <tr><td>e</td><td>215</td></tr> <tr><td>f</td><td>252</td></tr> <tr><td>g</td><td>482</td></tr> <tr><td>h1</td><td>160</td></tr> <tr><td>h1a</td><td>233</td></tr> <tr><td>h2</td><td>355</td></tr> <tr><td>k</td><td>492,5</td></tr> <tr><td>m1</td><td>287,5</td></tr> <tr><td>m2</td><td>210</td></tr> <tr><td>n1</td><td>310</td></tr> <tr><td>n2</td><td>254</td></tr> <tr><td>s</td><td>14,5</td></tr> </tbody> </table>		Dimensions in mm		a	140	b	64	c	22	d	234	DNd	125	DNs	150	e	215	f	252	g	482	h1	160	h1a	233	h2	355	k	492,5	m1	287,5	m2	210	n1	310	n2	254	s	14,5
Dimensions in mm																																									
a	140																																								
b	64																																								
c	22																																								
d	234																																								
DNd	125																																								
DNs	150																																								
e	215																																								
f	252																																								
g	482																																								
h1	160																																								
h1a	233																																								
h2	355																																								
k	492,5																																								
m1	287,5																																								
m2	210																																								
n1	310																																								
n2	254																																								
s	14,5																																								
		Weight 208 kg																																							

Appendix III Picture of original output file from loggings

Row	Time (Integer, R)	Minutt (Integer, R)	Sekund (Integer)	TT1 (Float)	TT2 (Float)	TT3 (Float)	TT4 (Float)	TT5 (Float)	PT1 (Float)	PT2 (Float)	DPT1 (Float)	DPT2 (Float)	DPT3 (Float)	DPT4 (Float)	FT1 (Float)	FT2 (Float)
0	9	31	24	13,83	13,56	5,01	5	4,86	1,43	0,03	0,01	-0,5	1,36	-0,5	51,78	131,48
1	9	31	25	13,83	13,56	5,01	5	4,86	1,43	0,03	0,01	-0,5	1,34	-0,5	51,95	131,46
2	9	31	26	13,83	13,56	5,01	4,99	4,86	1,43	0,03	0,01	-0,5	1,34	-0,5	51,92	131,3
3	9	31	27	13,83	13,57	5,02	4,96	4,86	1,43	0,03	0,01	-0,5	1,34	-0,5	51,92	131,3
4	9	31	28	13,83	13,57	5,02	4,96	4,86	1,42	0,03	0,01	-0,5	1,34	-0,5	52,07	131,3
5	9	31	29	13,84	13,58	5,02	4,97	4,86	1,42	0,03	0,01	-0,5	1,34	-0,5	51,88	131,3
6	9	31	30	13,84	13,59	5,02	4,97	4,86	1,42	0,03	0,01	-0,5	1,34	-0,5	51,86	131,3
7	9	31	31	13,84	13,59	5,01	4,96	4,86	1,42	0,03	0,01	-0,5	1,34	-0,5	51,88	131,25
8	9	31	32	13,85	13,59	5,01	4,97	4,86	1,42	0,03	0,01	-0,5	1,34	-0,5	51,9	131
9	9	31	33	13,85	13,59	4,99	4,98	4,86	1,42	0,03	0,01	-0,5	1,33	-0,5	51,77	130,88
10	9	31	34	13,85	13,59	5	4,99	4,86	1,42	0,03	0,01	-0,5	1,33	-0,5	51,79	130,4

Appendix IV Raw test data with standard deviation

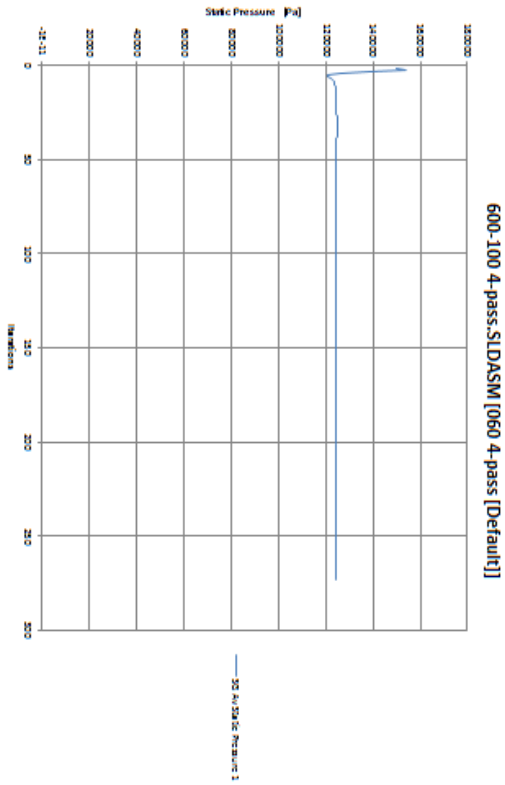
No Rack				4-pass Rack				2-pass Rack				2-pass Full Rack			
DP T3	FT2	STD EV	Rel STDEV	DP T3	FT2	STD EV	Rel STDEV	DP T3	FT2	STD EV	Rel STDEV	DP T3	FT2	STD EV	Rel STDEV
1,29	134,91	0,60	0,45	1,34	130,61	0,56	0,43	1,33	130,35	0,75	0,58	1,33	129,42	0,52	0,40
1,29	134,91	0,59	0,44	1,33	131,19	0,67	0,51	1,33	130,77	0,41	0,31	1,33	129,47	1,44	1,12
1,21	129,39	0,92	0,71	1,33	130,58	0,43	0,33	1,33	130,65	0,51	0,39	1,33	128,92	0,41	0,32
1,04	120,52	0,47	0,39	1,17	123,71	0,95	0,77	1,14	121,02	0,56	0,46	1,16	120,39	0,64	0,54
0,87	111,49	0,55	0,49	1,15	121,13	1,04	0,86	1,13	119,62	0,76	0,64	0,98	110,64	0,54	0,49
0,73	99,95	0,47	0,47	0,95	111,24	0,75	0,68	0,96	111,06	0,60	0,54	0,97	110,36	0,86	0,78
0,74	101,58	0,51	0,50	0,81	102,35	0,77	0,75	0,96	111,01	0,81	0,73	0,82	101,15	0,26	0,25
0,60	92,15	1,20	1,30	0,80	101,94	0,46	0,45	0,95	110,68	0,83	0,75	0,81	99,09	0,82	0,83
0,60	91,64	0,71	0,77	0,77	99,71	0,53	0,53	0,78	100,71	0,32	0,31	0,68	90,33	0,39	0,43
0,48	81,09	0,91	1,12	0,66	92,39	0,69	0,75	0,77	99,52	0,77	0,78	0,54	80,20	0,52	0,65
0,47	81,10	0,53	0,65	0,65	92,24	0,73	0,79	0,77	99,31	0,39	0,39	0,42	70,67	0,72	1,01
0,37	71,39	0,79	1,10	0,51	81,82	0,50	0,61	0,64	89,96	0,95	1,05	0,42	69,80	0,37	0,54
0,37	70,64	0,49	0,70	0,50	80,88	0,83	1,02	0,64	91,15	0,74	0,81	0,31	59,82	0,69	1,15
0,27	59,83	0,50	0,83	0,39	70,95	0,70	0,98	0,64	91,94	0,78	0,85	0,22	50,32	0,81	1,62
0,27	60,34	0,65	1,07	0,39	70,47	0,26	0,37	0,51	79,75	0,55	0,69	0,21	49,96	0,73	1,47
0,20	50,14	0,33	0,65	0,30	61,54	0,72	1,17	0,41	70,97	0,36	0,50	0,15	40,77	0,84	2,07
0,13	39,89	0,60	1,51	0,21	50,08	0,71	1,42	0,39	68,57	0,69	1,00	0,14	39,99	0,82	2,04
0,13	39,95	0,93	2,33	0,13	38,48	0,64	1,67	0,30	60,17	0,66	1,10	0,07	29,39	0,68	2,32
0,07	30,02	0,42	1,39	0,14	40,41	0,62	1,53	0,30	59,99	0,64	1,06	0,08	30,40	0,47	1,53
0,03	19,95	0,37	1,86	0,14	41,09	0,60	1,45	0,21	49,87	0,41	0,83	0,04	20,43	0,43	2,09
0,02	14,71	0,37	2,51	0,08	29,12	0,64	2,19	0,14	39,44	0,81	2,05	0,02	15,26	0,35	2,27
0,02	15,57	0,78	5,03	0,08	29,36	0,52	1,78	0,08	30,33	0,80	2,63	0,01	10,77	0,43	4,02
0,01	10,52	0,36	3,43	0,04	19,41	0,60	3,11	0,08	29,91	0,56	1,87	Average:		0,63	1,27
0,01	9,59	0,65	6,79	0,04	20,50	0,69	3,37	0,04	20,06	0,95	4,72				
Average:		0,61	1,52	0,02	15,53	0,45	2,87	0,02	15,23	0,36	2,36				
				0,01	9,51	0,41	4,34	0,02	15,37	0,29	1,86				
				Average:		0,63	1,34	0,01	10,05	0,51	5,03				
								0,01	10,02	0,38	3,78				
								Average:		0,61	1,36				

Appendix V Result file from SolidWorks Flow Simulation

600-1000 4-pass.SLDASM [060 4-pass [Default]]

Goal Name	Unit	Value	Averaged Value	Minimum Value	Maximum Value	Progress [%]	Use In Convergence	Delta	Criteria
SG Av Static Pressure 1	[Pa]	124356.8065	124350.7665	124321.6873	124363.4619	100	Yes	41,77452683	531,1389045

Iterations: 273
Analysis interval: 137



Static Pressure (Pa)	Iterations	SG Av Static Pressure 1
	Yes	9
	100	
41,77452683		
531,1389045		
124350,7665		
124321,6873		
124363,4619		
150253,6735	1	
153918,1795	2	
138529,0371	3	
126283,8883	4	
120824,4069	5	
121243,2353	6	
122612,0846	7	
123363,0809	8	
123877,1533	9	



Appendix VI Full report 600-1000S 4-pass Simulation (Mesh 5)

FULL REPORT

System Info

Product	Flow Simulation 2013 SP4.0. Build: 2401
Computer name	TFFL4-04
User name	lassis
Processors	Intel(R) Xeon(R) CPU E3-1230 v3 @ 3.30GHz
Memory	16297 MB / 8388607 MB
Operating system	Windows 7 Service Pack 1 (Build 7601)
CAD version	SolidWorks 2013 SP4.0
CPU speed	3301 MHz

General Info

Model	D:\Lasse\Test\700-1000 Simulation\600-1000 4-pass\600-100 4-pass.SLDASM
Project name	-060 4-pass
Project path	D:\Lasse\Test\700-1000 Simulation\600-1000 4-pass\9
Units system	SI (m-kg-s)
Analysis type	Internal
Exclude cavities without flow conditions	On
Coordinate system	Global coordinate system
Reference axis	X

INPUT DATA

Initial Mesh Settings

Automatic initial mesh: On
 Result resolution level: 5
 Advanced narrow channel refinement: Off
 Refinement in solid region: Off

Geometry Resolution

Evaluation of minimum gap size: Automatic
 Evaluation of minimum wall thickness: Automatic

Local Mesh Settings

Local Initial Mesh 1

Components	Bend mesh-1
Solid/fluid interface	Small solid features refinement level: 4 Curvature refinement level: 3 Curvature refinement criterion: 0.318 rad Tolerance refinement level: 2 Tolerance refinement criterion: 0.122 m
Refining cells	Refine fluid cells: On Level of refining fluid cells: 4

	Refine solid cells: Off Refine partial cells: On Level of refining partial cells: 3
Narrow channels	Advanced narrow channel refinement: On Characteristic number of cells across a narrow channel: 10 Narrow channels refinement level: 3 The minimum height of narrow channels: Off The maximum height of narrow channels: Off

Local Initial Mesh 2

Components	Inlet outlet mesh-1
Solid/fluid interface	Small solid features refinement level: 3 Curvature refinement level: 2 Curvature refinement criterion: 0.390 rad Tolerance refinement level: 2 Tolerance refinement criterion: 0.040 m
Refining cells	Refine fluid cells: On Level of refining fluid cells: 3 Refine solid cells: Off Refine partial cells: On Level of refining partial cells: 1
Narrow channels	Advanced narrow channel refinement: On Characteristic number of cells across a narrow channel: 10 Narrow channels refinement level: 3 The minimum height of narrow channels: Off The maximum height of narrow channels: Off

Computational Domain

Size

X min	-0.233 m
X max	0.233 m
Y min	-1.105 m
Y max	-0.006 m
Z min	-0.284 m
Z max	0.284 m

Boundary Conditions

2D plane flow	None
At X min	Default
At X max	Default
At Y min	Default
At Y max	Default
At Z min	Default
At Z max	Default

Physical Features

Heat conduction in solids: Off

Time dependent: Off
 Gravitational effects: On
 Flow type: Laminar and turbulent
 Cavitation: Off
 High Mach number flow: Off
 Default roughness: 1.5 micrometer

Gravitational Settings

X component	0 m/s ²
Y component	-9.81 m/s ²
Z component	0 m/s ²

Default wall conditions: Adiabatic wall

Initial Conditions

Thermodynamic parameters	Static Pressure: 101325.00 Pa Temperature: 323.15 K
Velocity parameters	Velocity vector Velocity in X direction: 0 m/s Velocity in Y direction: 0 m/s Velocity in Z direction: 0 m/s
Turbulence parameters	Turbulence intensity and length Intensity: 2.00 % Length: 0.005 m

Material Settings

Fluids

Water

Boundary Conditions

Inlet Volume Flow 1

Type	Inlet Volume Flow
Faces	Face<1>@LID2-1
Coordinate system	Face Coordinate System
Reference axis	X
Flow parameters	Flow vectors direction: Normal to face Volume flow rate normal to face: 0.0167 m ³ /s Fully developed flow: No Inlet profile: 0
Thermodynamic parameters	Temperature: 323.15 K
Turbulence parameters	Turbulence intensity and length Intensity: 2.00 % Length: 0.005 m
Boundary layer parameters	Boundary layer type: Turbulent

Environment Pressure 1

Type	Environment Pressure
Faces	Face<2>@LID1-1
Coordinate system	Face Coordinate System

Reference axis	X
Thermodynamic parameters	Environment pressure: 101325.00 Pa Temperature: 323.15 K
Turbulence parameters	Turbulence intensity and length Intensity: 2.00 % Length: 0.005 m
Boundary layer parameters	Boundary layer type: Turbulent

Goals

Surface Goals

SG Av Static Pressure 1

Type	Surface Goal
Goal type	Static Pressure
Calculate	Average value
Faces	Face<1>@LID2-1
Coordinate system	Global coordinate system
Use in convergence	On

Calculation Control Options

Finish Conditions

Finish conditions	If one is satisfied
Maximum travels	4
Goals convergence	Analysis interval: 5e-001

Solver Refinement

Refinement: Disabled

Results Saving

Save before refinement	On
------------------------	----

Advanced Control Options

Flow Freezing

Flow freezing strategy	Disabled
------------------------	----------

RESULTS

General Info

Iterations: 366

CPU time: 40573 s

Log

Preparing data for calculation	00:32:55 , Apr 22
Calculation started 0	00:36:39 , Apr 22
Calculation has converged since the following criteria are satisfied: 365	11:50:03 , Apr 22
Goals are converged 365	



Calculation finished 366	11:58:08 , Apr 22
--------------------------	-------------------

Warnings: A vortex crosses the pressure opening Boundary Condition : Environment Pressure 1 ; Inlet flow/outlet flow=0.005153

Calculation Mesh

Basic Mesh Dimensions

Number of cells in X	14
Number of cells in Y	34
Number of cells in Z	18

Number Of Cells

Total cells	6109796
Fluid cells	1471876
Solid cells	1749960
Partial cells	2887960
Irregular cells	0
Trimmed cells	0

Maximum refinement level: 4

Goals

Name	Unit	Value	Progress	Use in convergence	Delta	Criteria
SG Av Static Pressure 1	Pa	110478.33	100	On	20.8664883	81.4607725

Min/Max Table

Name	Minimum	Maximum
Pressure [Pa]	101073.64	119559.18
Temperature [K]	323.15	323.15
Density (Fluid) [kg/m ³]	987.45	987.45
Velocity [m/s]	0	1.657
Velocity (X) [m/s]	-1.512	1.494
Velocity (Y) [m/s]	-1.657	1.478
Velocity (Z) [m/s]	-1.061	1.297
Temperature (Fluid) [K]	323.15	323.15
X (cartesian) [m]	-0.233	0.233
Vorticity [1/s]	8.537e-005	1091.239
Shear Stress [Pa]	0	19.37
Relative Pressure [Pa]	-251.36	18234.18
Heat Transfer Coefficient [W/m ² /K]	0	0
Surface Heat Flux [W/m ²]	0	0

Appendix VII Full report 600-1000S 4-pass Simulation (Mesh 4)

FULL REPORT

System Info

Product	Flow Simulation 2013 SP4.0. Build: 2401
Computer name	TFFL4-04
User name	lassis
Processors	Intel(R) Xeon(R) CPU E3-1230 v3 @ 3.30GHz
Memory	16297 MB / 8388607 MB
Operating system	Windows 7 Service Pack 1 (Build 7601)
CAD version	SolidWorks 2013 SP4.0
CPU speed	3301 MHz

General Info

Model	D:\Lasse\Test\700-1000 Simulation\600-1000 4-pass\600-100 4-pass.SLDASM
Project name	060 4-pass
Project path	D:\Lasse\Test\700-1000 Simulation\600-1000 4-pass\2
Units system	SI (m-k-g-s)
Analysis type	Internal
Exclude cavities without flow conditions	On
Coordinate system	Global coordinate system
Reference axis	X

INPUT DATA

Initial Mesh Settings

Automatic initial mesh: On
 Result resolution level: 4
 Advanced narrow channel refinement: Off
 Refinement in solid region: Off

Geometry Resolution

Evaluation of minimum gap size: Automatic
 Evaluation of minimum wall thickness: Automatic

Local Mesh Settings

Local Initial Mesh 1

Components	Bend mesh-1
Solid/fluid interface	Small solid features refinement level: 4 Curvature refinement level: 3 Curvature refinement criterion: 0.318 rad Tolerance refinement level: 2 Tolerance refinement criterion: 0.122 m
Refining cells	Refine fluid cells: On Level of refining fluid cells: 4 Refine solid cells: Off Refine partial cells: On Level of refining partial cells: 3
Narrow channels	Advanced narrow channel refinement: On Characteristic number of cells across a narrow channel: 10 Narrow channels refinement level: 3 The minimum height of narrow channels: Off The maximum height of narrow channels: Off

Local Initial Mesh 2

Components	Inlet outlet mesh-1
Solid/fluid interface	Small solid features refinement level: 3 Curvature refinement level: 2 Curvature refinement criterion: 0.390 rad Tolerance refinement level: 2 Tolerance refinement criterion: 0.040 m
Refining cells	Refine fluid cells: On Level of refining fluid cells: 3 Refine solid cells: Off Refine partial cells: On Level of refining partial cells: 1
Narrow channels	Advanced narrow channel refinement: On Characteristic number of cells across a narrow channel: 10 Narrow channels refinement level: 3 The minimum height of narrow channels: Off The maximum height of narrow channels: Off

Computational Domain

Size

X min	-0.233 m
X max	0.233 m
Y min	-1.105 m

Y max	-0.006 m
Z min	-0.284 m
Z max	0.284 m

Boundary Conditions

2D plane flow	None
At X min	Default
At X max	Default
At Y min	Default
At Y max	Default
At Z min	Default
At Z max	Default

Physical Features

Heat conduction in solids: Off
 Time dependent: Off
 Gravitational effects: On
 Flow type: Laminar and turbulent
 Cavitation: Off
 High Mach number flow: Off
 Default roughness: 1.5 micrometer

Gravitational Settings

X component	0 m/s ²
Y component	-9.81 m/s ²
Z component	0 m/s ²

Default wall conditions: Adiabatic wall

Initial Conditions

Thermodynamic parameters	Static Pressure: 101325.00 Pa Temperature: 323.15 K
Velocity parameters	Velocity vector Velocity in X direction: 0 m/s Velocity in Y direction: 0 m/s Velocity in Z direction: 0 m/s
Turbulence parameters	Turbulence intensity and length Intensity: 2.00 % Length: 0.005 m

Material Settings

Fluids

Water

Boundary Conditions

Inlet Volume Flow 1

Type	Inlet Volume Flow
Faces	Face<1>@LID2-1
Coordinate system	Face Coordinate System
Reference axis	X
Flow parameters	Flow vectors direction: Normal to face Volume flow rate normal to face: 0.0167 m ³ /s Fully developed flow: No Inlet profile: 0
Thermodynamic parameters	Temperature: 323.15 K
Turbulence parameters	Turbulence intensity and length Intensity: 2.00 % Length: 0.005 m
Boundary layer parameters	Boundary layer type: Turbulent

Environment Pressure 1

Type	Environment Pressure
Faces	Face<2>@LID1-1
Coordinate system	Face Coordinate System
Reference axis	X
Thermodynamic parameters	Environment pressure: 101325.00 Pa Temperature: 323.15 K
Turbulence parameters	Turbulence intensity and length Intensity: 2.00 % Length: 0.005 m
Boundary layer parameters	Boundary layer type: Turbulent

Goals

Surface Goals

SG Av Static Pressure 1

Type	Surface Goal
Goal type	Static Pressure
Calculate	Average value
Faces	Face<1>@LID2-1
Coordinate system	Global coordinate system
Use in convergence	On

Calculation Control Options

Finish Conditions

Finish conditions	If one is satisfied
Maximum travels	4

Goals convergence	Analysis interval: 5e-001
-------------------	---------------------------

Solver Refinement

Refinement: Disabled

Results Saving

Save before refinement	On
------------------------	----

Advanced Control Options

Flow Freezing

Flow freezing strategy	Disabled
------------------------	----------

RESULTS

General Info

Iterations: 273

CPU time: 12608 s

Log

Preparing data for calculation	21:28:48 , Apr 15
Calculation started 0	21:30:31 , Apr 15
Calculation has converged since the following criteria are satisfied: 272	00:59:24 , Apr 16
Goals are converged 272	
Calculation finished 273	01:02:47 , Apr 16

Calculation Mesh

Basic Mesh Dimensions

Number of cells in X	10
Number of cells in Y	24
Number of cells in Z	12

Number Of Cells

Total cells	2535865
Fluid cells	363175
Solid cells	779580
Partial cells	1393110
Irregular cells	0
Trimmed cells	0

Maximum refinement level: 4



Goals

Name	Unit	Value	Progress	Use in convergence	Delta	Criteria
SG Av Static Pressure 1	Pa	124356.81	100	On	41.7745268	531.138905

Min/Max Table

Name	Minimum	Maximum
Pressure [Pa]	101113.50	134488.17
Temperature [K]	323.15	323.15
Density (Fluid) [kg/m ³]	987.45	987.45
Velocity [m/s]	0	3.062
Velocity (X) [m/s]	-3.061	2.928
Velocity (Y) [m/s]	-3.046	3.019
Velocity (Z) [m/s]	-0.964	1.310
Temperature (Fluid) [K]	323.15	323.15
X (cartesian) [m]	-0.233	0.233
Vorticity [1/s]	3.443e-006	2342.688
Shear Stress [Pa]	0	75.61
Relative Pressure [Pa]	-211.50	33163.17
Heat Transfer Coefficient [W/m ² /K]	0	0
Surface Heat Flux [W/m ²]	0	0



Norwegian University
of Life Sciences

Postboks 5003
NO-1432 Ås, Norway
+47 67 23 00 00
www.nmbu.no